

# The **RISING** Project

Proposals for Stopped Beam Configuration



RISING Collaboration

February 2005



# Decay Studies of Exotic Nuclei using RISING and the GSI Fragment Separator

Spokesperson for the Stopped Beam RISING collaboration: P.H.Regan  
GSI contacts: J.Gerl & H.J.Wollersheim

This proposal forms part of the 'Stopped Beam' RISING experimental campaign at GSI.

## PARTICIPANTS

CENBG Bordeaux, France: B. Blank

GSI-Darmstadt, Germany: J.Gerl, H.J.Wollersheim, F.Becker, H.Grawe, M.Gorska, P.Bednarczyk, N.Saitoh, T.Saitoh

IKP Koeln, Germany: J. Jolie, P. Reiter, N. Warr, A. Richard, A. Scherillo, N. Warr

TU Munchen: R. Krücken, T. Faestermann

University of Camerino, Italy: D. Balabanski, K.Gladnishki,

IFJ PAN Krakow, Poland: A. Maj, J. Grebosz, M. Kmiecik, K. Mazurek

Warsaw University, Poland: M. Pfützner

Universidad Autonoma de Madrid, Spain: A. Jungclaus

Universidad de Santiago de Compostela, Spain: D. Cortina Gil, J. Benlliure, T. Kurtukian Nieto, E. Caserejos

IFIC Valencia, Spain: B. Rubio

INFN-Legnaro, Italy: A. Gadea, G. deAngelis, J.J. Valiente Dobon, N. Marginean, D. Napoli,

INFN-Padova, Italy: E. Farnea, D. Bazzacco, S. Lunardi, R. Marginean

University and INFN-Milano: A. Bracco, G. Benzoni, F. Camera, B. Million, O. Wieland, S. Leoni

University of Surrey, UK: Zs. Podolyák, P.H. Regan, P.M. Walker, W. Gelletly, W.N.Catford, Z. Liu, S. Williams

University of York, UK: M.A. Bentley, R. Wadsworth

University of Brighton, UK: A.M. Bruce

University of Manchester, UK: D.M. Cullen, S.J. Freeman

University of Liverpool, UK: R.D. Page

University of Edinburgh, UK: P. Woods, T. Davinson

CLRC Daresbury, UK: J. Simpson, D. Warner

Uppsala University, Sweden: H. Mach

Lund University, Sweden: D. Rudolph

Lawrence Berkeley National Lab, USA: R.M. Clark

University of Notre Dame, USA: M. Wiescher, A. Aprahamian

Youngstown State University, Ohio, USA: J.J. Carroll

Debrecen, Hungary: A. Algora

*for the STOPPED BEAM RISING COLLABORATION*

**Abstract:** *We will investigate new structures in exotic, heavy neutron-rich and N~Z nuclei formed following projectile fragmentation reactions using the Fragment Separator. The specific physics aims are:*

- *Investigating fundamental nuclear shell model interactions by identifying proton-hole states in the  $^{208}\text{Pb}$  double-magic closed shell;*
- *The evolution of nuclear dynamical symmetries and related nuclear shapes from the extreme 'single-particle region' around  $^{208}\text{Pb}$  towards the 'valence maximum' nucleus,  $^{170}\text{Dy}$ ;*
- *The identification of isomeric states in proton-hole configurations in the  $^{132}\text{Sn}$  doubly-closed core; and*
- *The study of isospin symmetry across the N=Z line.*

*The experimental technique involves the use of the FRagment Separator (FRS) at GSI to identify some of the most exotic, heavy nuclei synthesised to date. We will study the internal structure of these systems using  $\gamma$ -ray spectroscopy following: (i) the decay of metastable nuclear isomeric states with lifetimes in the nano-to-millisecond time scale; and (ii) the  $\beta^-$ -decay of highly neutron-rich nuclei with lifetimes in the seconds range. Events will be time correlated with respect to the detection of individually identified nuclei at the final focus of the FRS. The six proposed experiments will use the high-efficiency RISING  $\gamma$ -ray array of CLUSTER germanium detectors, complemented by BaF<sub>2</sub> detectors (which provide the opportunity for fast timing measurements in specific cases) and a segmented silicon 'active stopper' for  $\beta$ -decay measurements.*

## BACKGROUND

A major thrust of nuclear structure research is to determine and understand how the shell structure of nuclei changes for systems with highly asymmetric proton-to-neutron ratios. The proposed research for this portion of the *Stopped Beam RISING Experimental Campaign* will exploit radioactive beams, produced using projectile-fragmentation reactions to enable the first study of a range of highly exotic, heavy, neutron-rich nuclei and studies of isospin symmetry across the  $N=Z$  line. Some of these experiments will take advantage of the existence of nano-to-millisecond isomers in these nuclei to enable the first spectroscopic information to be obtained (more details on this technique from GSI-FRS-based work can be found in references [1-6]). The relatively low intensities of the secondary radioactive beams in such experiments (typically less than 1 ion per second) can often preclude the use of  $\gamma$ -ray coincidence measurements that are needed to confirm the nuclear decay schemes. However, isomeric decays and measurements of decays following  $\beta$ -emission [7] can provide the vital  $\gamma$ -ray ‘fingerprints’ which give the first glimpses of excited states and the internal structure of such nuclei. A systematic study of key experimental signatures, such as the energy of the first excited state and/or of the ratio of the excitation energies of the lowest-lying levels in even-even nuclei, can vividly demonstrate the erosion of the established magic numbers. This reveals both new regions of nuclear shell structure and the development of nuclear collective excitations. The current proposal aims to identify such fingerprints following radioactive-beam studies in selected exotic nuclei using isomer [1-6] and  $\beta^-$ -delayed  $\gamma$ -ray detection [7].

Figure 1 shows the predicted ground state nuclear decay modes as predicted by the Moller-Nix mass model [8]. While a very wide range of exotic nuclei can be populated in projectile fragmentation, in-beam spectroscopy of such systems (as performed in the ‘fast beam’ part of the RISING Campaign) is limited by the total germanium singles counting rate at the production target for the secondary radioactive ions. For very weakly produced secondary nuclei, this limitation makes their spectroscopy impossible at the current time using the in-beam technique. However, by using the Fragment Separator to select and transport the specific nuclei of interest to the final focal plane of the FRS, decays from both isomeric states [1-6] and following the radioactive decay of the daughter nuclei can be performed [7], often allowing the first spectroscopic information on these highly exotic systems.

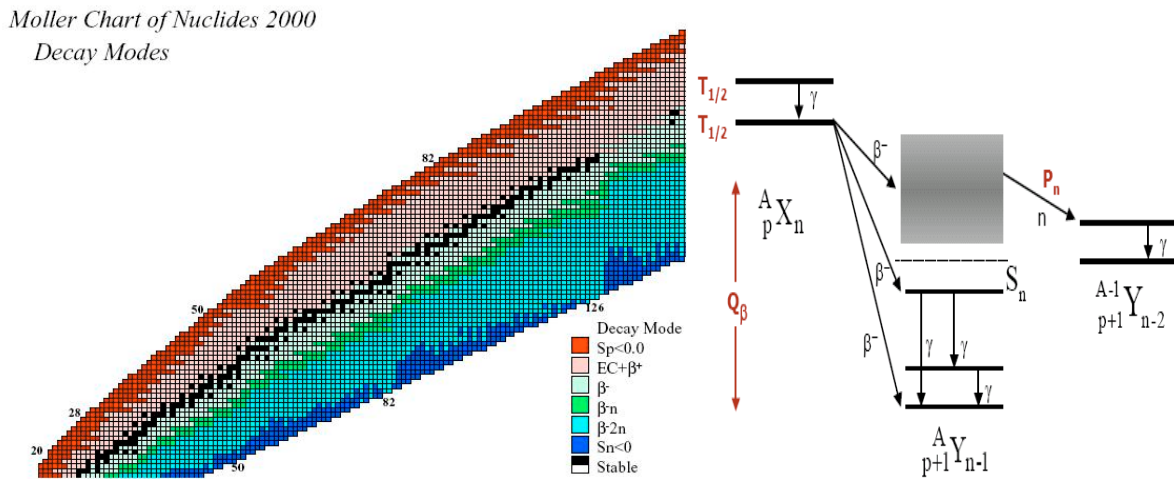


**Figure 1: Left:** Radioactive decay modes as predicted by the 2000 mass evaluation [8]. **Right:** Schematic of  $\beta$  and isomer decay modes of decay to populate excited states in specific daughter nuclei.

The stopped beam proposals have been prepared following a meeting to discuss the specific physics aims of the Stopped Beam RISING campaign, which took place at the University of Surrey in March 2004 (see [http://www.ph.surrey.ac.uk/~phs1pr/rising/stopped\\_workshop\\_04](http://www.ph.surrey.ac.uk/~phs1pr/rising/stopped_workshop_04)). Note that the proposals submitted in this, ‘active stopper’ phase of the stopped beam RISING campaign are complemented by the series of proposals aimed at measuring gyromagnetic ratios of isomeric states using a related set-up (see proposals by G. Neyens et al.,).



In the proposed geometry, the calculated photopeak efficiency for  $\gamma$ -ray detection from the active stopper detector placed in the centre of the RISING array (see below) is calculated to be 11% for a  $\gamma$ -ray energy of 1.33 MeV and 20% for 662 keV. In addition, an array of 8 BaF<sub>2</sub> detectors will also be placed in the array for the ‘fast-timing’ of lifetimes in the hundreds of pico to few nanoseconds time range. This will be useful in cases where the ordering of newly observed transitions in a cascade needs to be determined.

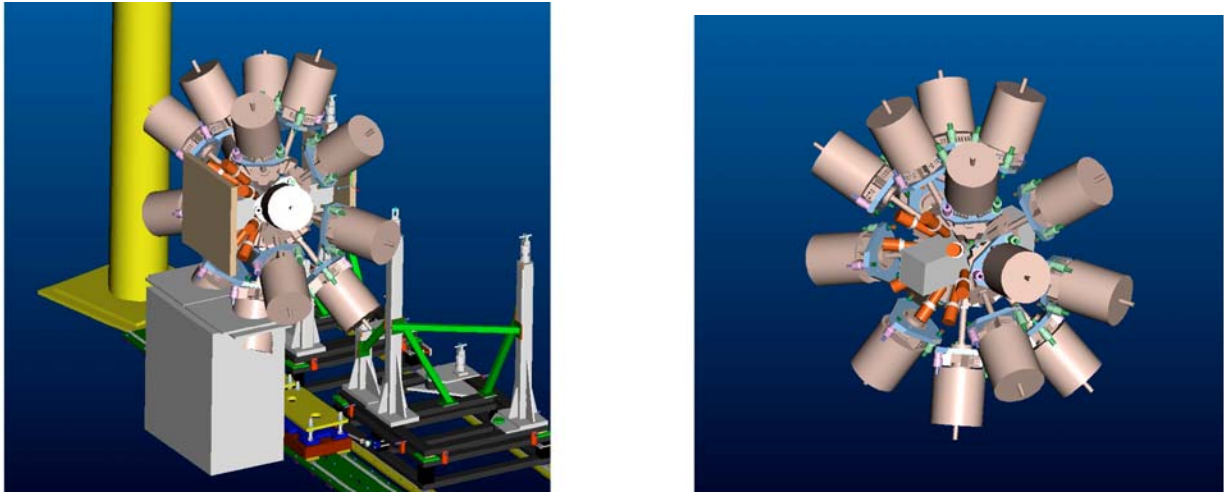


**Figure 3** CAD drawings of the Stopped Beam RISING array, plus 8 BaF<sub>2</sub> detectors, showing (left) the support structure and space for fast plastic scintillation detectors and (right) a 25cm x 25cm vacuum chamber in which to house the DSSSDs.

The FRS will be used in the monochromatic mode which enables individually selected ions to be stopped in a single 1mm thick silicon detector. This means that the experimenters can select specific elements of interest for  $\gamma$ -ray spectroscopy studies following  $\beta$ -decay. Figure 4 shows the effect of this ‘selective stopping’ using the monochromatic setting of the FRS from the experiment of J. Benlliure et al., (S227) following the fragmentation of a <sup>208</sup>Pb beam on a <sup>9</sup>Be target at a beam energy of 1 GeV per nucleon.

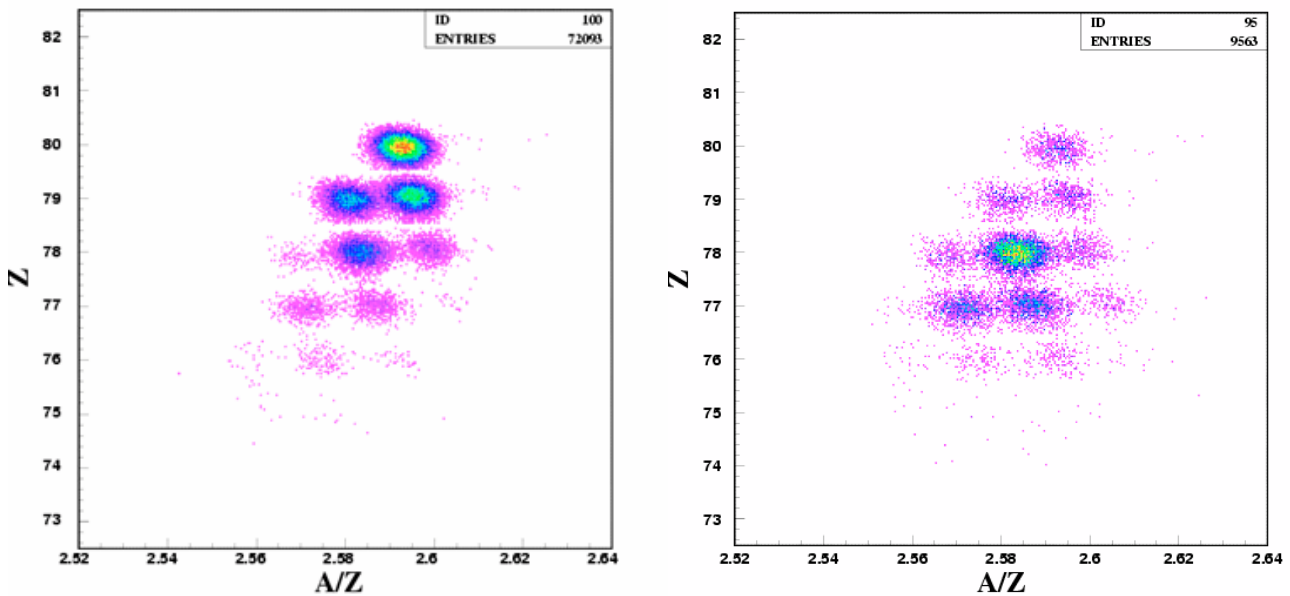


**Figure 4** Particle identification plots centred on <sup>198</sup>Ir ions produced following the fragmentation of 1 GeV per nucleon <sup>208</sup>Pb beam on a <sup>9</sup>Be target with the FRS used in monochromatic mode. The left hand figure shows the total production yield at the end of the FRS, while the right hand side is limited to those ions which were selected to stop in the 1mm thick DSSSD as will be used in the proposed experiments.

The active stopper will consist of three 5 cm by 5 cm double sided silicon strip detectors (DSSSDs) each with 16 horizontal and 16 vertical strips (giving each detector defined 256 pixels, or 768 pixels for the three detectors of active stopper). The active stopper detectors are 1 mm thick, which is enough to stop all the ions of a chosen element if the FRS is used in monochromatic mode (see figure 4). Heavier elements are stopped in the degrader or plastic scintillator which precedes the active stopper (see left-hand side of figure 2), while the lower-Z elements pass through the active stopper and are detected in the plastic veto scintillator detector.

A number of the proposed experiments for the Active Stopper RISING campaign rely on rate estimates assuming ‘cold fragmentation’ of the primary beam [12]. Figure 5 shows the robustness of these estimates when compared with the measured cross-sections for cold-fragmentation products following reactions between a  $^{197}\text{Au}$  beam on  $^9\text{Be}$  target at 950 MeV per nucleon [12].

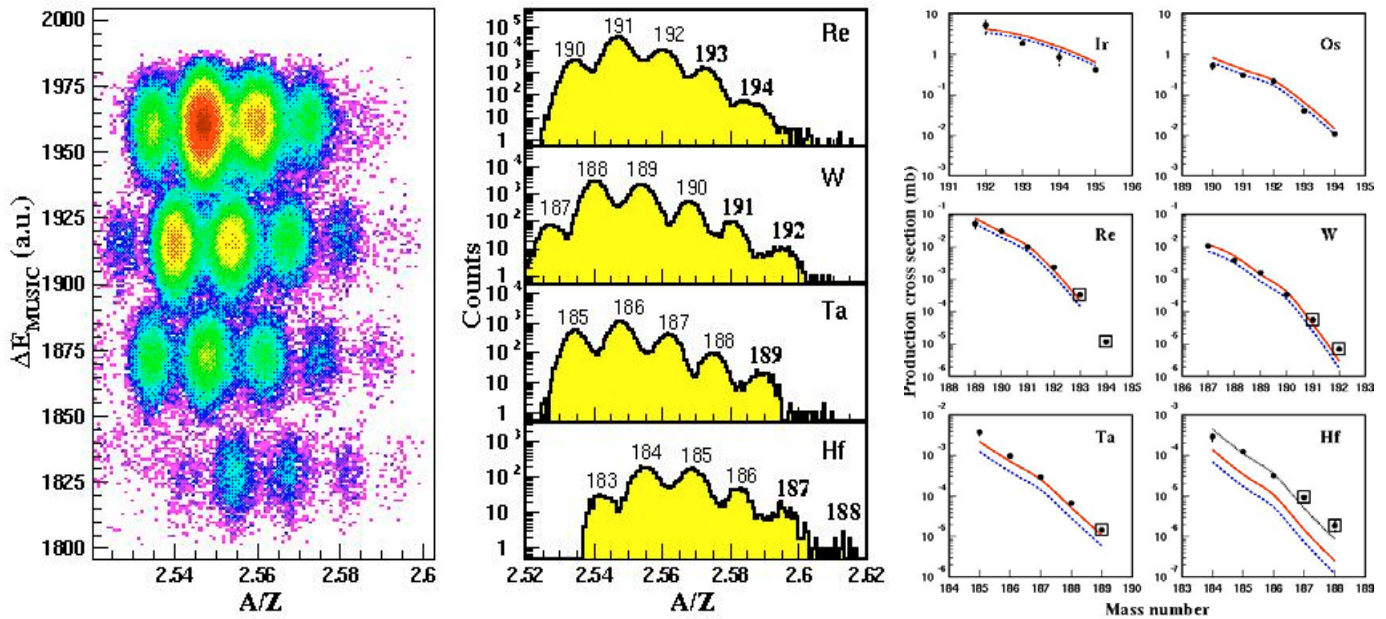


**Figure 5:** Particle identification plots and experimental cross-sections for the ‘cold fragmentation’ products in the  $^{197}\text{Au} + ^9\text{Be}$  reaction, highlighting the good agreement with the semi-empirical predictions for the cross-section as described in reference. Data taken from ref. [12].

Assuming upper-limit  $\beta$ -decay half-life measurements of up to 30 seconds for the less exotic nuclei such as  $^{204,5}\text{Au}$  [11], this implies each pixel can be hit by a new ion on average every 150 seconds (5 typical half-lives) for a reasonable peak to total ratio. This assumption leads to a maximum implantation rate at the active stopper of around 5 ions in total per second (50 per 10 second spill cycle), or 144k per 8 hour shift. The DSSSD array will have dual gain pre-amplifiers to obtain energy measurements for both the implanted heavy ion and the subsequently emitted  $\beta^-$ -particle. Each event will be time stamped with a MHz clock to allow time correlation between the implantation and the subsequent  $\beta$ -decay in the same pixel. Note, that typically the nuclei of interest have predicted  $\beta$ -decay half-lives of significantly less than 10 seconds (see figures 6-9) which will significantly improve the effective experimentally useful correlation-time limit.

## TIMELINESS

The current proposals precedes a massive investment in the GSI-FAIR facility. This €700M upgrade will make GSI the world’s leading laboratory to study heavy, radioactive nuclei. This proposal represents a unique opportunity for the nuclear structure community to build on initial projectile fragmentation isomer and reaction work at GSI to drive a major physics initiative in nuclear spectroscopy through the RISING project. The combination of the FRS and the RISING array mean that the experimental technology is only now available to enable the measurements outlined in the following proposals. The proposed campaign also provides an opportunity to test concepts of future experiments aimed for the DESPEC project at FAIR, for example in the use of fast timing measurements using an array of  $\text{BaF}_2$  detectors. The proposed experiments will also test the application of

the fast timing detectors and cold-fragmentation reactions in ‘large area’ source scenarios. The information gained in such studies will provide input for the design of a proposed future dedicated setup for high precision lifetime measurements.

91	Pa215 0.914s	Pa216 0.185s	Pa217 0.0934s	Pa218 0.000113s	Pa219 5.3e-08s	Pa220 7.6e-07s	Pa221 5.9e-06s	Pa222 0.0053s	Pa223 0.0049s	Pa224 0.25s	Pa225 1.7s	Pa226 1.8m	Pa227 66.3m	Pa228 22h	Pa229 1.5d
90	Th214 0.1s	Th215 1.2s	Th216 0.027s	Th217 0.000237s	Th218 1.09e-07s	Th219 1.05e-06s	Th220 9.7e-06s	Th221 0.00168s	Th222 0.002s	Th223 0.6s	Th224 0.812s	Th225 0.72m	Th226 30.6m	Th227 18.72d	Th228 1.913y
89	Ac213 0.731s	Ac214 8.2s	Ac215 0.17s	Ac216 0.000443s	Ac217 4e-07s	Ac218 1.06e-06s	Ac219 1.18e-05s	Ac220 0.0261s	Ac221 0.032s	Ac222 1.05m	Ac223 2.1m	Ac224 2.9h	Ac225 184	Ac226 1.225d	Ac227 21.77y
88	Ra212 13s	Ra213 2.74m	Ra214 2.46s	Ra215 0.00167s	Ra216 1.82e-07s	Ra217 1.7e-06s	Ra218 1.56e-05s	Ra219 0.01s	Ra220 0.018s	Ra221 28s	Ra222 38s	Ra223 11.44d	Ra224 3.66d	Ra225 14.9d	Ra226 1600y
87	Fr211 3.1m	Fr212 20m	Fr213 34.6s	Fr214 0.005s	Fr215 8.6e-08s	Fr216 7e-07s	Fr217 1.6e-05s	Fr218 0.022s	Fr219 0.02s	Fr220 27.4s	Fr221 4.9m	Fr222 14.2m	Fr223 22m	Fr224 3.3m	Fr225 4m
86	Rn210 2.42h	Rn211 14.6h	Rn212 23.9m	Rn213 0.0195s	Rn214 2.7e-07s	Rn215 2.3e-06s	Rn216 4.5e-05s	Rn217 0.00054s	Rn218 0.035s	Rn219 3.96s	Rn220 55.6s	Rn221 25m	Rn222 8.24d	Rn223 23.2m	Rn224 1.78h
85	At209 5.41h	At210 8.1h	At211 7.214h	At212 0.314s	At213 1.25e-07s	At214 7.6e-07s	At215 0.0001s	At216 0.0003s	At217 0.0323s	At218 1.6s	At219 96s	At220 3.71m	At221 2.3m	At222 54s	At223 50s
84	Po208 0.599s	Po209 103s	Po210 139.4d	Po211 25.2s	Po212 45.1s	Po213 4.2e-06s	Po214 0.000164s	Po215 0.001781s	Po216 0.145s	Po217 1.53s	Po218 3.1m	Po219 30.5m	Po220 36.3m	Po221 6.18m	Po222 9.3m
83	Bi207 31.55v	Bi208 3.68e+05v	Bi209 100	Bi210 3.04e+06	Bi211 2.14m	Bi212 1.009h	Bi213 45.59m	Bi214 19.9m	Bi215 7.7m	Bi216 2.25m	Bi217 1.64m	Bi218 33s	Bi219 0.87s	Bi220 4.73s	Bi221 5.42s
82	Pb206 24.1	Pb207 22.1	Pb208 82	Pb209 3.253h	Pb210 22.7v	Pb211 36.1m	Pb212 10.64h	Pb213 10.2m	Pb214 26.9m	Pb215 36s	Pb216 38.7s	Pb217 28.7s	Pb218 14.5s	Pb219 5.94s	Pb220 2.71s
81	Tl205 70.476	Tl206 4.199m	Tl207 4.77m	Tl208 3.053m	Tl209 2.161m	Tl210 1.3m	Tl211 4.18s	Tl212 2.09s	Tl213 1.13s	Tl214 1.45s	Tl215 1.22s	Tl216 0.811s	Tl217 0.63s	Tl218 0.479s	Tl219 0.44s
80	Hg204 6.87	Hg205 5.2m	Hg206 8.15m	Hg207 2.3m	Hg208 41m	Hg209 35s	Hg210 1.84s	Hg211 1.13s	Hg212 0.528s	Hg213 0.377s	Hg214 0.321s	Hg215 0.226s			
79	Au203 1m	Au204 39.8s	Au205 31s	Au206 1.59s	Au207 1.3s	Au208 1.23s	Au209 0.746s	Au210 0.917s	Au211 0.507s	Au212 0.411s	Au213 0.32s	Au214 0.267s	Au215 0.196s		
78	Pt202 1.8d	Pt203 41.1s	Pt204 6.75s	Pt205 0.674s	Pt206 0.465s	Pt207 0.562s	Pt208 0.302s	Pt209 0.379s	Pt210 0.179s	Pt211 0.177s					
77	Ir201 18.5s	Ir202 8.5s	Ir203 3.08s	Ir204 0.406s	Ir205 0.296s	Ir206 0.321s	Ir207 0.187s	Ir208 0.208s	Ir209 0.124s						
76	Os200 16s	Os201 2.44s	Os202 2.38s	Os203 0.316s	Os204 0.202s	Os205 0.243s									
75	Re199 1.94s	Re200 1.23s	Re201 0.535s	Re202 0.116s	Re203 0.0905s	Re204 0.114s									

Figure 6: Predicted (white squares)  $\beta$ -decay half-lives for the neutron-rich  $N \sim 126$  region [9].

83	Bi193 1.12m	Bi194 1.92m	Bi195 3.05m	Bi196 5.13m	Bi197 9.33m	Bi198 11.6m	Bi199 27m	Bi200 36.4m	Bi201 1.8h	Bi202 1.72h	Bi203 11.76h	Bi204 11.22h	Bi205 15.31d	Bi206 6.243d	Bi207 31.55y
82	Pb192 3.5m	Pb193 5.8m	Pb194 10m	Pb195 15m	Pb196 37m	Pb197 43m	Pb198 2.4h	Pb199 1.5h	Pb200 21.5h	Pb201 9.33h	Pb202 5.25e+04v	Pb203 2.161d	Pb204 1.4	Pb205 1.53e+07v	Pb206 24.1
81	Tl191 5.22m	Tl192 10.9m	Tl193 21.6m	Tl194 33m	Tl195 1.16h	Tl196 1.84h	Tl197 2.94h	Tl198 5.3h	Tl199 7.42h	Tl200 1.09d	Tl201 3.038d	Tl202 12.23d	Tl203 29.52d	Tl204 3.78y	Tl205 70.476
80	Hg190 20m	Hg191 50.8m	Hg192 4.85h	Hg193 11.8h	Hg194 520v	Hg195 1.73d	Hg196 0.15	Hg197 2.706d	Hg198 9.97	Hg199 16.87	Hg200 23.1	Hg201 13.18	Hg202 29.8s	Hg203 45.61d	Hg204 6.87
79	Au189 29.7m	Au190 42.9m	Au191 3.19h	Au192 4.94h	Au193 17.65h	Au194 1.584d	Au195 186.1d	Au196 6.167d	Au197 100	Au198 2.695d	Au199 3.139d	Au200 18.7h	Au201 26.4m	Au202 28.8s	Au203 1m
78	Pt188 10.2d	Pt189 10.87h	Pt190 0.014	Pt191 2.862d	Pt192 0.782	Pt193 50v	Pt194 32.967	Pt195 33.832	Pt196 25.242	Pt197 19.89h	Pt198 7.163	Pt199 30.8m	Pt200 12.5h	Pt201 2.5m	Pt202 1.8d
77	Ir187 10.5h	Ir188 1.73d	Ir189 13.2d	Ir190 11.78d	Ir191 37.3	Ir192 241v	Ir193 62.7	Ir194 171d	Ir195 3.8h	Ir196 1.4h	Ir197 8.9m	Ir198 8s	Ir199 1.61m	Ir200 19.3s	Ir201 18.5s
76	Os186 1.59	Os187 1.96	Os188 13.24	Os189 16.15	Os190 26.26	Os191 15.4d	Os192 40.78	Os193 1.295d	Os194 6v	Os195 6.5m	Os196 34.9m	Os197 1.36m	Os198 45.5s	Os199 17.2s	Os200 16s
75	Re185 37.4	Re186 2e+05v	Re187 62.6	Re188 17.02h	Re189 1.013d	Re190 3.2h	Re191 9.8m	Re192 16s	Re193 1.09m	Re194 16.1s	Re195 18.3s	Re196 5.13s	Re197 6.02s	Re198 2.17s	Re199 1.94s
74	W 184 30.64	W 185 75.1d	W 186 28.43	W 187 23.72h	W 188 69.4d	W 189 11.5m	W 190 30m	W 191 1.16m	W 192 36.6s	W 193 21s	W 194 8.08s	W 195 6.16s	W 196 4.79s	W 197 2.15s	W 198 1.32s
73	Ta183 5.1d	Ta184 8.7h	Ta185 49.4m	Ta186 10.5m	Ta187 1.82m	Ta188 24.1s	Ta189 34.7s	Ta190 8.51s	Ta191 9.52s	Ta192 4.42s	Ta193 2.86s	Ta194 1.9s	Ta195 1.62s	Ta196 0.768s	Ta197 0.577s
72	Hf182 0.9e+06v	Hf183 1.067h	Hf184 4.12h	Hf185 3.5m	Hf186 2.6m	Hf187 11.7s	Hf188 8.39s	Hf189 5.39s	Hf190 4.2s	Hf191 2.62s	Hf192 1.22s	Hf193 1.04s	Hf194 0.726s	Hf195 0.454s	
71	Lu181 3.5m	Lu182 18m	Lu183 58s	Lu184 18s	Lu185 6.75s	Lu186 3.88s	Lu187 4.96s	Lu188 2.11s	Lu189 2.16s	Lu190 1.13s	Lu191 0.65s	Lu192 0.625s	Lu193 0.475s	Lu194 0.298s	
70	Yb180 2.4m	Yb181 20.3s	Yb182 5.78s	Yb183 7.23s	Yb184 2.55s	Yb185 1.75s	Yb186 1.52s	Yb187 0.821s	Yb188 0.734s	Yb189 0.506s	Yb190 0.299s				
69	Tm179 4.88s	Tm180 3.38s	Tm181 1.87s	Tm182 2.01s	Tm183 0.793s	Tm184 0.594s	Tm185 0.559s	Tm186 0.349s	Tm187 0.319s	Tm188 0.249s	Tm189 0.182s				
68	Er178 1.64s	Er179 1.65s	Er180 0.8s	Er181 0.984s	Er182 0.321s	Er183 0.303s	Er184 0.261s	Er185 0.21s							
67	Hol77 0.711s	Hol78 0.607s	Hol79 0.35s	Hol80 0.403s	Hol81 0.171s	Hol82 0.167s	Hol83 0.15s	Hol84 0.13s							

Figure 7 Predicted (white squares)  $\beta$ -half-lives for the  $^{190}\text{W}$  Region [9].



$\beta$ -Decay Lifetimes,  $\beta^-$ -Delayed Spectroscopy Studies and  
Collective Evolution ‘South’ of  $^{208}\text{Pb}$

J. Benlliure, D. Cortina Gil, T. Kurtukian Nieto, E. Casarejos  
*Universidade de Santiago de Compostela, Spain*

P.H. Regan, Zs. Podolyák, P.M. Walker, W. Gelletly, W.N. Catford, P.D. Stevenson, S.J. Williams,  
A.B. Garnsworthy, N.J. Thompson, Z. Liu, S.F. Ashley  
*Department of Physics, University of Surrey, Guildford, GU2 7XH, UK*

J. Jolie, N. Warr, A. Richard, A. Scherillo  
*IKP, University of Cologne, 50937 Cologne, Germany*

J. Gerl, M. Gorska, P. Bednarczyk, H.J. Wollersheim  
*Planckstrasse 1, GSI, Germany*

R. Krücken  
*TU Muenchen, Germany*

M. Pfützner  
*Warsaw University, Poland*

H. Mach  
*Uppsala University, Sweden*

R.D. Page  
*Dept. of Physics, University of Liverpool, UK*

S.J. Freeman, D.M. Cullen  
*Dept. of Physics and Astronomy, University of Manchester, UK*

J. Simpson, D.D. Warner  
*CLRC Daresbury Laboratory, Cheshire, UK*

D. Balabanski, K. Gladnishki  
*University of Camerino, Italy*

A. Jungclaus, L. Caceres  
*Universidad Autonoma de Madrid, Spain*

**Abstract:** *We propose to measure  $\beta$ -decay lifetimes and study the internal structure of heavy, neutron-rich nuclei with  $Z < 82$  and  $N < 126$  produced following ‘cold-fragmentation’ reactions between a  $^{208}\text{Pb}$  beam and a  $^9\text{Be}$  production target. The GSI Fragment Separator will be used with a monoenergetic degrader, allowing the selection of specific elemental residues in a position-sensitive, three-element DSSSD active stopper. The subsequent  $\beta$ -decays of the neutron-rich reaction products (with decay lifetimes in the seconds range) will be temporally and position correlated with the implanted ions to provide unambiguous channel selection for subsequent  $\gamma$ -ray spectroscopic measurements in the daughter using the RISING array in its Stopped Beam configuration. Decays from microsecond isomeric states will also be measured from the primary reaction fragments implanted in the active stopper to provide internal calibrations for the particle identification. The  $\beta$ -delayed  $\gamma$ -ray spectroscopy following the decays of a number of odd-odd nuclei will also provide new nuclear structure information on the evolution of collective structures and nuclear shape/phase transitions with increasing proton and neutron hole valency from  $^{208}\text{Pb}$ .*

## Introduction

The understanding of how shell structure evolves with varying proton or neutron excess (compared with the isotopes along the valley of stability) represents a major current theme in nuclear physics. Nuclei lying close to the stability line exhibit structural effects associated with the well established spherical shell closures at the magic proton and neutron numbers of 2, 8, 20, 28, 50, 82, 126 etc. However, by exploring the properties of neutron-rich nuclei it is now known that this standard shell structure can be subject to dramatic rearrangements. Plausible evidence for the shell melting or ‘quenched’ of magic neutron numbers has been reported for  $N=8,20,28,50$  and even 82 [1].

The  $^{208}\text{Pb}$  nucleus, with 82 protons and 126 neutrons, represents a classic *doubly magic* closed-shell nucleus. One of the aims of the current proposal is to address the question of the robustness of the  $N=126$  neutron shell closure with reduced proton number. This will be tested by studying the electric quadrupole ( $E2$ ) polarisability and nuclear shape responses as protons or neutrons are removed from  $^{208}\text{Pb}$  and by investigating the  $\beta$ -decay lifetimes of nuclei in this region. As the proton-neutron valence product ( $N_\pi \cdot N_\nu$ ) increases away from  $^{208}\text{Pb}$  one expects to observe the development of collective excitations and associated ground state quadrupole ( $\beta_2$ ) deformation [2]. These collective quadrupole effects are expected to approach a maximum at the doubly mid-shell valence maximum nucleus,  $^{170}\text{Dy}$  [3].

Very little spectroscopic information is currently available on the neutron-rich nuclei ‘south’ of  $^{208}\text{Pb}$  i.e., proton-hole states in the  $^{208}\text{Pb}$  core. Such data are vital to pin down the basic shell model interactions in this region. Information on excited states for  $N=126$  isotones with  $Z<82$  is available only for the  $Z=81$  and 80 isotones,  $^{207}\text{Tl}$  [4] and  $^{206}\text{Hg}$  [5], while in  $^{205}\text{Au}$  ( $Z=79$ ) only the ground state has been identified [6]. The large  $\gamma$ -ray detection efficiency available using the Stopped Beam RISING array will permit new spectroscopic information in this largely unexplored region following both (i) decays from isomeric states and, of specific relevance to the current proposal, (ii) following  $\beta^-$ -decays to populate excited states in exotic, neutron-rich daughter nuclei. As demonstrated by our previous work which utilised fragmentation isomer spectroscopy of heavy nuclei, useful information can be obtained even when the exotic nuclei have transmission rates through the fragment separator of only a few per hour [7-9]. This opens up the possibility of probing this extreme part of the nuclear chart for the first time.

		N							
			p3/2	p1/2	p3/2	f5/2	p1/2		
		113	115	117	119	121	123	125	
81		194Tl 2-, 33m	196Tl 2-, 2h	198Tl 2-, 5h	200Tl 2-, 26h	202Tl 2-, 12d	204Tl 2-, 3.8y	206Tl 0-, 4.2m	s1/2
79		192Au 1-, 4h	194Au 1- 38h	196Au 2-, 6d	198Au 2-, 3d	200Au (1-), 48m	202Au (1-), 29s	204Au 2-, 40s	d3/2
77		190Ir 4+ 12d	192Ir 1- 1.5m 4+ 73d	194Ir 1-, 19h	196Ir (0-), 52s	198Ir (0-) 8s	I 200Ir 13s	202Ir 9s	d3/2
75		188Re 1-, 17h	190Re (2-) 3m	192Re 16s	I 194Re 16s	196Re 5s	198Re 2s		d3/2
73		186Ta (2,3) 10m	I 188Ta 24s	190Ta 9s	192Ta 4s	194Ta 2s			
71		184Lu ~20s	186Lu 4s	188Lu 2s	190Lu 1s				

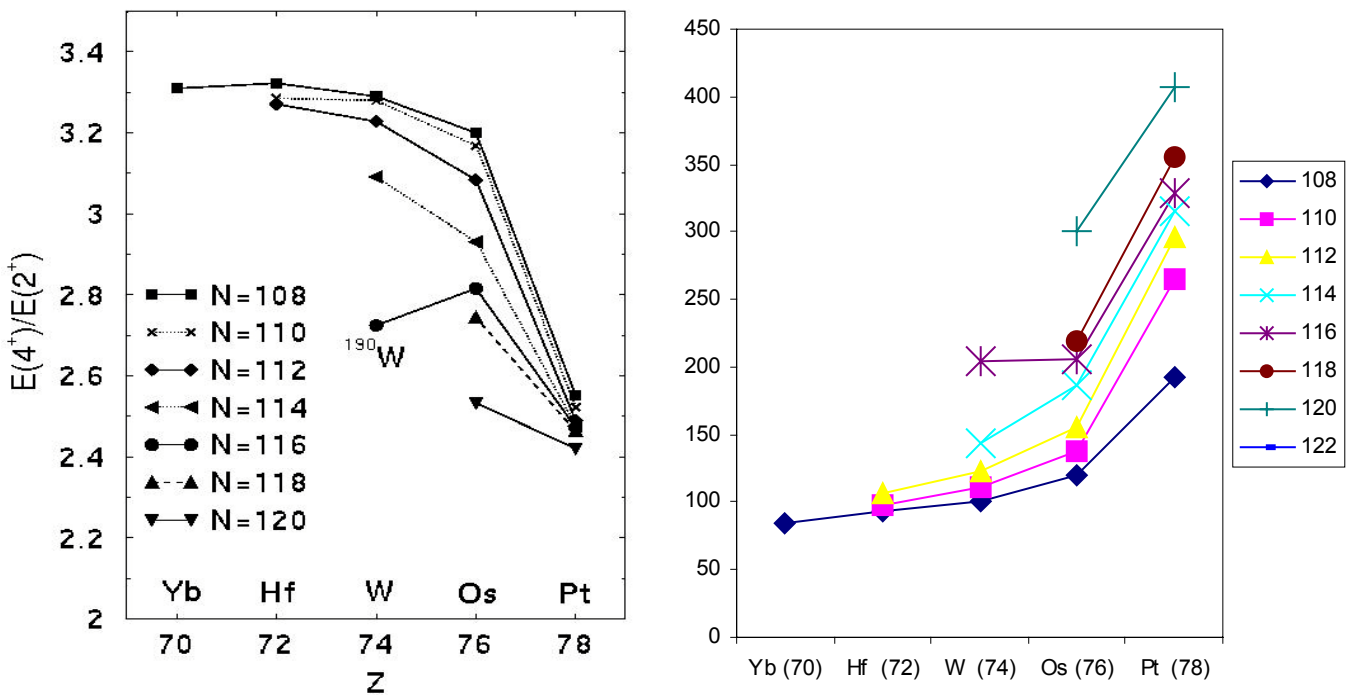
**Figure 4:** Odd-odd nuclei in the region of interest for the current proposal. The solid, thick, blue line separates regions of decay by  $\beta^+$  and  $\beta^-$  decay. The red, dotted line corresponds to the current limit of measured lifetimes for  $\beta^-$  decay. The italicised isotopes are the focus of the current study. The nominal, major single-particle orbital (from the ground state of the neighbouring odd-A isotope/isotones) is also shown as a guide for those nuclei closest to the doubly-magic  $^{208}\text{Pb}$  core. The symbol I corresponds to odd-odd nuclei where a micro-second isomer has been previously identified following  $^{208}\text{Pb}$  projectile fragmentation [8,9].

Figure 1 shows the experimentally observed [10] and theoretically predicted [11]  $\beta$ -decay half-lives for odd-odd mother nuclei in the region directly below the  $^{208}\text{Pb}$  closed shell, together with the assigned spin and parity of the mother nucleus. The general feature of these odd-odd systems is that they have low-spins (0,1,2) and negative parities, making the most likely mode of decay a first-forbidden decay to low-spin states ( $0^+$  and  $2^+$ ) in the even-even daughter nuclei. This means that in most cases, the  $\beta$ -delayed  $\gamma$ -ray decay flux would be expected to pass through the first excited  $2^+$  state (apart from cases of direct decay to the  $I^\pi=0^+$  ground state in the case of  $0^-$  spin/parities for the odd-odd mother system). One of the main thrusts of the current proposal is to use the decays of exotic, neutron-rich odd-odd nuclei to populate the even-even daughter systems and thereby study their internal structures. Simple signatures such as the energy of the first excited  $2^+$  state and the ratio of the energies of the first  $4^+$  to  $2^+$  state can be used to describe the global evolution of nuclear structure with changing nucleon number [2]. Discontinuities in these simple signatures can be used to highlight the presence of sub-shell closures or shape competition effects at the nuclear ground state (see later).

In addition to the information obtained following the decays into even-even systems, the decays between odd-A systems are extremely important in highlighting how the basic ‘spherical’ hole orbitals expected close to the  $^{208}\text{Pb}$  core (neutron  $i_{13/2}$ ,  $p_{3/2}$ ,  $p_{1/2}$ ,  $f_{7/2}$  and  $f_{5/2}$  and proton  $h_{11/2}$ ,  $s_{1/2}$ ,  $d_{5/2}$  and  $d_{3/2}$ ) evolve with the increasing configuration mixing and the associated increase in quadrupole collectivity.

### Shape Evolution With Increasing Hole-Hole Valency

Figure 2 shows the low-lying excitation energy systematics of even-even nuclei with  $N>108$  for the Yb ( $Z=70$ ) to Hg ( $Z=80$ ) isotopes. The data point associated with  $^{190}\text{W}$  has been deduced following our observation of a cascade populated via the  $I^\pi=(10^-)$  ‘K-isomer’ in this nucleus [9]. The clear discontinuity of this data point compared with its even-even neighbours is notable both in the ratio of the yrast  $4^+$  to  $2^+$  states and in the excitation energy of the first  $2^+$  level itself. This has been interpreted as possible evidence for a proton sub-shell closure in this heavy, neutron-rich region [9].



**Figure 5:** *Left:* Excitation energy ratio of the first  $2^+$  and  $4^+$  states in even-even Yb to Pt nuclei with  $N=108$  to  $120$ . *Right:* Excitation energies in keV of the first  $2^+$  states for the same nuclei. Note the discontinuity for the  $^{190}\text{W}$  data point in both of these plots [9].

An alternative explanation is the evolution of nuclear ground state deformation from a prolate to oblate shape around neutron number 116. This has long been predicted in the Osmium nuclei to occur

around  $^{194-6}\text{Os}$  [13-15], however the most recent data on the excited states of  $^{194}\text{Os}$  [14] suggests that this nucleus remains prolate in deformation in its low-energy excitations. Figure 3 shows Constrained Hartree-Fock calculations, of the type outlined in reference [15], for the ground state deformations in neutron-rich Hf, W and Os nuclei. These calculations also predict a change from prolate to (weakly-deformed) oblate ground state deformations between neutron numbers 114 and 116. Jolie and Linnemann [15] have suggested that these nuclei constitute a region of prolate-oblate *phase transition* between the well-deformed prolate systems and the weakly deformed oblate nuclei. These prolate and oblate shapes can be represented by the  $SU(3)$  and  $\overline{SU(3)}$  ( $'SU(3)\text{-bar}'$ ) dynamical symmetries in the Interacting Boson Approximation (IBA). The  $O(6)$  symmetry, which represents nuclei in the extreme  $\gamma$ -soft case of which  $^{196}\text{Pt}$  is the often quoted empirical example [16], can then be thought of as representing a nuclear phase transition or *critical point* [15]. The current proposal will allow an extension of the energy systematics of the first excited states in the even-even systems about these well defined symmetry limits. In particular it should provide the first information on the  $2^+$  energies in  $^{192}\text{W}$  and  $^{196}\text{Os}$ , as well as confirming the  $^{190}\text{W}$  and  $^{202}\text{Pt}$   $2^+$  assignments which both come from our previous isomer spectroscopy work.

In addition, the generally rather large  $Q_{\beta^-}$  values for the expected decays (typically between 3 and 5 MeV), should mean that some of the *non-yrast*, low-spin levels such as excited  $0^+$  states are also identified in the current work. These are of importance in the identification of such dynamical symmetry limits in the IBA.

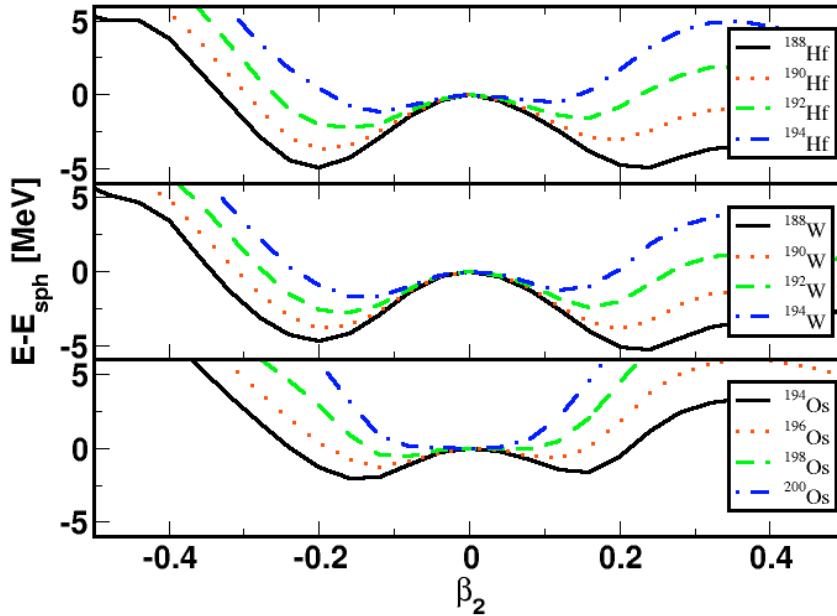


**Figure 6:** Constrained Hartree-Fock calculations using the separable monopole interaction, of the type described in reference [17], for the ground state configurations of neutron-rich Hf, W and Os nuclei of interest in the current proposal. Note the general trend to more a flat-bottom (spherical) potential for increasing neutron number and the evolution from prolate to oblate ground state deformations predicted for  $^{190}\text{Hf}$ ,  $^{192}\text{W}$  and  $^{196}\text{Os}$ .

## FRS SEPARATOR SETTINGS, COUNT RATE ESTIMATES AND BEAM TIME REQUEST

As in our previous work (experiment S227), we will use a monoenergetic degrader at S2. This has the dual advantage in the current proposal of both minimizing the dispersion in the implantation range for a given nuclear species in the active stopper, and providing a larger effective implantation surface at S4. This

effective defocussing of the secondary beam species minimises the implantation rate per pixel at the active stopper. Both of these aspects are crucial to the current experiment where correlation times up to the tens of seconds are expected between the implanted particle and its subsequent  $\beta^-$  decay. Following the initial analysis of our previous studies on the use of cold-fragmentation reactions to populate neutron-rich nuclei

using a 1 GeV per nucleon  $^{208}\text{Pb}$  beam on a  $^9\text{Be}$  target from experiment S227 (see figures 4 and 5), the production cross-sections for some of the nuclei of interest for spectroscopic study in the current proposal have been determined empirically. These compare well with the predictions of the COFRA simulations which have been used to provide the count rate estimate given below.

The current proposal aims to specifically investigate the decays into even-even systems from  $\beta^-$ -decay of their odd-odd, neutron-rich mothers. In particular, we aim to make studies centred on the following stopped ions, (i)  $^{203}\text{Au}$ ; (ii)  $^{201}\text{Ir}$ ; (iii)  $^{195}\text{Re}$ ; and (iv)  $^{191}\text{Ta}$ . The use of some initial  $2^+$  excitation energies in the even-even daughter nuclei for such settings (such as  $^{202,4}\text{Hg}$  [19],  $^{200,2}\text{Pt}$  [8] and  $^{190}\text{W}$  [9]) will be used to provide a validation of the experimental set-up. Note that in addition to the  $\gamma$ -ray spectroscopic information obtained for the even-even daughter nuclei, the apparent lifetimes of these characteristic decay  $\gamma$  rays observed relative to the implantation of the radioactive mother nucleus will give an extra (and extremely clean) method of determining the  $\beta^-$ -decay half-life of the parent.

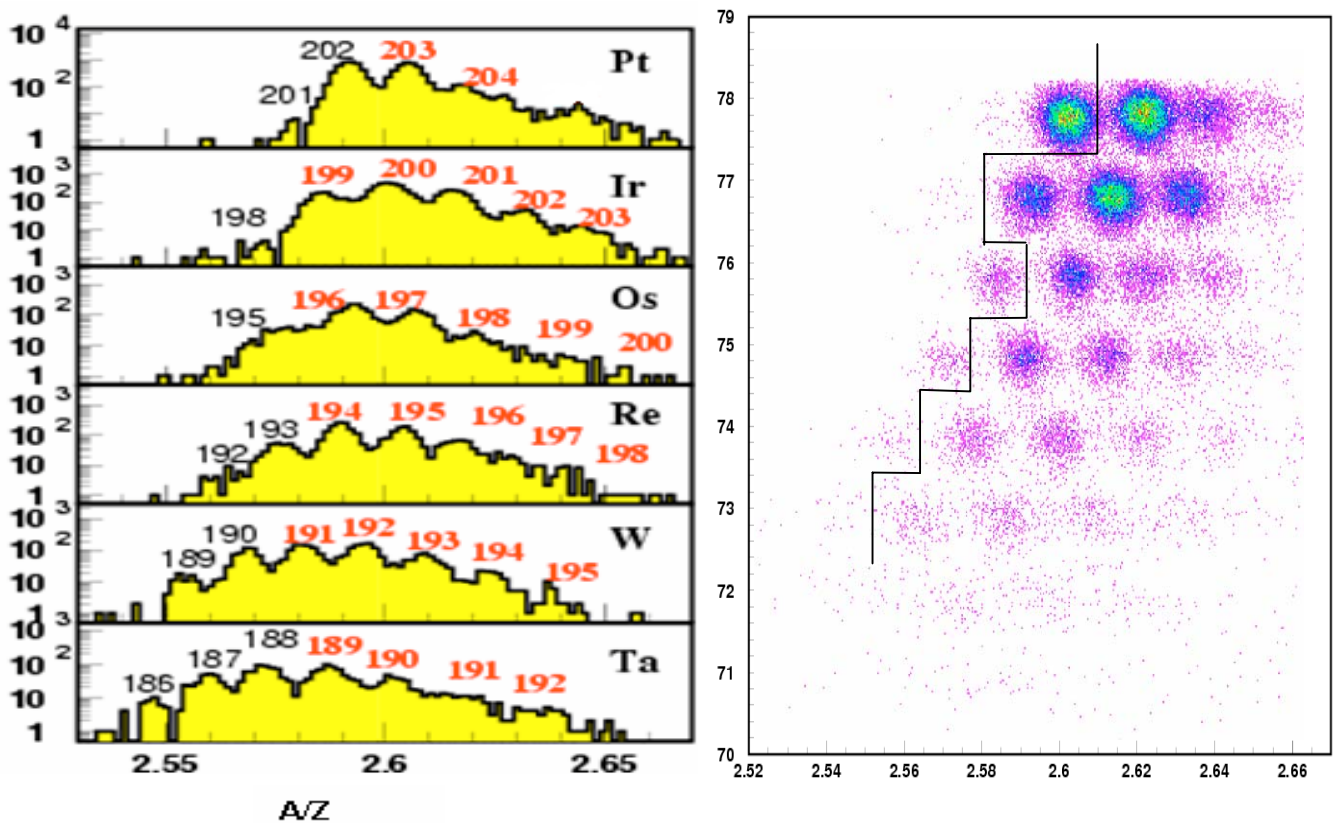


**Figure 4:** Particle identification projections from experiment S227 showing the population of some of the neutron-rich species below  $^{208}\text{Pb}$  following ‘cold’ fragmentation reactions [18]. The current proposal aims to specifically select settings centred on  $^{201}\text{Ir}$ ,  $^{195}\text{Re}$  and  $^{191}\text{Ta}$  all of which were identified in the previous work using the same production reaction.

Figure 5 shows the effect of running the FRS in monoenergetic mode in preferentially selecting specific elemental species to stop in the active stopper. The setting is set to be centred on  $^{198}\text{Ir}$  and these are stopped with high efficiency in the stopper. The (more heavily produced) higher-Z ions are stopped in the scintillator and degrader before the active stopper, while the lower-Z ions pass through the active stopper and are registered in the plastic veto detector placed directly behind. A similar set-up will be employed in the current proposal to select the species of interest in each run.

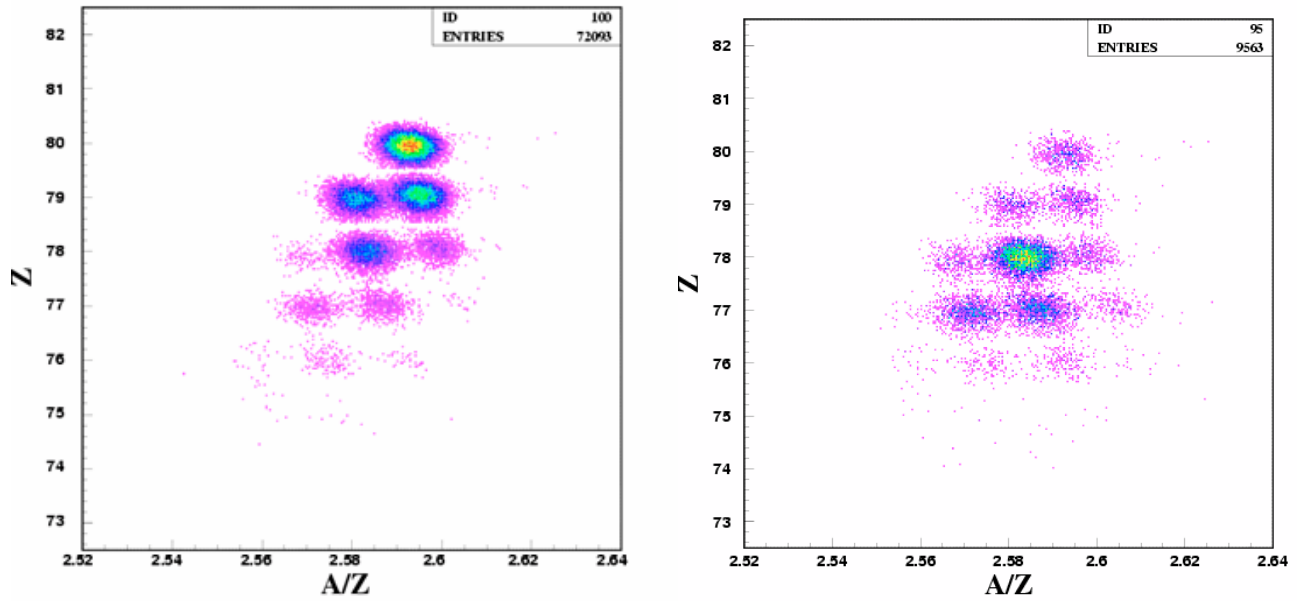


**Figure 5: Left:** Particle identification spectra for transmitted ions from the  $^{208}\text{Pb}$  fragmentation in experiment S227, centred on the transitions of  $^{198}\text{Ir}$  ions. production and implantation PID plots. **Right:** as left, but with condition that ions implanted in 1mm DSSSD active stopper.

Detailed simulations have been done for 3 settings assuming a 1 GeV per nucleon  $^{208}\text{Pb}$  beam incident on a  $2.5\text{ g/cm}^2$  Be target with a  $5.1\text{ g/cm}^2$  degrader and a total beam intensity of  $10^9$  particles per spill (3 second spill, 10 second cycle time). The predicted production rates per 8 hour shift are then:

**Setting 1: Centred on  $^{201}\text{Ir}$ :** Total Rate = 213 / spill  
 $^{204}\text{Hg}$ : 84,000       $^{203}\text{Hg}$ : 770,000       $^{202}\text{Hg}$ : 4,500,000  
 $^{200}\text{Ir}$ : 580,000       $^{201}\text{Ir}$ : 190,000       $^{202}\text{Ir}$ : 16,000  
 $^{198}\text{Os}$ : 61,000       $^{199}\text{Os}$ : 31,000       $^{200}\text{Os}$ : 5,900

Note that the total implantation rate for Setting 1 means that the primary beam current will be reduced by a factor of three to allow correlations between the implanted ions and subsequent  $\beta$  decays.

**Setting 2: Centred on  $^{195}\text{Re}$ :** Total Rate = 58 / spill  
 $^{196}\text{Os}$ : 710,000       $^{197}\text{Os}$ : 270,000       $^{198}\text{Os}$ : 60,000  
 $^{194}\text{Re}$ : 280,000       $^{195}\text{Re}$ : 120,000       $^{196}\text{Re}$ : 26,000  
 $^{192}\text{W}$ : 120,000       $^{193}\text{W}$ : 50,600       $^{194}\text{W}$ : 13,000

**Setting 3: Centred on  $^{191}\text{Ta}$ :** Total Rate = 8.7 / spill  
 $^{193}\text{W}$ : 57,000       $^{194}\text{W}$ : 12,000       $^{195}\text{W}$ : 1,300  
 $^{190}\text{Ta}$ : 63,000       $^{191}\text{Ta}$ : 29,000       $^{192}\text{Ta}$ : 6,090  
 $^{187}\text{Hf}$ : 33,000       $^{188}\text{Hf}$ : 30,000       $^{189}\text{Hf}$ : 15,000       $^{190}\text{Hf}$ : 3,900

Assuming a typical 50% implantation rate of the ions of interest, a conservative estimate of 20% for the absolute photopeak gamma-ray efficiency (for 662 keV), 50% effective  $\beta^-$ -detection efficiency and a 100% population of the first  $2^+$  in the daughter nucleus following  $\beta^-$ -decay, this leads to an absolute combined  $\gamma$  and  $\beta$  coincidence detection efficiency of 5% ( $0.5 \times 0.5 \times 0.2 = 5\%$ ).

Assuming this, the yields estimates for the number of photopeak  $\gamma$  rays to be observed for the  $2^+ \rightarrow 0^+$  transitions identified in the specific even-even nuclei per shift are as follows:

Setting 1:  $^{200}\text{Pt} = 9,666$  ;  $^{202}\text{Pt} = 267$  ( for a primary beam intensity reduced to  $3 \times 10^9$  per spill)  
Setting 2:  $^{194}\text{Os} = 14,000$  ;  $^{196}\text{Os} = 1,300$   
Setting 3:  $^{190}\text{W} = 3,150$  ;  $^{192}\text{W} = 350$

On the basis of these estimates and to enable a minimum of 1,500 counts in the photopeak for the most exotic even-even daughter in the setting, we request the following time

Setting 1: 2 day (6 shifts)  
Setting 2: 1 day (3 shifts)  
Setting 3: 2 days (6 shifts)

We also request 2 days (6 shifts) for beam preparation and calibration of the FRS. This leads to a total beam time request of 21 shifts (7 days).

## REFERENCES:

- [1] I. Dillmann et al., *Phys. Rev. Lett.* **91** (2003) 162503.
- [2] R.F. Casten, *Nucl. Phys.* **A443** (1985) 1; R.F. Casten and N.V. Zamfir *Phys. Rev. Lett.* **70** (1993) 402
- [3] P.H. Regan et al., *Phys. Rev.* **C65** (2002) 037302
- [4] D. Eccleshall, M.J.L.Yates, *Phys. Lett.* **19** (1965) 301
- [5] B. Fornal et al., *Phys. Rev. Lett.* **87** (2001) 212501
- [6] Ch. Wennemann et al., *Z.Phys.* **A347** (1994) 185; F.G. Kondev, *Nucl. Data Sheets* **101** (2004) 521
- [7] M. Pfützner et al., *Phys. Lett.* **444B** (1998) 32
- [8] M. Caamano et al., *Eur. Phys. Jour.* **A23** (2005) 201
- [9] Zs. Podolyák et al., *Phys. Lett.* **B491** (2000) 225
- [10] Table of Isotopes, 8<sup>th</sup> Edition Volume II, Richard B. Firestone and Virginia S. Shirley, John Wiley & Sons, New York (1996)
- [11] T. Tachibana and M. Yamada, *Proc. Int. Conf.on Exotic Nuclei and Masses*, Arles (1995) p763 and <http://www.ndc.tokai.jaeri.go.jp/CN04/inex.html>
- [12] J. Benlliure et al., *Nucl. Phys.* **A660** (1999) 87
- [13] A. Ansari *Phys. Rev.* **C33** (1986) 321
- [14] C. Wheldon et al., *Phys. Rev.* **C63** (2001) 011304
- [15] J. Jolie and A. Linneman, *Phys. Rev.* **C68** (2003) 031301(R)
- [16] R.F. Casten & J.Cizewski, *Phys. Lett.* **185B** (1987) 293
- [17] P. Stevenson et al., *Phys. Rev.* **C63** (2001) 054309
- [18] J. Benlliure, T. Kertukian Nieto et al., *to be published*
- [19] D.A. Craig and H.W. Taylor, *J. Phys. G: Nucl. Phys.* **10** (1984) 1133

Nuclear Dynamical Symmetries and Shape Evolution in  
K-isomeric Nuclei from  $^{190}\text{W}$  to the  $^{170}\text{Dy}$  Valence Maximum.

P.H. Regan, Zs. Podolyák, P.M. Walker, W. Gelletly, W.N. Catford, P.D. Stevenson, S.J. Williams,  
A.B. Garnsworthy, N.J. Thompson, Z. Liu, S.F. Ashley  
*Department of Physics, University of Surrey, Guildford, GU2 7XH, UK*

J. Benlliure, D. Cortina-Gil, T. Kurtukian Nieto, E. Casarejos  
*University of Santiago de Compostela, Spain*

J. Jolie, N. Warr, A. Richard, A. Scherillo  
*IKP, University of Cologne, 50937 Cologne, Germany*

J. Gerl, M. Gorska, P. Bednarczyk, H.J. Wollersheim  
*Planckstrasse 1, GSI, Germany*

M. Pfützner  
*Warsaw University, Poland*

H. Mach  
*Uppsala University, Sweden*

J. Simpson, D.D. Warner  
*CLRC Daresbury Laboratory, Cheshire, UK*

D. Balabanski, K. Gladnishki  
*University of Camerino, Italy*

S.J. Freeman, D.M. Cullen  
*University of Manchester, UK*

J.J. Carroll  
*Youngstown State University, Ohio, USA*

*Abstract:* We will use isomer and  $\beta^-$ -delayed  $\gamma$ -ray spectroscopy to obtain new spectroscopic information on a host of very neutron-rich nuclei which will map out the central region of K-isomerism in rare-earth and transitional elements. The proposal consists of two main threads: (i) The use of K-isomerism as a probe of predicted prolate-to-oblate shape change in heavy, neutron-rich rare-earth nuclei around neutron  $N=116$ ; and (ii) The investigation of the proton-neutron valence product ( $N_\pi \cdot N_\nu$ ) maximum nucleus,  $^{170}\text{Dy}$ . The structure of  $^{170}\text{Dy}$  is of unique interest as it is potentially the best example of both K-isomerism and the dynamical  $SU(3)$  symmetry in atomic nuclei.

**Shape Evolution and the Limits of K-isomerism:  $^{188}\text{Hf}$**

The structure of well-deformed nuclei in the Ytterbium ( $Z=70$ ) to Osmium ( $Z=76$ ) region is characterised by the presence of K-isomeric states [1]. These correspond to broken pairs of orbitals whose large angular momentum projections on the axis of nuclear shape symmetry,  $\Omega$ , add together to give rise to states of high-K (where  $K=\Sigma_i \Omega_i$ ) which are hindered in their decay to the, usually lower-K values, of low-lying excitations in the same nucleus. The most favoured conditions for the formation of K isomers arise in deformed nuclei when the neutron and proton Fermi levels are mid-to-high in their respective single-

particle shells. Proton numbers around  $Z=72$  (Hafnium) are strongly favoured, as are neutron numbers around  $N=116$ . However, access to nuclei with optimal values of *both*  $N$  and  $Z$  requires the study of neutron-rich nuclei that to date, have been experimentally inaccessible.

The centre of  $K$  isomerism in the neutron-rich domain is expected to be located in the vicinity of the  $Z=72$  and  $N=116$  nucleus  $^{188}\text{Hf}$  [2] which, following the above discussion, may be coined ‘doubly- $K$  magic’. The neutron-rich nature of this nucleus and its neighbours means that, to date, this central region of  $K$  isomerism has not yet been studied in detail. We propose to investigate the internal structure of  $^{188}\text{Hf}$ , focussing on both its excited collective rotational states and non-collective multi-quasiparticle structures.  $K$  isomers provide real insight into the robustness or ‘stiffness’ of the quadrupole deformations of both the isomeric state and the level(s) to which it decays. They also serve as an excellent spectroscopic tool providing access to excited states in these very neutron-rich nuclei where dramatic prolate-to-oblate shape changes may manifest themselves [3,4]. For  $^{188}\text{Hf}$  both neutron ( $K^\pi=10^-$ ) and proton ( $K^\pi=8^-$ ) high- $K$  couplings are predicted to be energetically favoured [2]. Experimentally, the clearest observable is predicted to be the decay of the proton  $K^\pi=8^-$  isomer into the ground state ( $K^\pi=0^+$ ) band. This decay is observed in the less neutron-rich even-even Hafnium isotopes from  $^{180-184}\text{Hf}$ . The  $K^\pi=8^-$  state decay half-life reduces from 5 hours in  $^{180}\text{Hf}$  [5]; to 1 hour in  $^{182}\text{Hf}$  [6]; and to 48 seconds in  $^{184}\text{Hf}$  [7]. Half-lives in the few seconds range are anticipated for the decay of the  $K^\pi=8^-$  two quasi-proton isomers in  $^{186}\text{Hf}$  and  $^{188}\text{Hf}$ , in part due to their (expected) reduced deformation compared with the lighter isotopes. Note that  $\beta^-$ -decay directly from the  $K$ -isomeric states in these neutron-rich nuclei is potentially an additional mode of de-excitation. An active stopper, which could in principle be used to measure  $\beta$ - $\gamma$  coincidences which follow the decay of these isomers is thus necessary for the temporal correlation of such decays with the identified  $^{188}\text{Hf}$  fragments.

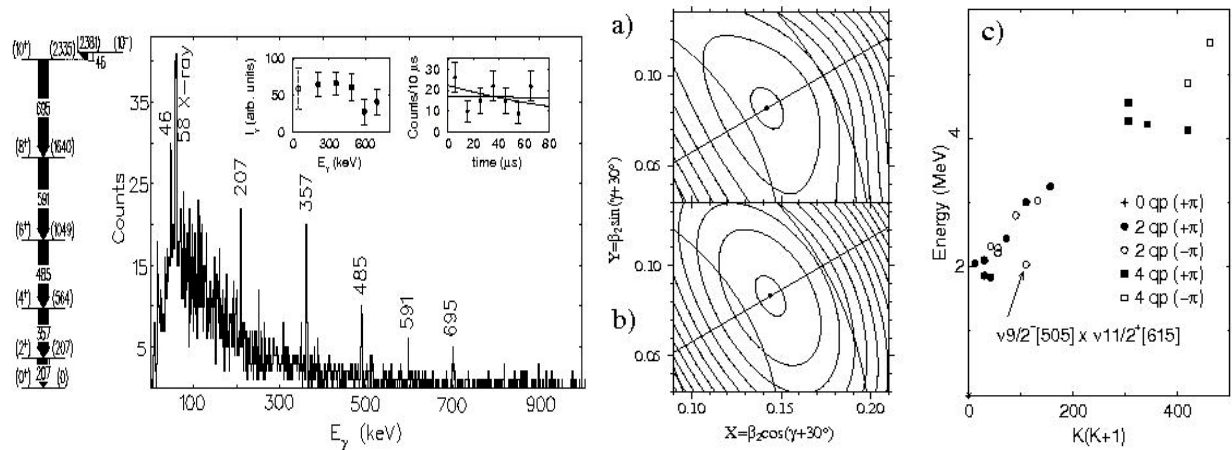


**Figure 7:** (Left) Isomer-spectroscopy spectrum showing the decay of the  $K^\pi=10^-$  isomer in the  $N=116$  isotone,  $^{190}\text{W}$ . (Centre) Potential Energy Surface (PES) calculations for the ground state (a) and  $K=10^-$  isomer configuration in this nucleus. (Right) Blocked Nilsson quasi-particle calculations [8] for  $^{190}\text{W}$  with BCS pairing showing the prediction of the favoured  $K^\pi=10^-$  two-quasi-neutron state in this system which is the proposed basis for the isomer in  $^{190}\text{W}$ . These figures are all taken from reference [3].

The internal decays from these proposed isomeric states can also be used to populate the yrast ground state band in the same nucleus. Figure 1 shows the decay of the proposed  $K^\pi=10^-$  isomer in  $^{190}\text{W}$  which was identified in our previous work following the projectile fragmentation of a 1 GeV per nucleon  $^{208}\text{Pb}$  beam at GSI [3,9]. The proposed yrast sequence of this nucleus, as deduced from that work, suggested a change in structure compared to the heavier isotones. As figure 2 shows, by plotting the ratio of excitation energies of the lowest lying  $4^+$  and  $2^+$  states in the even-even nuclei of the  $A\sim 175-195$  region, a clear change in structure appears is evident for  $^{190}\text{W}$ . Assuming a simple harmonic vibrator and static deformed rotor picture, a perfect axially symmetric quadrupole deformed nucleus should have a value of 3.33 for this ratio, with an ideal harmonic vibrational sequence giving a ratio closer to 2.0 [10]. The apparent reduction in this ratio for  $^{190}\text{W}$  compared to its  $N=116$  isotone  $^{192}\text{Os}$  is particularly unusual since  $^{190}\text{W}$  has a larger number of valence holes compared to  $^{192}\text{Os}$  ( $N_\pi \cdot N_v = 8 \times 10 = 80$  for  $^{190}\text{W}$  and  $6 \times 10 = 60$  for  $^{192}\text{Os}$ ). This increase

in valence product is usually associated with an increase in quadrupole collectivity [10]. Thus, one would naively expect an increase in the  $E(4^+)/E(2^+)$  energy ratio towards the rotational limit, as is observed in the  $N=108,110,112$  and  $114$  isotonic chains. The *reduction* for this ratio associated with  $^{190}\text{W}$  may possibly represent a new sub-shell effect which is present only for specific neutron numbers (greater than  $114$ ) [3] or alternatively with a shape change in the ground state deformations of the nuclei in this region [4]. One of the aims of the current proposal is to study the lighter,  $N=116$  isotones,  $^{188}\text{Hf}$  and  $^{186}\text{Yb}$ , to see whether this bifurcation trend continues with increasing neutron excess, or is simply a local phenomenon associated only with  $^{190}\text{W}$ .

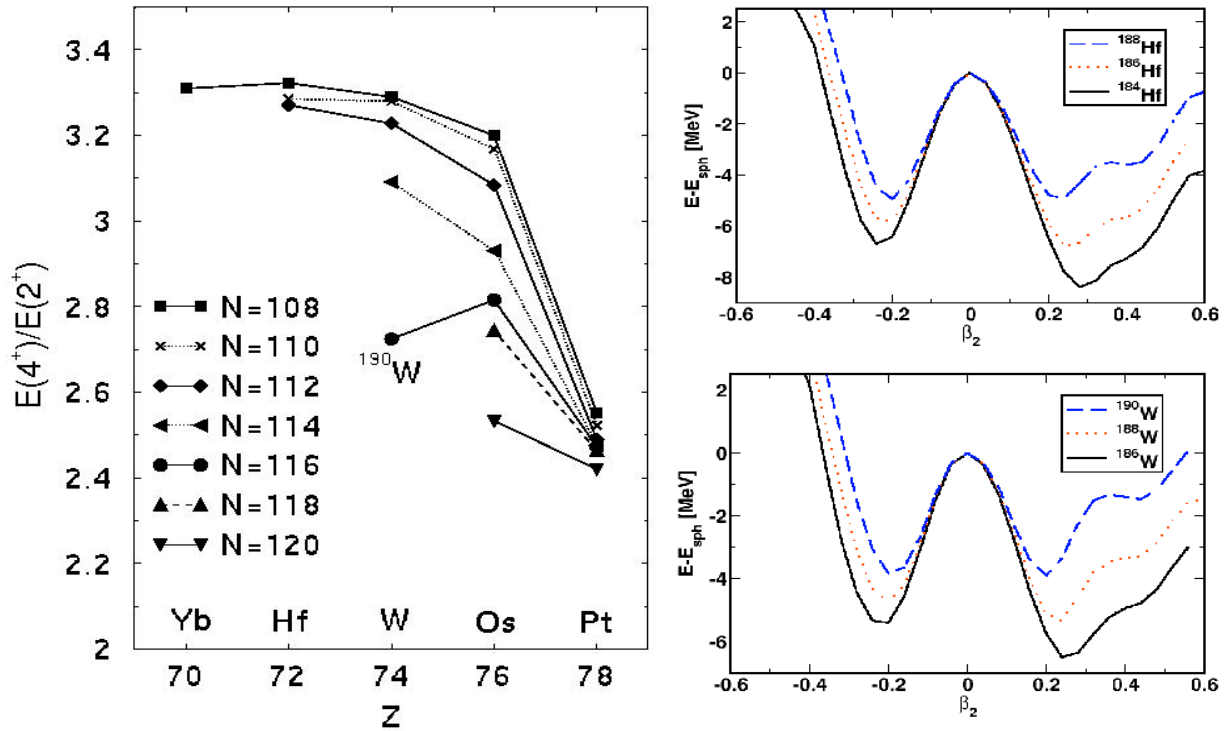


**Figure 8:** (Left) Experimentally deduced  $E(4^+)/E(2^+)$  ratios for even-even nuclei in the Yb-Pt region. Note the bifurcation of the plot for the new data point at  $^{190}\text{W}$ . (Right) Constrained Hartree-Fock calculations using a separable monopole interaction [11] calculations for the evolution of ground state deformation in Hf (upper) and W (lower) isotopes with neutron numbers  $N=112,114$  and  $116$ .

The current proposal will aim to identify the first  $2^+$  states in  $^{192}\text{W}$ ,  $^{188,190}\text{Hf}$  and  $^{186,188}\text{Yb}$ . It is intended that these nuclei will be populated both by direct projectile fragmentation of a  $^{198}\text{Pt}$  beam and also following the  $\beta^-$ -delayed spectroscopy of their odd-odd mother nuclei  $^{192}\text{Ta}$ ,  $^{188,190}\text{Lu}$  and  $^{186,188}\text{Tm}$ . Each of the even-even systems are predicted to have similar  $K^\pi=10^-$  isomeric states associated with the  $9/2^- [505] \times 11/2^+ [615]$  two-quasi-neutron configuration. In addition the Hafnium isotopes are expected to have favoured  $K^\pi=8^-$  2-quasi-proton isomers which are likely to directly feed the ground-state bands in these nuclei. The lifetimes of the predicted isomers depends on the purity of the  $K$  values of both the isomeric state and the ground state configuration to which it decays. The right side of figure 2 shows Constrained Hartree-Fock calculations of the type described in reference [11]. These calculations show the predicted ground state deformations in Hf and W isotopes with neutron numbers  $N=112, 114$  and  $116$  and suggest a change in deformation from pure prolate to competing prolate/oblate when going from neutron number  $114$  to  $116$ . This should be reflected both in the excitation energy of the first  $2^+$  states and also in the transition rate between the prolate  $K$ -isomer and the oblate/prolate mixed ground state configuration.

### Valence Maximum at $^{170}\text{Dy}$ : Nature's Most Axially Symmetric Deformed Nucleus?

Nuclear ground-state collectivity requires many interacting particles and/or holes and is thus usually found in regions away from the standard spherical magic numbers. By this simple argument, the most collective nuclei should be found in the *doubly mid-shell* regions, halfway between successive proton and neutron major shell closures. Our calculations [12,13] predict that the doubly mid-shell system,  $^{170}\text{Dy}$ ,

exhibits an unusually rigid quadrupole deformation, implying an exceptional purity of the  $K$  quantum number. The purity of the  $K$  value associated with states in such deformed systems provides an insight into the constancy or ‘goodness’ of axial symmetry of the nucleus. Assuming the standard spherical magic numbers at  $N, Z = 50, 82$  and  $126$ ,  $^{170}\text{Dy}$  ( $Z=66, N=104$ ) is the *only* even-even doubly mid-shell system with  $A>100$  which can realistically be reached experimentally. No excited states are currently known in  $^{170}\text{Dy}$ . Indeed, its ground state has only been tentatively observed in our previous fragmentation reaction work at GSI [9]. There is a general paucity of nuclear data in this region, which is at the very edges of possible population by asymmetric fission. The heaviest Dy isotope for which any spectroscopic information is currently known is the  $N=102$  case of  $^{168}\text{Dy}$ , as reported by Asai et al.[14]. This was populated following the  $\beta^-$ -decay of the odd-odd  $^{168}\text{Tb}$  mother nucleus ( $T_{1/2} = 8$  seconds) and identified the excitation energy of the first  $2^+$  state together with a candidate for the  $4^+ \rightarrow 2^+$  transition. Figure 3a shows the first  $2^+$  excitation energies and  $E(4^+)/E(2^+)$  ratios for the Dysprosium isotopes. The lowest transition energy is observed at the  $N=98$  case of  $^{166}\text{Dy}$  which has been suggested as evidence for a maximum deformation and collectivity in these isotopes before the  $N=104$  midshell [15]. However, the data point for  $^{168}\text{Dy}$  suggested a continuing trend towards the perfect rotor limit for the energy ratio of 3.33 with increasing neutron number towards  $^{170}\text{Dy}$ .

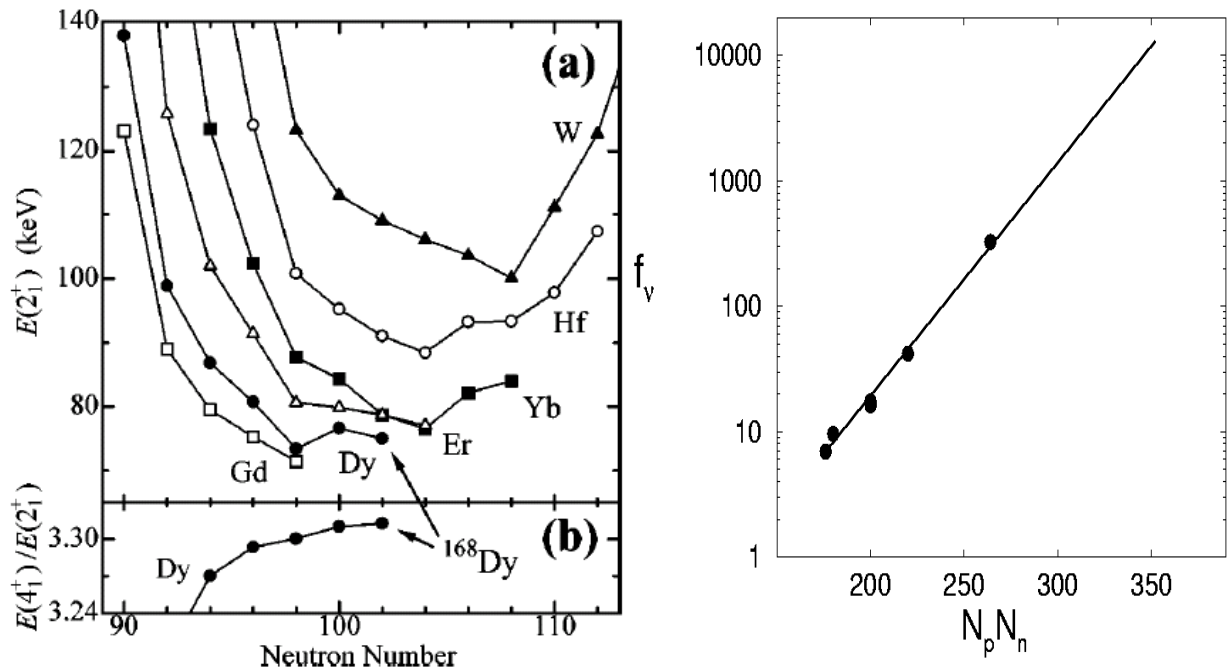


**Figure 9:** (Left) (a) Level energies of first  $2^+$  states in even-even Gd, Dy, Er, Yb, Hf and W isotopes. (b) Energy ratios between the first  $4^+$  and  $2^+$  states for even-even dysprosium isotopes, taken from reference [14]. (Right) Reduced hindrance of  $K$ -isomeric states in  $N=104$  isotones as a function of proton-neutron valence product. The extrapolation of these systematics suggests a particularly large reduced hindrance for the valence maximum ( $N_\pi, N_\nu = 16 \times 22 = 352$ ) nucleus,  $^{170}\text{Dy}$ .

In common with other  $N=104$  isotones,  $^{170}\text{Dy}$  is expected to have an energetically favoured,  $K=6^+$  two-quasi-neutron isomeric state. The right hand side of figure 3 shows the reduced hindrance for  $K$ -isomeric states in the  $N=104$  isotonic chain<sup>1</sup>. As pointed out in references [12,16], there appears to be a correlation between this quantity and the valence proton-neutron product. This can be qualitatively understood in terms of the valence maximum forming a nucleus with maximum quadrupole collectivity and thus a very ‘stiff’ axial symmetry. This is the requirement for keeping the  $K$ -quantum number ‘good’ as small deviations in the triaxial degree of freedom can be responsible for significant apparent breakdowns of the  $K$ -selection rule. From the systematics shown on the right hand side of figure 3, it could be that  $^{170}\text{Dy}$

<sup>1</sup> The reduced hindrance is defined as the  $(1/\nu)^h$  power of the ratio of the observed lifetime for decay divided by the Weisskopf single particle estimate for the same transition, where  $\nu = \lambda - K$  and  $\lambda$  is the multipole order of the electromagnetic transition.

arguably represents the ‘best case’ of  $K$  isomerism yet observed. This is due to its unusual stability with regard to axial-symmetric prolate deformation.

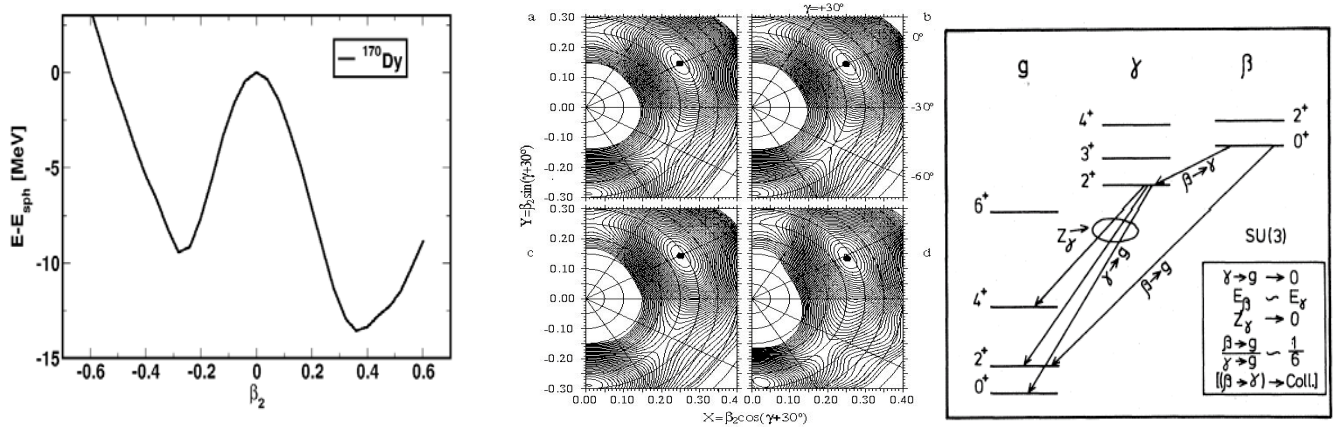


**Figure 10:** (Left) Constrained Hartree-Fock calculations for the ground state configuration in the doubly mid-shell nucleus  $^{170}\text{Dy}$ , which predict a very favoured prolate deformed shape. (Centre) Cranked Total Routhian Surface calculations for  $^{170}\text{Dy}$  at rotational frequencies of (a) 0.0 MeV/h; (b) 0.1 MeV/h; (c) 0.2 MeV/h; and (d) 0.4 MeV/h. Note the deep, axially symmetric prolate deformed ( $\beta_2=0.3$ ,  $\gamma=0^\circ$ ) minimum which remains constant in shape for spins up to 16  $\hbar$  (from reference [12]). (Right) Theoretical signatures for the dynamical  $SU(3)$  symmetry in nuclei as described in reference [17].

Intriguingly, the double mid-shell at  $^{170}\text{Dy}$  may also represent the single best case of the  $SU(3)$  dynamical symmetry in nuclei [17]. In even-even nuclei the excitation energy of the first  $I^\pi=2^+$  state and the ratio of the excitation energies of the first  $4^+$  and  $2^+$  states can be used to classify nuclei into different regimes of structure. Limiting cases can be linked to well-defined dynamical symmetries in the nuclear Interacting Boson Approximation. A spherical vibrational nucleus is described by the  $U(5)$  limit, while pure triaxial and perfect axially symmetric quadrupole rotors are associated with the  $O(6)$  and  $SU(3)$  dynamical symmetry limits, respectively. The spectroscopy of  $^{170}\text{Dy}$  and its near neighbours is of fundamental interest to group-theoretical descriptions of nuclear structure. While representative examples of the  $U(5)$  [18] and  $O(6)$  [19] dynamical symmetries have been identified in a variety of nuclei, the specific signatures which are evidence of the  $SU(3)$  limit have been more challenging to demonstrate empirically (see figure 4). As was pointed out two decades ago by Casten et al. [17], while many axially deformed prolate nuclei display *some* of the features of the  $SU(3)$  dynamical symmetry, no nucleus currently studied displays all of them. The systematics for  $SU(3)$  candidate nuclei appear to show an underlying  $SU(3)$  symmetry associated with the neutron mid-shell at  $N=104$  [17]. In addition to a  $E(4^+)/E(2^+)$  ratio of 3.33, additional signatures for pure  $SU(3)$  symmetry include hindered (forbidden in the  $SU(3)$  limit) transitions between the  $K^\pi=2^+$  ( $\gamma$ ) band and the ground state configuration, and that the nominal  $\gamma$ - and  $\beta$ -vibrational bands are at approximately the same excitation energy. These studies require detailed non-yrast spectroscopy, which might be possible following population by the low-spin  $\beta^-$ -decaying parent  $^{170}\text{Tm}$ . In the  $^{168}\text{Dy}$  case reported by Asai et al. [14], in addition to the first  $4^+$  and  $2^+$  states being identified, tentative evidence for states in the  $\gamma$ -vibration band were also reported. The increase in  $Q_{\beta^-}$  value expected for the  $^{170}\text{Tm}$  to  $^{170}\text{Dy}$  decay compared to the  $A=168$  isotopes (where the value was more than 5 MeV) should also increase the likelihood of access to spectroscopy of the non-yrast states in the daughter nucleus.

The channel selection available using the combination of the FRS, RISING and the active stopper means that  $^{170}\text{Dy}$  and its near neighbours can be studied in detail following both  $\beta^-$ -decay of the  $^{170}\text{Tm}$  mother nucleus and also following the isomeric decay of the predicted  $K^\pi=6^+$  state which has a predicted half-life in the seconds range [8]. Following the fragmentation of a  $^{198}\text{Pt}$  beam, we estimate a rate of  $^{170}\text{Tm}$  at the final focus of the FRS of approaching 1 ions per spill ( $10^9$  particles of primary beam), making this region experimentally accessible for spectroscopic study for the first time.

## Rate Calculations and Beam Time Request:

Following a series of detailed simulations using different 'standard' SIS beams such as  $^{197}\text{Au}$ ,  $^{208}\text{Pb}$  and  $^{238}\text{U}$ , it has been decided that the most appropriate beam for use in this experiment is  $^{198}\text{Pt}$ . This decision has been arrived at following arguments to both (i) maximise the production cross-sections for the nuclei of interest, and also (ii) to provide sufficient angular momentum input for the Yb, Hf and W region, thereby giving sufficient isomeric ratios for useful measurements.

*A  $^{198}\text{Pt}$  beam has not been accelerated by the SIS group before and will need development prior to the experiment.*

The following rate simulations were performed assuming a primary  $^{198}\text{Pt}$  beam intensity of  $10^9$  particles per spill, over a 10 second spill cycle. A beam energy of 1 GeV per nucleon was assumed, as were a  $2.5\text{ g/cm}^2$  thick Be production target was used, together with a  $5.1\text{g/cm}^2$  Aluminium degrader at S2 followed by a  $108\text{mg/cm}^2$  Niobium stripper. The cross-section estimates come from the COFRA [20], the analytical version of the ABRABLA Monte Carlo codes, which is appropriate for the production of neutron-rich nuclei. The estimated values for transmission of specific isotopes per eight hour shift are then calculated to be:

**Setting 1: Centred on  $^{191}\text{W}$**   
 $^{190}\text{W}$   $1 \times 10^7$        $^{191}\text{W}$   $0.4 \times 10^7$        $^{192}\text{W}$   $0.4 \times 10^7$

**Setting 2: Centred on  $^{187}\text{Hf}$**   
 $^{187}\text{Hf}$   $3.7 \times 10^5$        $^{188}\text{Hf}$   $9 \times 10^4$        $^{189}\text{Hf}$   $1 \times 10^4$

**Setting 3: Centred on  $^{185}\text{Yb}$**   
 $^{184}\text{Yb}$   $2 \times 10^4$        $^{185}\text{Yb}$   $6 \times 10^3$        $^{186}\text{Yb}$  240

Assuming a 20%  $\gamma$ -ray efficiency for 662 keV, attenuated by 50% for the prompt-flash reduction, and an isomeric ratio of 5%, this yields the following estimates for observed photopeak  $\gamma$  rays per 8 hour shift of

$^{190}\text{W}$  250,000 ;  $^{192}\text{W}$  100,000 ;  $^{188}\text{Hf}$  2,250 ;  $^{184}\text{Yb}$  500 ;  $^{186}\text{Yb}$  6

**Setting 4: Centred on  $^{170}\text{Dy}$**   
 $^{170}\text{Dy}$   $1.4 \times 10^5$        $^{170}\text{Tb}$  4,500       $^{168}\text{Tb}$   $4.9 \times 10^4$

Assuming an overall  $\gamma$ -ray (0.2) and  $\beta$ -detection (0.5) efficiency for decays of  $^{170}\text{Tb}$  to  $^{170}\text{Dy}$ , this would yield an estimate of 450 photopeak  $\gamma$  rays from the decay of the first  $2^+$  state in  $^{170}\text{Dy}$  per shift.

Based on these rate estimates we request the following beam time:

Setting 1: 3 shifts (1 day)

Setting 2: 3 shifts (1 days)

Setting 3: 6 shifts (2 days)

Setting 4: 6 shifts (2 days)

We also request an extra two days (six shifts) for primary beam tuning and initial particle identification calibrations, based on the  $^{191}\text{W}$  setting, making a total beam request of 24 shifts (8 days).

## REFERENCES:

- [1] P.M. Walker & G.D. Dracoulis, *Nature* **399** (1999) 35; *Hyperfine Interactions* **135** (2001) 83
- [2] F.R. Xu, P.M. Walker & R. Wyss, *Phys. Rev.* **C62** (2000) 014301
- [3] Zs. Podolyák et al., *Phys. Lett.* **B491** (2000) 225
- [4] J. Jolie & A. Linnemann, *Phys. Rev.* **C68** (2003) 021301(R)
- [5] M. Deutsch and R.W. Bauer, *Nucl. Phys.* **21** (1960) 128 ; W.F. Edwards and F. Boehm *Phys. Rev.* **121** (1961) 1499
- [6] T.E. Ward & P.E. Haustein, *Phys. Rev.* **C4** (1971) 244
- [7] K. Krumbholz et al., *Z. Phys.* **A351** (1995) 11
- [8] K. Jain et al., *Nucl. Phys.* **A591** (1995) 61
- [9] M. Caamano et al., *Eur. Phys. Jour.* **A23** (2005) 201
- [10] R.F. Casten, *Nucl. Phys.* **A443** (1985) 1; R.F. Casten and N.V. Zamfir *Phys. Rev. Lett.* **70** (1993) 402
- [11] P.D. Stevenson et al., *Phys. Rev.* **C63** (2001) 054309
- [12] P.H. Regan et al., *Phys. Rev.* **C65** (2002) 037302
- [13] A.K. Rath et al., *Phys. Rev.* **C68** (2003) 044315
- [14] M. Asai et al., *Phys. Rev.* **C59** (1999) 3060
- [15] S.A. Kerr et al., *Proceedings on the 5<sup>th</sup> International Conference on Capture Gamma-ray Spectroscopy and Related Topics, Knoxville 1984*, (American Institute of Physics, NY, 1985), p416
- [16] P. Walker *J. Phys.* **G16** (1990) L233
- [17] R.F. Casten et al., *Phys. Rev.* **C31** (1985) 1991
- [18] A. Aprahamian et al., *Phys. Rev. Lett.* **59** (1987) 535
- [19] R.F. Casten & J. Cizewski, *Phys. Lett.* **185B** (1987) 293
- [20] J. Benlliure et al., *Nucl. Phys.* **A660** (1999) 87

**Search for the  $8^+$  ( $\pi g_{9/2}$ )<sup>-2</sup> isomer in N=82  $^{130}\text{Cd}$  populated via the  
6 proton knockout channel in the fragmentation of  $^{136}\text{Xe}$**

A. Jungclaus<sup>1</sup>, A. Algora<sup>2</sup>, J. Benlliure<sup>3</sup>, L. Caceres<sup>1,4</sup>, B. Fogelberg<sup>5</sup>, W. Gelletly<sup>6</sup>, J. Gerl<sup>4</sup>, M. Gorska<sup>4</sup>, H. Grawe<sup>4</sup>, J. Jolie<sup>7</sup>, H. Mach<sup>5</sup>, M. Pfützner<sup>8</sup>, Z. Podolyak<sup>6</sup>, P.H. Regan<sup>6</sup>, A. Richard<sup>7</sup>, B. Rubio<sup>9</sup>, D. Rudolph<sup>10</sup>, A. Scherillo<sup>7</sup>, H.-J. Wollersheim<sup>4</sup>

*1 Universidad Autónoma de Madrid, Spain*

*2 Institute of Nuclear Research, Debrecen, Hungary*

*3 Universidad de Santiago de Compostela, Spain*

*4 GSI Darmstadt, Germany*

*5 Uppsala University, Sweden*

*6 University of Surrey, UK*

*7 Universität zu Köln, Germany*

*8 University Warsaw, Poland*

*9 IFIC Valencia, Spain*

*10 Lund University, Sweden*

**Abstract**

The aim of this proposal is to study the  $\gamma$ -decay of the  $8^+$  ( $\pi g_{9/2}$ )<sup>-2</sup> isomer in the neutron rich semi-magic N=82 nucleus  $^{130}\text{Cd}$ , which is one of the classical r-process waiting-point nuclei.  $^{130}\text{Cd}$  will be produced in cold projectile fragmentation at relativistic energies using a  $^{136}\text{Xe}$  beam with energy of about 1 GeV/u. The energies of the first excited states in  $^{130}\text{Cd}$  as well as the lifetime of the  $8^+$  ( $\pi g_{9/2}$ )<sup>-2</sup> isomer to be determined in the proposed experiment will provide important new information concerning the shell structure close to doubly-magic  $^{132}\text{Sn}$  and in particular address the question whether a N=82 shell quenching exists “south” of  $^{132}\text{Sn}$ .

**Introduction**

The region around doubly-magic  $^{132}\text{Sn}$  has been subject of numerous experimental and theoretical studies in the last years. The reason is that it is of special importance both for nuclear astrophysics as well as nuclear structure. Concerning the former the interest is due to the close relation between the N=82 shell closure and the A $\approx$ 130 peak of the solar r-process abundance distribution. It has been suggested already in 1993 that a spherical shell quenching of the N=82 neutron shell “below”  $^{132}\text{Sn}$  would allow to properly reproduce the observed abundances. While this is still heavily debated among astrophysicists, the question of shell quenching towards the neutron dripline remains a key topic of nuclear structure research. The study of the region around  $^{132}\text{Sn}$ , a well bound spherical nucleus, is of great importance for nuclear structure physics because this is the only region around a heavy doubly closed shell nucleus far-off stability (8 neutrons relative to the last stable isotope  $^{124}\text{Sn}$ ) for which spectroscopic information can be obtained using modern state-of-the-art techniques. It therefore plays an essential role in testing the shell model and serves as input for any reliable future microscopic nuclear structure calculations towards the neutron drip line. Over the last decade spectroscopic studies of  $\beta$ -decays at on-line mass separator facilities, e.g. OSIRIS and ISOLDE, have provided a large amount of information about nuclei around  $^{132}\text{Sn}$  (see overview in [1]). Today, the  $\nu$ -hole structure of  $^{131}\text{Sn}$ , the  $\pi$ -particle structure of  $^{133}\text{Sb}$ , the lowest  $\nu$ -particle states in  $^{133}\text{Sn}$  and part of the  $\pi$ -hole structure of  $^{131}\text{In}$  have been established. Also for the two-valence particle/hole systems  $^{134}\text{Sn}$ ,  $^{130}\text{Sn}$  and  $^{134}\text{Te}$  some experimental information is available. Despite the considerable amount of experimental information already available in the region around  $^{132}\text{Sn}$ , or maybe because of it, the shell structure around  $^{132}\text{Sn}$  is not yet fully understood. Going further away from  $^{132}\text{Sn}$  towards the neutron dripline, both “south” along the N=82 line as well as “east” along the Z=50 line, important questions concerning the nuclear structure still are waiting to be answered. A quenching of the N=82 shell gap “below”  $^{132}\text{Sn}$  has been predicted by different calculations. This effect is suggested to be caused by a lowering of single-particle energies of low-j orbitals relative to those of high-j orbitals due to the strong interaction between bound orbitals and the low-j continuum. However, experimental evidence for this effect is still scarce as discussed in the next section. Going along the Z=50 line towards the neutron drip line a modification of the single-particle energies is expected for nuclei with an N/Z ratio that exceeds 1.6 possibly caused by a more diffuse nuclear surface or even the existence of neutron skins.

## Is there a N=82 shell quenching ?

Some years ago it had been proposed [2] that the assumption of a spherical quenching of the N=82 neutron shell closure could provide a possible solution to the puzzle in the r-process nucleosynthesis which existed in the 1990s. The pronounced abundance troughs prior to the peaks at  $A \approx 130$  and 195 seemed to have their origin in an overestimation of the N=82 and 126 shell closures. In Hartree-Fock-Bogoliubov (HFB) calculations using Skyrme-type interactions, Dobaczewski et al. [3] indeed found that the N=82 shell gap drastically decreases near the neutron drip line. They attributed this effect to a lowering of single-particle energies of low-j orbitals relative to those of high-j orbitals resulting from a strong interaction between bound orbitals and low-j continuum states. The use of the masses from this HFB calculation has shown to lead to a considerable improvement in the global abundance fit in r-process calculations [4] as shown in Fig. 1, namely a filling of the troughs around  $A \approx 120$  and 140 and a better overall reproduction of the heavy-mass region.

Experimental evidence for a quenching of the N=82 neutron closed shell is still scarce. Since direct mass measurements on the nuclei around  $^{132}\text{Sn}$  have not yet been reported, there exists only very vague indirect evidence today. In the recent study of the  $\beta$ -decay of the classical r-process “waiting-point” nucleus  $^{130}\text{Cd}$  [5] a large  $Q_\beta$  value of 8.34 MeV has been measured which is in agreement only with recent mass models which include N=82 shell quenching. In addition the observed high excitation energy (2.12 MeV) of the  $\pi g_{9/2} \otimes \nu g_{7/2} 1^+$  level in  $^{130}\text{In}$ , populated by the main Gamov-Teller transition in the  $\beta$ -decay of  $^{130}\text{Cd}$ , required a change of the TBME for the  $^{130}\text{Cd}$  decay in order to get agreement between shell model calculations and experiment. As a consequence of this change the  $\beta$ -decay half-lives of the so far unknown N=82 waiting-point nuclei  $^{128}\text{Pd}$  to  $^{122}\text{Zr}$  will become longer than those predicted by recent large-scale shell models. This change in the assumption of important half-lives results in significant changes in dynamical r-process abundance calculations as illustrated in Fig. 1. The longer lifetimes lead to a better reproduction of the rising wing of the  $A \approx 130$  peak compared to the calculations with the previous short shell-model half-lives. These results clearly show that the r-process abundances in the solar system are governed by nuclear structure. Clearly more experimental information on nuclear quantities in the vicinity of the classical, neutron-magic (N=82) waiting-point nuclei below  $^{132}\text{Sn}$  would be needed for a complete understanding of the r-process matter flow through the  $A \approx 130$  “bottleneck” region.

There is one more experimental study claiming to have found experimental signatures of a weakening of the N=82 shell closure already one proton-pair below  $^{132}\text{Sn}$ . In that study, the  $2^+$  and  $4^+$  levels in  $^{126,128}\text{Cd}$  and tentatively the  $2^+$  state in  $^{130}\text{Cd}$  have been identified for the first time in the  $\beta$ -decays of  $^{126,128,130}\text{Ag}$  at ISOLDE [6] (see Fig. 2). It is important to notice at this point that - as stated by the authors - the case of the  $^{128}\text{Ag} \rightarrow ^{128}\text{Cd}$  decay is close to the present limit which can be achieved using the available beam yields and instrumentation. Consequently the authors of Ref. [6] consider the assignment of the  $2^+$  state in  $^{130}\text{Cd}$  as “speculative”. The surprising result of this experiment is that the  $2^+$  state in  $^{128}\text{Cd}$  at an excitation energy of 645 keV lies 7 keV lower than the  $2^+$  level in  $^{126}\text{Cd}$ . That means that whereas the proton-rich Cd nuclei exhibit a rather steep increase of the  $2^+$  energies towards N=50 with  $E(2^+) = 1395$  keV the neutron-rich Cd isotopes show only a moderate increase up to N=78, followed by a constant value in N=80  $^{128}\text{Cd}$  and tentatively a steep increase towards N=82  $^{130}\text{Cd}$  as illustrated in Fig. 3a – in contrast to the behaviour of the heavy Sn and Te isotopes. The  $B(E2)$  values for the Cd, Sn and Te isotopic chains calculated from the  $E(2^+)$  values using the empirical relation given in [7] are shown in Fig. 3b. From this figure it is evident that both the two-proton-hole Cd as well as the two-proton-particle Te isotopes have considerably higher  $B(E2)$  values than the proton-magic Sn, indicating that sizeable collectivity persists close to the  $Z=50$  magic shell. However, whereas the  $B(E2)$  values decrease continuously up to N=82 for the Te isotopes, they remain more or less constant between N=78 and N=80 for the Cd isotopes and then steeply increase for semi-magic  $^{130}\text{Cd}$ . This might indicate that in the Cd isotopic chain some kind of collectivity persists up to the neutron shell closure or at least up to N=80. However, the important question is whether the observed differences in the structures of the Te and Cd isotopes for  $N \geq 76$  are really due to a difference in the underlying shell gap at N=82 for  $(Z_{\text{magic}}-2)$  relativ to  $(Z_{\text{magic}}+2)$  as claimed by the authors of Ref. [6] or whether they are rather due to a weakening of ideal sphericity with a slight onset of quadrupole collectivity below  $^{132}\text{Sn}$ .

As mentioned in Ref. [6] none of the published microscopic meanfield calculations in the region around  $^{132}\text{Sn}$  predicts quadrupole collectivity near the N=82 shell closure. They all agree in that for the heavy Pd, Cd and Te isotopes there is a sudden drop of deformation around  $N \approx 72$  reaching sphericity ( $\beta_2 \leq 0.03$ ) already at  $N \approx 76$ . However, things are probably a bit more complicated. In order to further investigate this question we have calculated the HFB meanfield energies as a function of the deformation parameter  $\beta_2$  for the nuclei  $^{126,128,130}\text{Cd}$ ,  $^{132}\text{Sn}$  and for comparison also  $^{208}\text{Pb}$  using the Gogny force. As expected the energy curves of all these nuclei have a spherical minimum and the width is decreasing from  $^{126}\text{Cd}$  over  $^{128}\text{Cd}$  to N=82  $^{130}\text{Cd}$  and finally to doubly-magic  $^{132}\text{Sn}$ . However, the important observation is that the energy curve for  $^{132}\text{Sn}$  is much broader than the corresponding for the other doubly-magic nucleus, namely  $^{208}\text{Pb}$ . That means that fluctuations in the quadrupole moment are much larger in  $^{132}\text{Sn}$  indicating that a higher degree of collectivity remains as compared to  $^{208}\text{Pb}$ . Already the beyond-meanfield studies of the N=20 shell closure and in particular  $^{32}\text{Mg}$  have shown that a nucleus with a spherical minimum at the meanfield level might show deformation after angular momentum projection [8] – in agreement with the experimental findings. Clearly further beyond-meanfield studies around the N=82

shell closure are needed. The knowledge of  $2^+$ ,  $4^+$ ,  $6^+$  and  $8^+$  excitation energies in  $^{128,130}\text{Cd}$  aimed for in the proposed experiment would provide experimental information about the degree of deformation in these nuclei close to  $N=82$ .

### Isomeric states around doubly magic $^{100}\text{Sn}$ and $^{132}\text{Sn}$

In analogy to the  $8^+$  isomer observed in  $^{98}\text{Cd}$  some years ago [9], an isomer is also expected in  $^{130}\text{Cd}$  since both nuclei have two proton holes with respect to the doubly-magic  $^{100}\text{Sn}$  resp.  $^{132}\text{Sn}$  and the same proton orbitals are involved in both cases. In all of the other three two-particle or two-hole nuclei around  $^{132}\text{Sn}$ , namely  $^{134}\text{Sn}$ ,  $^{134}\text{Te}$  and  $^{130}\text{Sn}$ , as well as in many more isotopes in this region isomers have already been observed (see Fig. 4). The isomer spectroscopy has the advantage over the population in  $\beta$ -decay that excited states up to relatively high spin are populated in the isomer decay and the lifetime of the isomer gives additional information about the shell structure.

The  $8^+$  isomer in  $^{130}\text{Cd}$  with  $(\pi g_{9/2})^{-2}$  configuration has already been searched for both in relativistic projectile fission of  $^{238}\text{U}$  in an experiment performed at the FRS at GSI [10] as well as in thermal-neutron induced fission reactions with Pu targets at the LOHENGRIN mass spectrometer at the ILL, Grenoble [11]. In both cases no  $\gamma$ -ray could be assigned to the decay of the hypothetic isomer probably due to limitations in statistics and/or too short half-life. The transport time through the LOHENGRIN spectrometer is about 2.2  $\mu\text{s}$  and therefore limits these studies to isomers with half-lives longer than about 0.5  $\mu\text{s}$ . At the FRS the flight time is much shorter (about 0.5  $\mu\text{s}$ ) and in addition most of the fragments are fully stripped leading to an effective increase of the isomer lifetime because the conversion electron decay branch is “switched off”. (Assuming an  $8^+ \rightarrow 6^+$  transition energy of 100 keV - taken from the SM calculation [11] - and E2 multipolarity, the conversion coefficient is 1.5.) In this way, the  $\gamma$ -decay of an isomer in  $^{200}\text{Pt}$  with a half-life as short as 14 ns has recently been observed at the FRS after  $^{208}\text{Pb}$  fragmentation [12].

### Experimental method

We propose to study the isomeric decay of the  $8^+$  state in  $^{130}\text{Cd}$  produced as the 6-proton knockout channel in the cold fragmentation of an 1 GeV/u  $^{136}\text{Xe}$  beam on a  $^9\text{Be}$  target. This reaction has recently been studied by J. Benlliure et al. at the FRS and considering the measured cross section of  $\sigma(^{130}\text{Cd})=0.154$  nb [13] it constitutes a very promising alternative approach to study the very neutron-rich Cd isotopes. The identified fragments will be implanted in an active stopper and the decay  $\gamma$ -rays detected in the RISING setup consisting of 15 EUROBALL Cluster detectors.

#### **Beamtime estimate:**

#### **The implantation rate at the focal plane is given by**

$$I [\text{sec}^{-1}] = \sigma [\text{cm}^2] \cdot d [\text{g/cm}^2] \cdot A^{-1} [\text{mol/g}] \cdot \phi [\text{sec}^{-1}] \cdot T_{\text{tot}} \cdot N_A [\text{mol}^{-1}]$$

with  $\sigma$ : cross section  
 $d$ : target thickness  
 $A$ : atomic mass of the target  
 $\phi$ : primary beam current  
 $T_{\text{tot}}$ : total transmission to the catcher  
 $N_A$ : Avogadro constant

The number of isomeric decays per second is:  $R [\text{sec}^{-1}] = I [\text{sec}^{-1}] \cdot R_{\text{iso}} \cdot \varepsilon_\gamma$

with  $R_{\text{iso}}$ : isomeric ratio  
 $\varepsilon_\gamma$ :  $\gamma$ -ray detection efficiency

For  $^{130}\text{Cd}$  produced in fragmentation of 1 GeV/nucleon  $^{136}\text{Xe}$  we have:

$$\begin{aligned} \sigma(^{130}\text{Cd}) &= 0.154 \text{ nb} \\ d &= 2.5 \text{ g/cm}^2 \quad \text{Be target} \\ \phi &= 5 \cdot 10^9 \text{ ions per spill} \quad (\text{with cycle length } 5 \text{ s}) \\ T_{\text{tot}} &= 95\% \end{aligned}$$

→  $I = 1.4$   $^{130}\text{Cd}$  implants per minute or  $\approx 2000$  implants per day

Assuming further

$$R_{\text{iso}} = 10\% \text{ and } \varepsilon_{\gamma} = 8\text{-}15\% \text{ (for } E_{\gamma}=0.6\text{-}1.3 \text{ MeV, taking into account a 25\% reduction of the efficiency due to the prompt flash)}$$

we expect to observe 15-30 counts per day in each of the  $\gamma$ -lines from the isomer decay. These numbers are valid in case that the half-life of the  $8^+$  isomer is long enough that no decay losses during the flight time through the FRS have to be considered.

In the setting optimized for  $^{130}\text{Cd}$  about hundred times more  $^{128}\text{Cd}$  nuclei will be implanted as well. This might allow the first observation of the decay of the  $8^+$  state in this nucleus even in case of a relatively short half-life. At the same time, the known isomeric decays in  $^{127}\text{Cd}$  and  $^{130}\text{In}$  [14] will serve as an internal check for the particle identification.

The beamtime request is

- **6 shifts** for radioactive beam preparation and the calibration of the particle identification procedure and the  $\gamma$ -ray detection setup using known isomeric decays (for example  $^{132}\text{Sn}$  and  $^{129}\text{In}$ )
- **15 shifts** to search for the  $8^+$  isomers in  $^{130}\text{Cd}$  and  $^{128}\text{Cd}$

The total requested beamtime amounts to 21 shifts. This assumes that a  $^{136}\text{Xe}$  primary beam intensity of at least  $5 \cdot 10^9$  ions/spill (5 second cycle) is available.

#### References:

- [1] Mach, Acta Phys. Pol. B32 (2001) 887
- [2] Kratz et al., Ap. J. 403 (1993) 216
- [3] Dobaczewski et al., Phys. Rev. Lett. 72 (1994) 981
- [4] Chen et al., Phys. Lett. B355 (1995) 37
- [5] Dillmann et al., Phys. Rev. Lett. 91 (2003) 162503
- [6] Kautsch et al., Eur. Phys. J. A9 (2000) 201
- [7] Raman et al., Phys. Rev. C43 (1991) 556
- [8] Rodriguez-Guzman et al., Phys. Rev. C62 (2000) 054319 and Nucl. Phys. A709 (2002) 201
- [9] Gorska et al., Phys. Rev. Lett. 79 (1997) 2415
- [10] Mineva et al., Eur. Phys. J. A and PhD Thesis, University of Lund, 2004
- [11] Scherillo et al., Phys. Rev. C70 (2004) 054318 and Scherillo, PhD thesis Cologne 2005
- [12] Caamaño et al., Eur. Phys. J. A23 (2005) 201
- [13] J. Benlliure, private communication
- [14] Hellström et al., Proc. of the Third International Conference on Fission and Properties of the Neutron-Rich Nuclei, Ed. J. Hamilton, World Scientific, 2003, p.22 and Proc. of the International Workshop on Gross Properties of Nuclei and Nuclear Excitations, Ed. H. Feldmeier, GSI imprint 2003, p.72

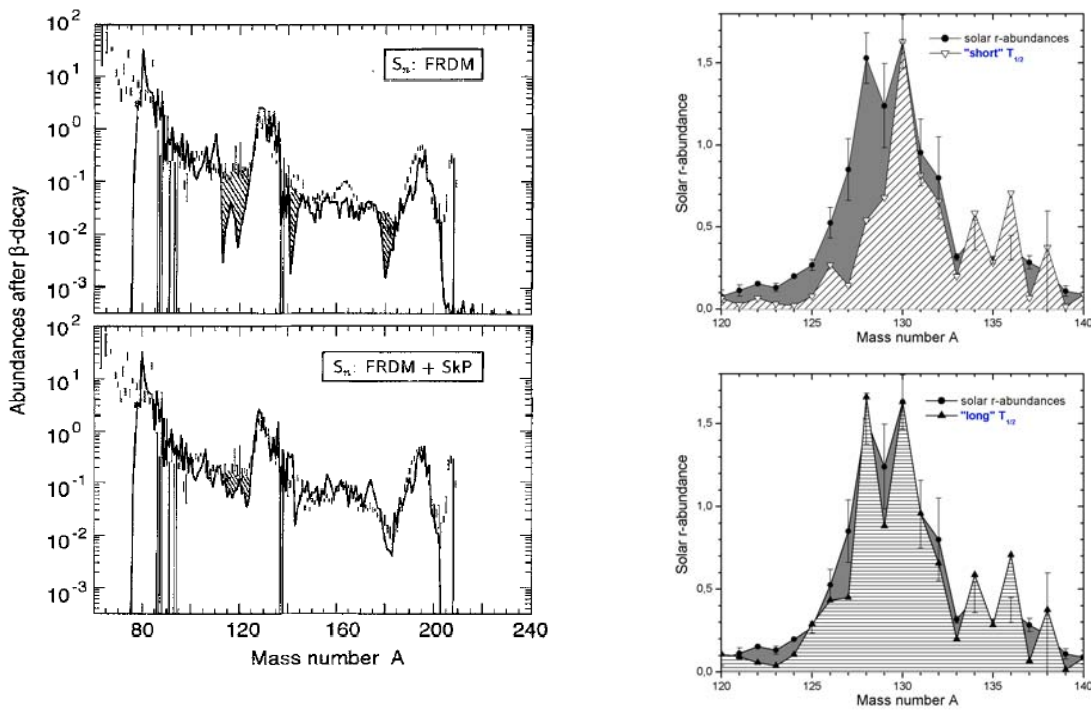


Figure 1: Left: r-process abundances calculated with (lower part) and without (upper part) a  $N=82$  neutron shell quenching [4]. Right: Calculated solar r-process abundances assuming short (upper part) or long (lower part) half-lives in comparison to experiment (see text for details) [5].

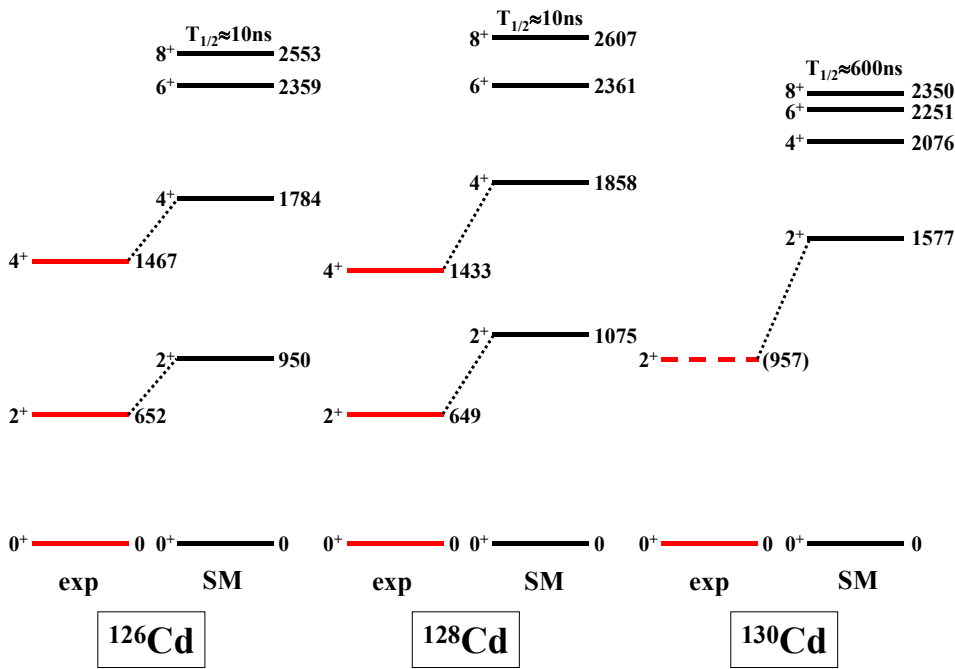


Figure 2: Experimental [6] and shell model [11]  $2^+$  and  $4^+$  excitation energies in  $^{126,128,130}\text{Cd}$ . The assignment of the  $2^+$  state in  $^{130}\text{Cd}$  at 957 keV is still very speculative [6]. The calculated half-lives (SM) of the  $8^+$  states are indicated as well.

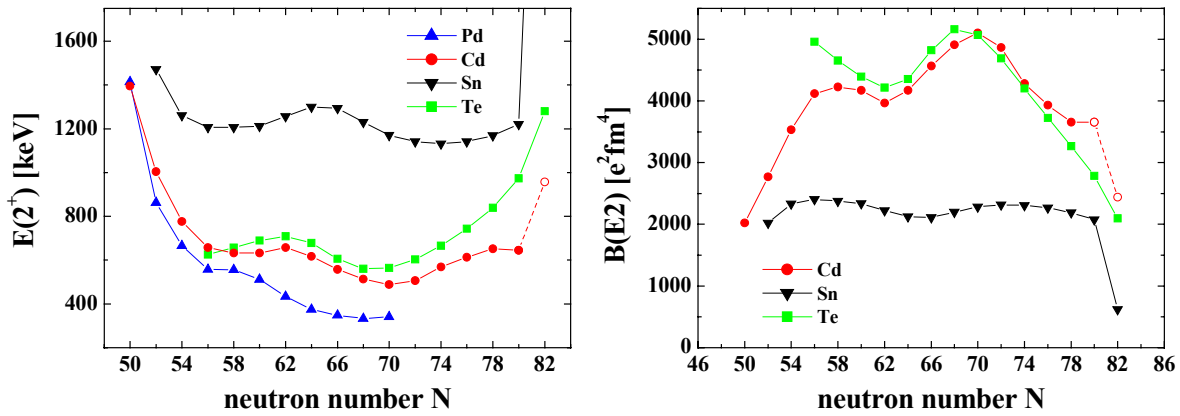


Figure 3: Systematics of  $E(2^+)$  and  $B(E2)$  values (determined using the  $B(E2) \sim E(2^+)^{-1}$  relation from [7]) for the even-even  ${}_{46}\text{Pd}$ ,  ${}_{48}\text{Cd}$ ,  ${}_{50}\text{Sn}$  and  ${}_{52}\text{Te}$  isotopes. Note the discontinuities for the Cd isotopic chain around  $N=80,82$  (see text for details).

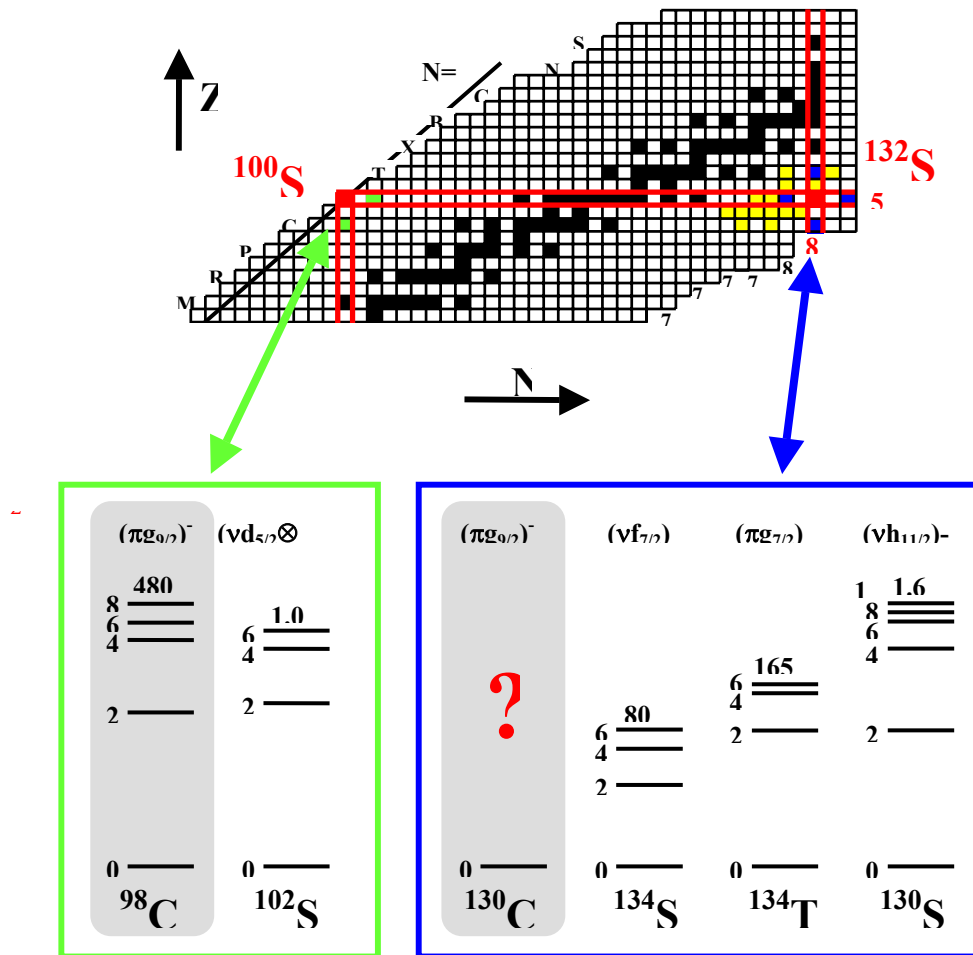


Figure 4: Overview over known isomers around doubly magic  ${}^{132}\text{Sn}$  (yellow and blue squares). The known isomers in the two-particle and two-hole nuclei  ${}^{134}\text{Sn}$ ,  ${}^{134}\text{Te}$  and  ${}^{130}\text{Sn}$  are shown with their measured lifetimes. A  $8^+$   $(\pi g_{9/2})^{-2}$  isomer is expected in  ${}^{130}\text{Cd}$  in analogy to the one observed in  ${}^{98}\text{Cd}$  [9].

# Exotic beta decays near the proton-drip line: study of the beta decay of $^{70,71}\text{Kr}$ .

**A. Algora, B. Nyakó, J. Timár, Z. Dombrádi, D. Sohler,  
A. Krasznahorkay**

*Institute of Nuclear Research, Debrecen, Hungary*

**B. Rubio, A. Perez, L. Caballero**

*IFIC, University of Valencia, Valencia, Spain*

**W. Gelletly, Z. Podolyak, P. H. Regan, W. Catford, A. Garnsworthy,  
N. Thompson, S. Williams**

*University of Surrey, Guildford, UK*

**J. Benlliure, D. Cortina-Gil**

*University Santiago de Compostela, Santiago, Spain*

**Y. Fujita, A. Tamii, T. Adachi, H. Matsubara**

*Osaka University, Osaka, Japan*

**A. Jungclaus**

*Universidad Autonoma de Madrid, Madrid, Spain*

**T. Martinez**

*CIEMAT, Madrid, Spain*

**M. Gorska, H. Geissel, H. Weick, J. Gerl**

*GSI, Darmstadt, Germany*

**A. Gadea, G. deAngelis**

*LNL, Legnaro, Italy*

**Spokesperson: A. Algora, B. Rubio, W. Gelletly**

**GSI Contact: M. Gorska**

**Abstract:** *This proposal is aimed at the study of the beta decay of the proton rich  $^{70,71}\text{Kr}$  nuclei. The goal of the proposed experiment is twofold: first, to determine the  $I^\pi$  of the ground state (g.s) of  $^{71}\text{Kr}$  which should allow us to answer several questions such as the deformation of the ground state of this nucleus, and secondly to search for states populated in the beta decay of  $^{70}\text{Kr}$ , that may indicate the existence of the proton-neutron condensate.*

## 1. Background and physics motivation to study $^{71}\text{Kr}$ decay

Nuclei in the region of  $N \approx Z$  around  $Z=36-38$  have been the subject of numerous theoretical and experimental investigations to answer questions about deformation, shape coexistence, shape transitions, np pairing and isospin symmetry. This region is characterized by drastic shape changes depending on the competition in energy between prolate and oblate shapes (closely related to the occupation of particular single particle orbits).

In this context the beta decay between mirror  $T=1/2$  pairs is of special interest in terms of pinning down the characteristic structure of particular states. For instance the  $T_z=-1/2$  parent state will decay through a super-allowed Fermi transition to the isobaric analogue state in the daughter nucleus which should be identical to the parent state except for the  $T_z$  quantum number. One of the objectives of this proposal will be to identify

the IAS of  $^{71}\text{Kr}$  which is not known at the moment. Although the beta decay of  $^{71}\text{Kr}$  was studied some years ago at Isolde, the fact that the g.s and the first excited state in  $^{71}\text{Br}$  are separated by only 9 keV made the identification of the IAS impossible. One of the two states (or even both) was clearly populated in the decay but it was impossible to tell which one. The decay scheme resulting from the work of Oinonen *et al.* [1] is shown in fig.1.

In the decay of  $^{71}\text{Kr}$  Gamow Teller beta-decay is also possible and, in fact, a sizeable feeding to the second excited state at 207 keV was observed in ref. [1]. One of either the ground state or the 9 keV state (or both) also receives some Gamow Teller strength since the observed feeding there exhausted more than the expected Fermi strength. One extra difficulty the authors encountered at that time was that the  $I^\pi$  assignments of the three states in question were not known. In this respect we are now in a better position because we have performed an in-beam experiment (Martinez *et al.* [2]), where we were able to show that the lowest three states in  $^{71}\text{Br}$ , at 0, 9 and 207 keV, have spins and parities  $5/2^-$ ,  $1/2^-$ , and  $3/2^-$ , in accord with the tentative assignments of Oinonen [1].

Looking at the decay data of [1] three spins are possible for the g.s of  $^{71}\text{Kr}$ , namely  $1/2^-$ ,  $3/2^-$ , and  $5/2^-$ . From mirror symmetry arguments  $1/2^-$  and  $5/2^-$  are the most probable values, but a real measurement is needed to clarify the situation. This is also important in relation to the question of oblate/prolate competition in these nuclei since a  $1/2^-$  assignment to the  $^{71}\text{Kr}$  g.s will probably mean an oblate shape while  $3/2^-$  has been interpreted in the heavier Br isotopes as being associated with a prolate shape (see for instance Griffiths *et al.* [3])

Another source of information concerning the shape of the ground states of nuclei in this region comes from the work of Hamamoto *et al.* [4] and Sarriguren *et al.* [5]; according to them it is possible to obtain information on the deformation of the ground-states of nuclei in this region by measuring the B(GT) distribution of the decay to the daughter nucleus. These authors showed that in the vicinity of the drip-line a large part of the B(GT) will be available in the beta decay of the nuclei of interest [4] and that in some cases the distribution of the B(GT) differs markedly with the assumed shape of the ground-state of the parent [5]. Recent experimental results using the total absorption technique on  $^{74}\text{Kr}$ ,  $^{76}\text{Sr}$  have shown the validity of these conclusions [6,7]. We plan to carry out a measurement of this type on the beta decay of  $^{71}\text{Kr}$  at Isolde. However, in order to compare our results with the calculations we need to know the correct  $I^\pi$  for the  $^{71}\text{Kr}$  g.s.

Finally Urkedal and Hamamoto have also discussed the decay between these mirror nuclei [8]. In their article they proposed an explanation for the feeding to the two low lying states based on the idea that these two states are the band head and the first rotational member of the first intrinsic state. Although they assumed  $3/2^-$  and  $5/2^-$  for the first and second excited states in  $^{71}\text{Br}$ , the same argument holds if they are  $1/2^-$  and  $3/2^-$  as we know now, but the argument requires that the state populated in the decay is the  $1/2^-$  and not the  $5/2^-$ . The clarification of the  $1/2^-$  or  $5/2^-$  character of the g.s. of  $^{71}\text{Kr}$  will clarify this situation as well.

In summary there are a number of reasons why it is important to determine the  $I^\pi$  of the  $^{71}\text{Kr}$  g.s. Unfortunately this is experimentally not an easy task since the measurement of the highly converted 9 keV transition is extremely difficult.

We propose here a possible way which is to study the decay scheme of  $^{71}\text{Kr}$  in more detail than was done before. With the limited statistics achieved in the work by Oinonen *et al.*, only two gamma rays could be observed, both de-exciting the already mentioned 207 keV state. We believe however that other states are

populated in this decay, an assumption based on our study of the decay of other Kr isotopes (see ref. [7]) and on the fact that feeding has been observed at quite high excitation energy in  $^{71}\text{Br}$  (about 4 to 5 MeV) when the de-excitation proceeds through beta delayed protons which are easier to detect than gamma rays.

We believe that in the proposed set up, with better detection efficiency for gammas of high energy, with a factor of 20 improvement in the production of  $^{71}\text{Kr}$  and with a detailed knowledge of the  $^{71}\text{Br}$  level scheme at low excitation energy (Martinez *et al.* [2]) we will be able to determine the spin and parity of the g.s of  $^{71}\text{Kr}$  and hence shed light on several of the problems outlined above.

## 2. The $^{70}\text{Kr}$ physics case

Considerable effort has been expended over the last few years to find a clear signature of n-p pairing in  $N = Z$  nuclei. Until now the possibility of exploring the pn condensate in beta decay has not been exploited. According to Iachello [9], this is a possibility worthy of study. Elliott and co-workers have shown that the introduction of proton-neutron bosons in addition to the proton-proton and neutron-neutron bosons allows the description of light nuclei in terms of the Interacting Boson Model [10] (IBM-4). In light nuclei, where protons and neutrons are similar in number, proton-neutron pairs play a major role as building blocks of nuclear structure, but in medium and heavy mass nuclei, due to the large neutron excess, the effects of proton-neutron pairs are hidden. There is, however, one phenomenon where proton-neutron pairing, if it exists, will play a major role and that is beta decay. According to Iachello some results obtained in light nuclei confirm the use of the pn boson classification scheme of the GT decay (IBM-4 picture). In the case of heavy nuclei, however, the neutron excess pushes the energy of the pn pairs to values larger than that of pp and nn pairs. The low-lying states of even-even nuclei can then be discussed primarily in terms of pp and nn bosons. This is why the use of IBM-1,2 instead of IBM-4 is justified in medium and heavy nuclei. However, if proton-neutron pairing survives at all in heavy nuclei, it will lead to the population of a p-n condensate in beta decay with large matrix elements. Exploring this possibility is one of the goals of this proposal.

Even though the idea of proton-neutron pairing in nuclei has been discussed often, it is difficult to find clear evidence of its existence. This problem has been addressed in in-beam studies of  $N \approx Z$  nuclei with no definite answer [11]. From the perspective of beta decay a clear signature of the existence of the proton neutron condensate would be the observation of a Gamow-Teller (GT) decay with a small log ft between a state with  $J=0$ ,  $T=1$ ,  $T_z=-1$ , and a final state with  $J=1$ ,  $T=0$ ,  $T_z=0$ . If there is p-n pairing with  $T=0$ , the log ft for the  $0^+$  to  $1^+$  GT transition should be of the same order-of-magnitude as the log ft value for the  $0^+$  to  $0^+$  Fermi transition in the same nucleus, i. e.  $\log ft < 4.0$  [9] (see fig.2 for an schematic picture).

To observe this decay, it is necessary to study a case where several pn pairs can contribute to the  $1^+$  state near the  $N \approx Z$  line. A good candidate for this study is the decay of  $^{70}\text{Kr}$  into  $^{70}\text{Br}$ . This measurement is relatively simple, one expects a strong decay to the IAS which is the g.s. in this case and has  $I^\pi 0^+$ , and several  $1^+$  excited states. If most of the strength is concentrated in one  $1^+$  state, this will be already a good indication that the proton-neutron condensate exists.

## 4. The Measurements

It is proposed to produce the separated beams of  $^{70,71}\text{Kr}$  using a primary beam of  $10^9$  ions/s of  $^{92}\text{Mo}$  on a Be target of thickness  $4000 \text{ mgcm}^{-2}$ . Calculations with LIESCHEN code suggest that, after passage through

the FRS, with the appropriate settings of slits, magnets etc one will obtain yields of these two parent isotopes of  $1.1\text{E}+03$  and  $6.3\text{E}+04$  ions per hour distributed over an area of about  $4 \times 4 \text{ cm}^2$  [12].

The experimental arrangement at the focal plane will be the standard RISING setup with the ions implanted into a double-sided strip detector system (DSSDs) of area  $5 \times 5 \text{ cm}^2$  with  $16 \times 16$  strips. The ions arriving at the detector will be tagged by A and Z in the conventional way. Their time of arrival will be correlated with the subsequent detection of the beta particle emitted in the radioactive decay in the same pixel of the DSSD and the beta-delayed gammas which follow. The DSSD will be operated with two sets of electronics in parallel, set on high and low gain in order to be able to detect both the heavy ion and the beta particle. Each event will be time-stamped in order to allow us to determine the correlation in time of the ions, betas and gammas.

If we assume conservatively that the overall efficiency for gamma ray detection is 10% at 1.0 MeV and 30% at 200.0 keV and that there is a gamma-ray multiplicity of 2 then we can estimate the number of counts per day in the gamma-gamma coincidence spectrum in  $^{71}\text{Kr}$  to be 500. This number can be obtained assuming a production of 18 atoms/s and a feeding intensity of 1 % to the level that decays consequently with the gamma cascade of two gammas. In the case of  $^{70}\text{Kr}$  we can expect a feeding of 50% at approximately 700 keV excitation assuming that Iachello's assumption is valid. Considering a gamma efficiency of 0.15% for a gamma ray of 700 keV and a production of 0.3 atoms/s we can expect 2000 counts per day in the gamma-beta coincidence spectrum. Based in these calculations in total we will need 4 days for  $^{71}\text{Kr}$  and 2 days for  $^{70}\text{Kr}$  plus one day to adjust settings. Thus we request one week for the experiment.

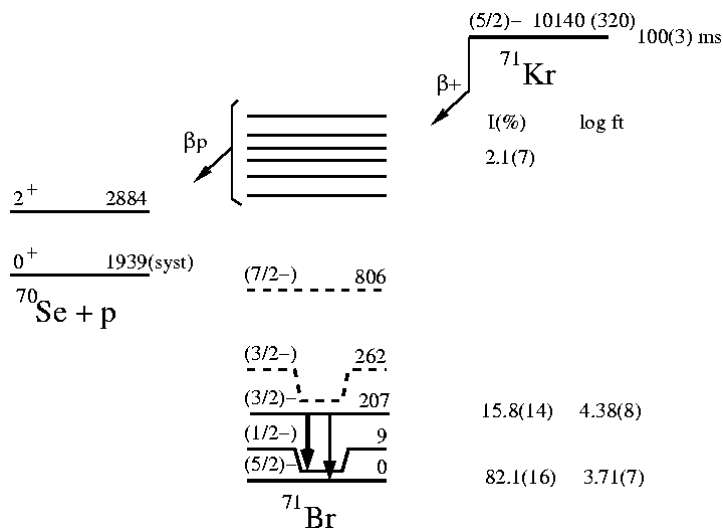


**Fig. 1** Known level scheme of  $^{71}\text{Br}$  populated in the  $^{71}\text{Kr}$  beta decay [1]. The level at 262 keV excitation was not confirmed experimentally in [2].

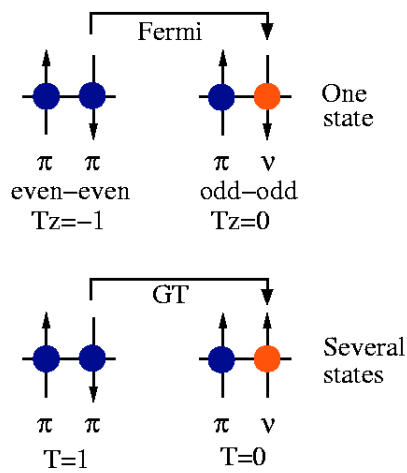


**Fig. 2** Schematic picture of the Fermi and the Gamow-Teller decay.

## References

- [1] M. Oinonen *et al.*, Phys. Rev. C 56 (1997) 745
- [2] T. Martinez, PhD Thesis, Valencia, 2004, T. Martinez *et al.*, in preparation
- [3] A. G. Griffiths *et al.* Phys. Rev. C 46 (1992) 2228.
- [4] I. Hamamoto *et al.*, Z. Phys. A353(1995) 145.
- [5] P. Sarriguren *et al.*, Nucl. Phys. A 635 (1998) 55.
- [6] E. Nacher *et al.*, Phys. Rev. Lett. 92 (2004) 232501
- [7] E. Poirier *et al.*, Phys. Rev. C 69 (2004) 034307, and P. Dessage and B. Rubio Isolde proposal IS370.
- [8] P. Urkedal, and I. Hamamoto, Phys. Rev. C 58 (1998) R1889
- [9] F. Iachello, Proc. Int. Conf. on Shell Model and Nuclear Structure, A. Covello, ed., World Scientific, Singapore (1989), p. 407 and private communication
- [10] J. P. Elliott and A. P. White, Phys. Lett. 97B (1980) 169; J. P. Elliott and J. A. Evans, Phys. Lett. 101B (1981) 216.
- [11] G. DeAngelis *et al.*, Phys. Lett 415B (1997) 217.
- [12] J. Benlliure, D. Cortina-Gil, private communication

## Proton-Neutron pairing effects in the beta decay of $^{62}\text{Ge}$

A.Gadea, G.deAngelis, N.Marginean, D.R.Napoli, J.J.Valiente-Dobón, Q.Zhong

*INFN-Laboratori Nazionali di Legnaro, Padova, Italy*

E.Farnea, D.Bazzacco, S.Lunardi, R.Marginean

*University and INFN-sezione di Padova, Italy*

A.Bracco, G.Benzoni, F.Camera, B.Million, S.Leoni, O.Wieland

*University and INFN-sezione di Milano, Italy*

Zs.Podolyák, P.H.Regan, W.Gelletly, W.N.Catford, S.Williams

*University of Surrey, UK*

M.Gorska, J.Gerl, H.J.Wollersheim, F.Becker, H.Grawe, L.Caceres, P.Bednarczyk, N.Saitio, T.Saito

*GSI-Darmstadt, Germany*

D.Rudolph, L.L.Andersson, E.K.Johansson

*University of Lund, Sweden*

J. Benlliure, D. Cortina Gil

*University of Santiago de Compostela, Spain*

B.Rubio

*IFIC Valencia, Spain*

A.Algora

*Institute of Nuclear Research, Debrecen, Hungary*

### 1. Introduction

Correlations between pairs of identical particles are very important in many-body systems. Superconductivity and superfluidity are phenomena arising from the interaction between pairs of electrons moving in opposite directions. The superconducting state that is realized in certain materials can be expressed as a freely moving (non-interacting) collection of such strongly correlated “Cooper pairs” and described with Bardeen-Cooper-Schrieffer (BCS) theory. In nuclear physics neutrons and protons couple (separately) in pairs giving rise to nuclear superfluidity: a description in terms of strong correlations involving Cooper pairs is therefore appropriate also here. In the nuclear domain, the strongest interactions involve nucleon pairs that are close in space, reflecting the short range of the nucleon-nucleon force. In addition, nuclei consist of a combination of two fermionic fluids (neutrons and protons) and as a consequence, the nucleons can form four types of Cooper pairs, each of which can be in a state of relative orbital angular momentum zero and hence well correlated in space. The ground states of the majority of nuclei are very well described in terms of superfluid condensates, in which the pairs of nucleons are formed like the Cooper pairs of electrons in superconductors. This is reflected by nuclear binding energies, *e.g.* by odd-even mass differences. To date, only the nuclear superconducting phases associated with Cooper pairs of like nucleon --protons with protons (pp) or neutrons with neutrons (nn)-- have been observed. Whether there also exists a deuteron-like condensate based on strongly correlated isoscalar ( $T=0$ ) np pairs remains an open question. The reason is that in order for a nucleon pair to exploit the short-range nuclear force and form a correlated Cooper pair, the constituent nucleons must occupy orbits within the same valence shell. Such “normal” pairing couples the nucleons in pairs with opposite spins and occupying orbits which are symmetric with respect to time inversion (isovector pairing;  $T=1, S=0$ ).

For proton-rich nuclei, approaching the double shell closure at  $N=Z=50$  ( $^{100}\text{Sn}$ , the heaviest particle stable  $N=Z$  nucleus) the two different types of nucleons occupy very similar orbitals, and there is a very large spatial overlap of their wave functions. Theoretical predictions suggest that np isoscalar pairing in such cases may compete effectively, or perhaps even dominate over, the isovector pairing modes.

Several manifestations of such an isoscalar superconducting state are going to be tested experimentally:

- 1) Enhanced probability to add or remove a spin-one (deuteron-like) np pair.
- 2) The presence of energy gaps in the spectra of odd-odd  $N=Z$  nuclei.

- 3) A new np-coupling scheme replacing seniority coupling for near-spherical nuclei.
- 4) Significantly different behaviour at medium to high spins of rotational bands built on deformed states due to the quenching of the Coriolis anti-pairing effect.
- 5) Enhanced  $\beta$ -decay rates between the ground state of an even-even  $N=Z$  nucleus and the lowest  $I=1$  state of its odd-odd neighbour.

## 2. Proton-Neutron Pairing in $\beta$ -decay process

The role played in  $\beta$ -decay by proton-neutron coherent pairs (bosons) have been extensively discussed by F. Iachello [1,2] in the framework of the proton-neutron boson scheme (IBM-4). The observed properties of the  $\beta$ -decay in light nuclei are consistent with such scheme and it has been suggested the importance of the scheme for heavier nuclei ( $A > 50$ ) close to the  $N=Z$  line.

The Interacting Boson Model (IBM) is a truncation of the shell model to a space built of correlated nucleon pairs exploiting the concept of generalized seniority. In heavy nuclei close to the stability, it considers traditionally only proton-proton and neutron-neutron pairs. In the early 80's it was suggested the necessity to introduce proton-neutron coherent pairs to treat the light nuclei in terms of the IBM [3,4]. Light nuclei, in fact, have almost equal number of protons and neutrons and therefore proton-neutron pairs play a major role in the structure of the nucleus. The same characteristic is present in heavy nuclei in the vicinity of  $N=Z$ .

In the framework of IBM-4, in addition to the proton ( $\pi$ ) and neutron ( $\nu$ ) bosons the proton-neutron isovector  $T=1$   $S=0$  ( $\delta$ ) and isoscalar  $T=0$   $S=1$  ( $\theta$ ) bosons are introduced. In this case the boson space has the following configuration:

$$T=1 \begin{pmatrix} \pi \\ \delta \\ \nu \end{pmatrix} \quad L = 0,2 \quad S=0 \quad J=0,2$$

$$T=0 : [ \theta ] \quad L = 0,2 \quad S=1 \quad J=1; 1,2,3$$

and the  $\beta$ -decay processes can be described as a transition between the boson states:

Fermi decay

$$\beta^+ : \pi \rightarrow \delta \quad \text{or} \quad \delta \rightarrow \nu$$

$$\beta^- : \nu \rightarrow \delta \quad \text{or} \quad \delta \rightarrow \pi$$

Gamow-Teller decay

$$\beta^+ : \pi \rightarrow \theta \quad \text{or} \quad \theta \rightarrow \nu$$

$$\beta^- : \nu \rightarrow \theta \quad \text{or} \quad \theta \rightarrow \pi$$

The low lying part of the Gamow-Teller (GT) strength distribution in medium mass and heavy nuclei will be dominated by boson transitions with one or two states absorbing the majority of the strength.

If proton-neutron pairing survives at all in heavy nuclei, it will be manifest, in the  $\beta$ -decay processes, through large matrix elements (small  $\log ft$  values) of the Gamow-Teller strength. It is well known that single GT fermion transitions in medium mass and heavy nuclei are highly retarded with measured  $\log ft$  values frequently above 4. A clear fingerprint of the presence of proton-neutron pairs will be GT transitions to low lying collective states with  $\log ft < 4$ .

Neutron-proton pairing in such nuclei will give rise to low-lying collective modes with  $J^\pi=1^+$ . These collective modes are associated with spin excitation ( $S=1$ ) and differ from those associated with orbital motion.

In such context a particularly interesting case is the Gamow-Teller  $\beta$ -decay process of even-even nuclei with  $N=Z-2$ . This decay provides information on the structure of the  $1^+$  state in the  $N=Z$  odd-odd nuclei. If

we consider a description of these nuclei in the framework of the IBM-4, one expect superallowed GT transition with  $\log ft$  values around 3 ( $\langle M_{GT} \rangle^2 \sim 1$ ) [1]. The main reason here is that we are dealing with collective transitions in which a  $\pi$  boson is changed into a  $\theta$  boson and a  $\theta$  boson into a  $\nu$  boson. Superallowed  $\beta$ -transitions with such characteristics are observed in light nuclei. The collective states formed by n-p pairs are expected to be at particularly low excitation energy in odd-odd N=Z nuclei. This suggests that the  $\beta$ -decay in the heavy N=Z nuclei might be dominated by this new mode. In Fig. 1 it is schematically described how the  $\beta$ -decay is expected to proceed from a even-even N=Z-2 nucleus to the odd-odd N=Z daughter and then to the even-even N=Z+2.

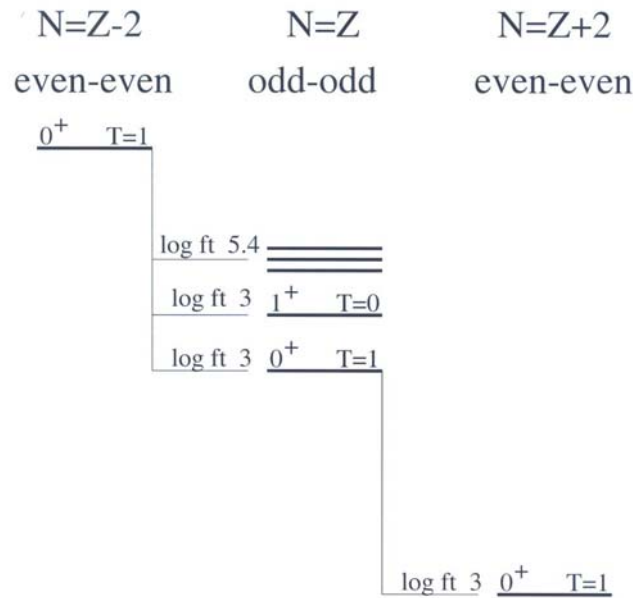


Figure 1. Schematic  $\beta$ -decay of an even-even N=Z-2 and of the odd-odd N=Z nucleus.

### 3. $\beta$ -decay into the N=Z $^{62}\text{Ga}$

The N=Z  $^{62}\text{Ga}$  is a good candidate to investigate the effects of the proton-neutron pairing. Spectroscopic information suggests the major role of this kind of pairing in the structure of this nucleus at high spin [5]. The characteristics of this nucleus and of the Tz=-1 neighbour  $^{62}\text{Ge}$  makes this system ideal for the study of the aforementioned p-n pairing effects in  $\beta$ -decay.

The spectrum of  $^{62}\text{Ga}$  populated in the  $\beta$ -decay of  $^{62}\text{Ge}$  is completely unknown, and the only available information on the  $^{62}\text{Ge}$  ground state is its lifetime with a value of  $T_{1/2}=129(35)\text{ms}$  [6]. Of the same order of magnitude is the lifetime of the  $^{62}\text{Ga}$  ground state ( $T_{1/2}=116\text{ms}$ ). The level scheme of  $^{62}\text{Ga}$  presents a low lying  $1^+$  state at 571 keV excitation energy (see Fig.2)[5,7]. The decay of the  $0^+$  ground state of  $^{62}\text{Ge}$  will proceed by a Fermi transition into the T=1  $0^+$  state in  $^{62}\text{Ga}$  and by a Gamow-Teller transition to the T=0  $1^+$  state. The population of the first  $1^+$  will give information on the degree of collectivity of this state. Additional  $1^+$  states might be identified and will give information about possible mixing, which is expected to be important in heavy nuclei.

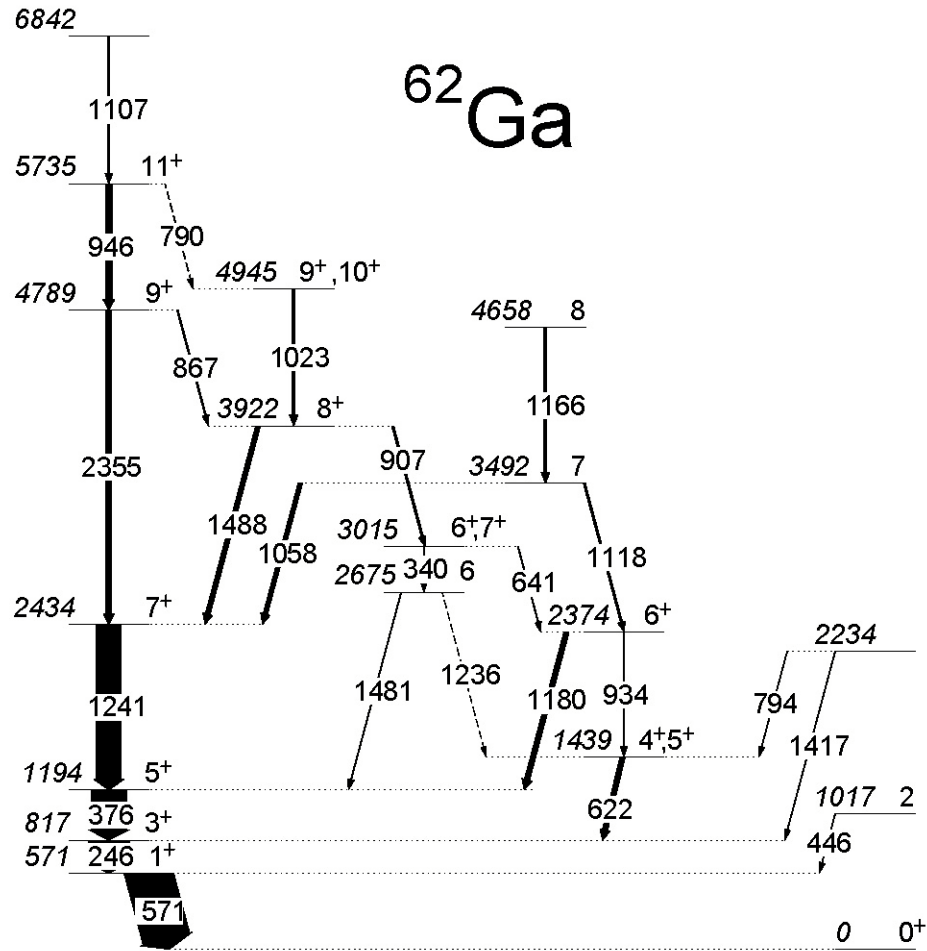


Figure 2. In beam level scheme for  $^{62}\text{Ga}$

#### 4. Experiment

The  $^{62}\text{Ge}$  nucleus will be produced by fragmentation of a  $^{78}\text{Kr}$  beam at  $\sim 400$  MeV/u. The  $^{62}\text{Ge}$  production cross section calculated with EPAX is  $\sim 10^{-7}$  barns. By considering the 20% transmission of the FRS, an intensity of the primary  $^{78}\text{Kr}$  beam of  $\sim 10^9$  atoms/s and a  $1.6\text{g/cm}^2$  Be target, the rate of  $^{62}\text{Ge}$  at the implantation site will be of the order of 2 atoms/s, and with an energy of  $\sim 150$  MeV/u (the ratio between the thickness of the production target and the intensity of the primary beam might be modified if necessary to keep the production rates).

The  $^{62}\text{Ge}$  atoms surviving implantation in the active stopper (95%) will partially decay to the  $0^+$  ground state in  $^{62}\text{Ga}$  and partially to excited states and in particular to the  $1^+$ , at 571 keV excitation energy, which will de-excite by emission of a M1 transition of the same energy to the  $0^+$  ground state. Sequentially the ground state of  $^{62}\text{Ga}$  will decay into the  $0^+$  ground state of  $^{62}\text{Zn}$  through a Fermi transition.

The  $Q_{\text{EC}}$  value of the  $^{62}\text{Ge}$   $\beta^+$ -decay has been estimated to be approximately 10 MeV [8] and therefore more than 90% of the decay will proceed through  $\beta^+$  emission. Therefore, a further discrimination for the surviving  $^{62}\text{Ge}$  will be the two sequential  $\beta^+$  decays within few hundred milliseconds.

The precise measurement of the 571 keV transition intensity, compared with the total number of decays of  $^{62}\text{Ge}$  nuclei will give the logft of the GT transition to the low lying  $1^+$ , and this value will allow to extract important information on the nature of the state.

In the same experiment we will explore the population of other  $1^+$  states that might carry also a consistent fraction of the expected collectivity.

The efficiency of the Rising array in the stopped beams configuration is 11% for a gamma-ray energy of 1.33 MeV and 20% at 662 keV.

The investigation of the decay level scheme will require a minimum of  $\sim 10^5$  decays and therefore, considering the efficiency of the array, the  $^{62}\text{Ge}$  production and the maximum implantation rate ( $>4$  atoms/s), a beam time of 5 days (15 shifts) of measurement will be necessary. The setup of RFD and the different detectors will require an extra day of beam time.

**Total  $^{78}\text{Kr}$  beam time requested: 6 days (18 shifts)**

### References.

- [1] F.Iachello, Proceeding Int. Conf. on Perspectives for the IBM, Padova Italy 1994, p.1
- [2] F.Iachello, Yale University preprint YCTP-N13-88
- [3] J.P.Elliot and A.P.White, Phys.Lett. B97 (1980) 169
- [4] J.P.Elliot and J.A.Evans, Phys.Lett. B101 (1981) 216
- [5] G.deAngelis et al., Nucl.Phys. A630 (1998) 426c
- [6] M.J.Lopez Jimenez et al, Phys. Rev. C 66 (2002) 025803
- [7] D.Rudolph et al., Phys. Rev. C 69 (2004) 034309
- [8] G.Audi et al., Nucl. Phys. A729 (2003) 1

# Isospin Symmetry of Transitions Probed by Weak and Strong Interactions: the beta decay of $^{54}\text{Ni}$ , $^{50}\text{Fe}$ , $^{46}\text{Cr}$ .

Y.Fujita, T.Adachi, H.Matsubara and A.Tamii  
(Osaka University, Osaka, Japan)

B.Rubio, A.Perez, and L.Caballero  
(IFIC, CSIC, Valencia, Spain)

W.Gelletly, Z.Podolyak, P.H.Regan, W.Catford, A.Garnsworthy,  
N.Thompson, S.Williams  
(University of Surrey, Guildford, UK)

A.Algora  
(Inst.for Nuc.Phys., Debrecen, Hungary)

A.Jungclaus  
(Universidad Autonoma de Madrid, Spain)

D.Warner  
(CCLRC, Daresbury, UK)

J.Benlliure, D.Cortina-Gil  
(University of Santiago de Compostela, Santiago, Spain)

P.Van Duppen, M.Huyse, D.Pauwels, M.Sawicka, O.Ivanov and Y.Kudryavtsev  
(University of Leuven, Leuven, Belgium)

M. Gorska, H. Geissel, H. Weick, J. Gerl  
(GSI, Darmstadt, Germany)

Spokespersons: Y.Fujita, B.Rubio and W.Gelletly  
GSI Contact: M.Gorska

**Abstract:-** *The main goal of the proposed experiments is to test Isospin symmetry by a comparison of the Gamow-Teller strength in beta decay and charge exchange reactions. It is proposed to carry out such a test by studying the nuclei with  $A=46$ ,  $50$  and  $54$  in both beta decay, as part of the RISING campaign, and charge exchange at Osaka.*

## The Background:-

One of the cornerstones of nuclear physics is the idea that the nuclear interaction is charge-independent. As a result *isospin* is a good quantum number. If so, this should be reflected in a symmetric structure for states in the isobaric nuclei (isobars) with the same value of  $T$  and having  $\pm T_Z$ , where  $T_Z$  is the  $z$  component of the isospin defined by  $(N - Z)/2$ . Although the concept of isospin is widely accepted, our knowledge of

isospin symmetry, in particular how well it is obeyed, is restricted largely a) to states in the vicinity of the ground state and b) to nuclei of low mass in the sd-shell.

If we now assume that corresponding states in a set of isobars are analogue states then Gamow Teller decays between identical mirror parent nuclei and a common daughter should have identical strengths, in the absence of isospin mixing. As a result it should be possible to test how good isospin symmetry is, by comparing the strengths of corresponding transitions between analogue states. Such a comparison is made easier by choosing transitions which, as a result of quantum mechanical selection rules, select states with specific spin and parity ( $J\pi$ ). The  $\Delta L = 0$ ,  $\Delta S = 1$  transitions induced by the  $\sigma\tau$ -type operator, the so-called Gamow-Teller (GT) transitions, are particularly well suited to this purpose. They are the subject of this proposal.

The most direct way to obtain the transition strengths  $B(GT)$  is from measurements of beta-decay ft values. They are derived from measurements of the Q value, the half-life and the branching ratio of the transition of interest in the beta decay. However we can also determine the  $B(GT)$  values from studies of the corresponding charge exchange reactions. It is well established [1,2] that studies of (p,n) and ( $^3\text{He}$ ,t) reactions at intermediate energies allow us to determine  $B(GT)$  values up high excitation energies in the daughter nucleus. Such studies have the considerable advantage that they are not limited by the Q-window as in beta decay. This is a consequence of the fact that (i) at  $0^\circ$  the momentum transfer is small and hence the  $\sigma\tau$  part of the effective interaction dominates and (ii) the reaction proceeds mainly as a one-step process at these energies. Recently, the poor resolution of the initial (p,n) studies has been overcome by the use of the equivalent ( $^3\text{He}$ ,t) reactions since it is now possible to analyse the triton ejectiles with an energy resolution  $\cong 30$  keV using a magnetic spectrometer in combination with the dispersion matching technique[3,4].

It is possible to measure the  $T_z = 1$  to  $T_z = 0$  transitions in charge exchange reactions on stable nuclei up to the fp-shell. At the same time we can also measure the  $T_z = -1$  to  $T_z = 0$  transitions in beta decay. This is shown in fig.1. To date only a few measurements for light nuclei, such as the  $A = 26$  system[5], have been made. One major limitation is that the beta-decay Q-values are low in these nuclei so the number of excited states populated is small. In the fp-shell, however, the Q-values are larger and, in principle, one can measure  $B(GT)$  values up to higher excitation energies in beta decay, while at the same time the charge exchange studies on stable nuclei are still possible.

We propose here a test of isospin symmetry for the transitions from the ground states of  $T = 1, T_z = \pm 1$  nuclei to excited states of the  $T_z = 0$  isobar. In order to study the isospin symmetry of these transitions, we propose to perform an accurate comparison of Gamow-Teller transitions for the mass  $A = 46, 50$  and  $54$  systems. The relevant ( $^3\text{He}$ ,t) reactions on  $^{54}\text{Fe}$ ,  $^{50}\text{Cr}$  and  $^{46}\text{Ti}$  have been or will be studied with high resolution at RCNP,Osaka. Examples of the spectra recorded at Osaka are shown in figs.2-4.

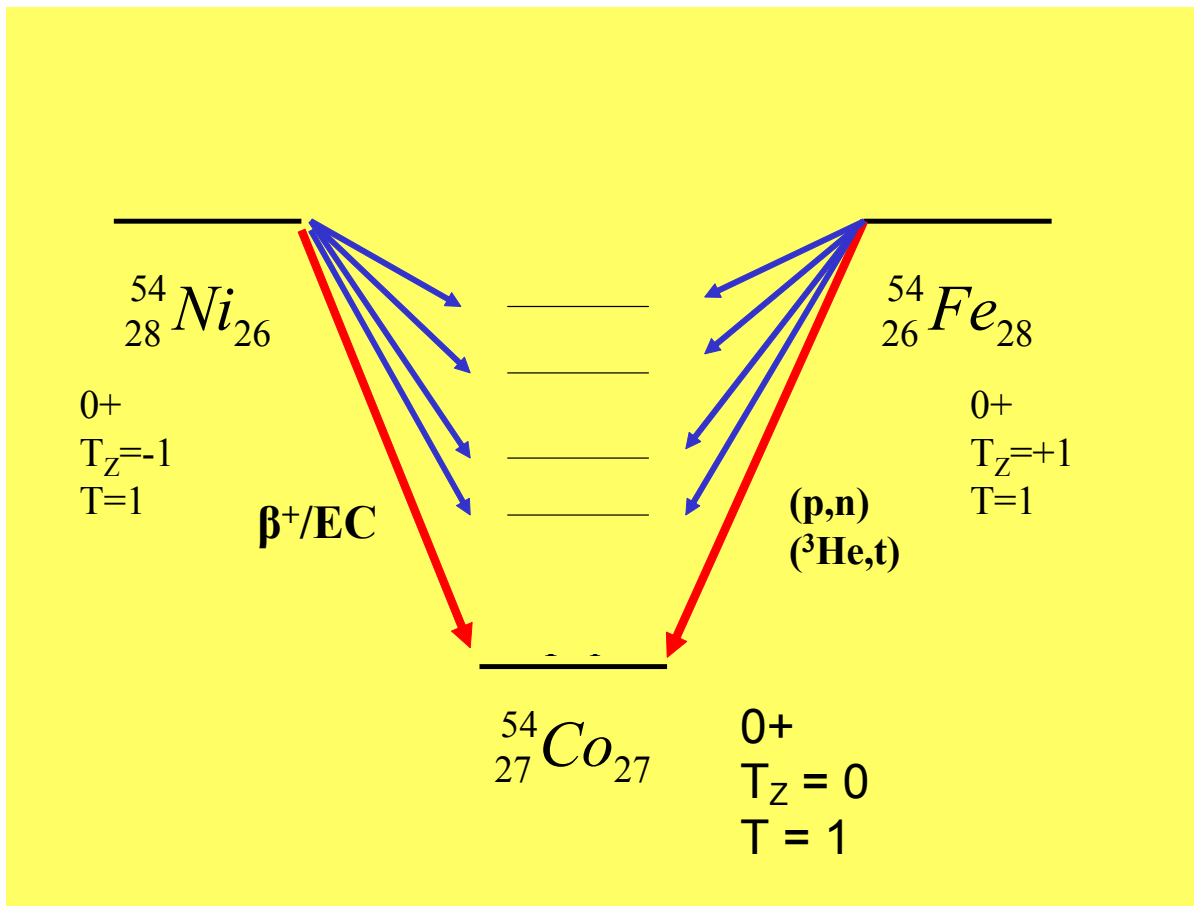


Figure 1:- A schematic illustration of the transitions to levels in the  $N = Z$  nucleus  $^{54}\text{Co}$  by beta decay and charge exchange reactions.

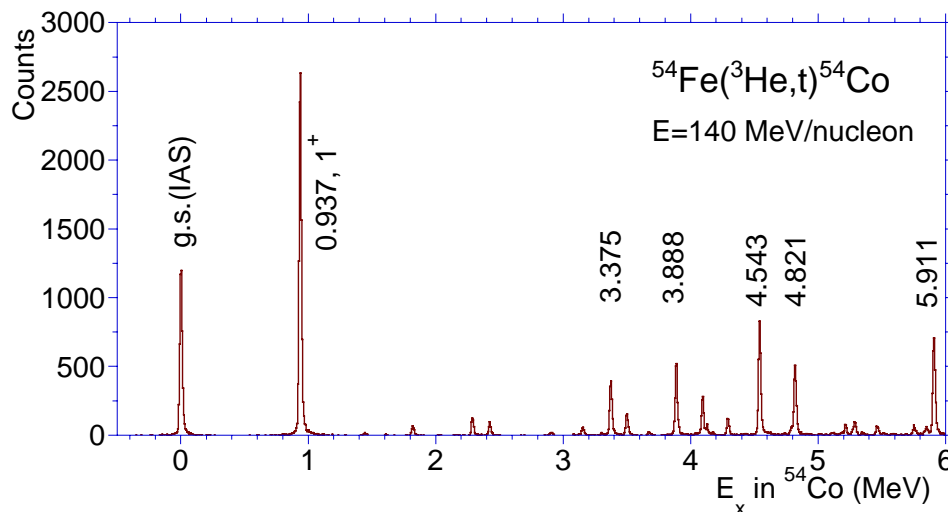
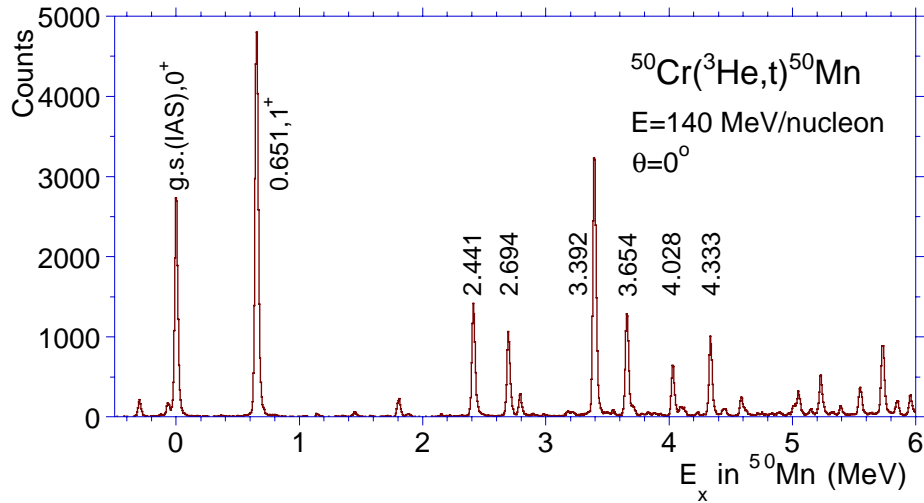
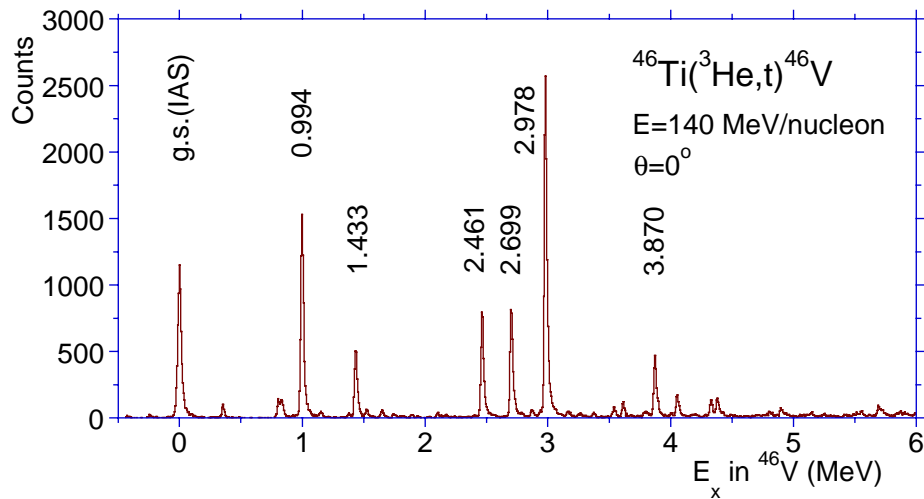


Figure 2:- Part of the  $^{54}\text{Fe}(^3\text{He},t)^{54}\text{Co}$  spectrum recorded with the Grand Raiden spectrometer at Osaka.

It is proposed to study the corresponding beta decays of  $^{46}\text{Cr}$ ,  $^{50}\text{Fe}$  and  $^{54}\text{Ni}$  as part of the RISING Stopped Beam campaign at the FRS. The experimental goals will be to measure the  $B(\text{GT})$  for these decays as a function of energy as precisely as possible for comparison with the strengths measured in the charge exchange reactions.



**Figure 3:- Part of the spectrum of the  $^{50}\text{Cr} (^3\text{He},t)^{50}\text{Mn}$  reaction recorded with the Grand Raiden spectrometer at Osaka.**



**Figure 4:- Part of the spectrum of the  $^{46}\text{Ti} (^3\text{He},t)^{46}\text{V}$  reaction recorded with the Grand Raiden spectrometer at Osaka.**

It should be noted that in the  $(^3\text{He},t)$  reaction, the  $B(\text{GT})$  values for the transitions to states at high excitation rely on the relationship between the  $B(\text{GT})$  value and the cross-section. In the accurate determination of  $B(\text{GT})$  values, the most important task is to find an accurate and reliable "calibration standard". One of the by-products of the proposed experiments is that accurate beta-decay studies will give us the "calibration standard", if we assume that isospin symmetry holds.

In earlier studies[6] of the beta decay of  $^{54}\text{Ni}$  at Louvain-la-Neuve it was established that the 937 keV first excited  $1+$  state in  $^{54}\text{Co}$  is fed in 22.4(4.4)% of the decays. No other gamma rays were seen. This was the first study of this decay and it is important for the present work in that it allows us to establish the amount of feeding we can expect to the various levels in the daughter nucleus from the measured cross-sections in charge-exchange.

The reader should note that absolute  $B(\text{GT})$  values for these nuclei are also of interest to astrophysicists. In the early stages of the collapse of the core in type II supernovae, electron capture and beta decay of  $pf$ -shell nuclei play important roles. Under these extreme conditions the electron capture and

beta decays are dominated by Fermi and allowed GT decays. Thus measurements of the absolute B(GT) values will allow us to place constraints on the core-collapse models of type II supernovae.

### The Measurements:

The charge exchange reactions for the mass  $A = 46, 50$  and  $54$  systems have recently been studied at Osaka. In figs. 2-4 one can see the spectra recorded at  $0^\circ$ . They are of excellent quality and have high resolution. As yet the analysis of these spectra is only at a preliminary stage.

In terms of the beta decays the most important experimental requirement is a sufficiently high intensity and pure beam of the parent nuclei ( $^{54}\text{Ni}$ ,  $^{50}\text{Fe}$ ,  $^{46}\text{Cr}$ ) and an efficient and accurately calibrated beta-gamma detection set-up. It is proposed to produce the separated beams of  $^{46}\text{Cr}$ ,  $^{50}\text{Fe}$  and  $^{54}\text{Ni}$  with a primary beam of  $0.1\text{nA}$  of  $^{58}\text{Ni}$  on a Be target of thickness  $4000\text{ mgcm}^{-2}$ . After passage through the FRS calculations with LISE3 suggest that, with the appropriate settings of slits, magnets etc one will obtain beams of these three parent isotopes with 280, 240 and 190 ions per sec. distributed over an area of about  $4 \times 4\text{ cm}^2$ . The calculations suggest that the beams have essentially no contaminants.

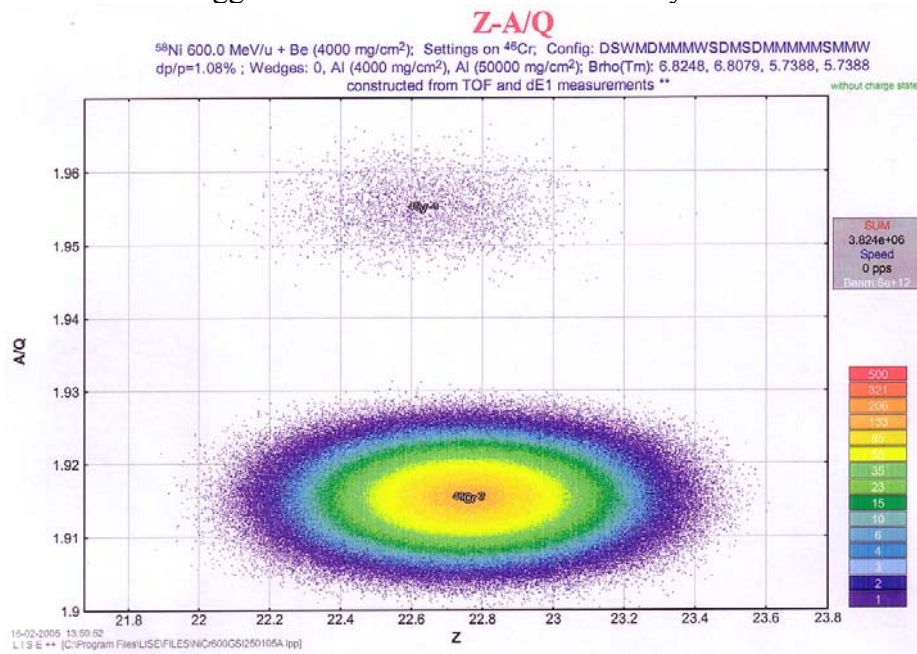


**Figure 5:- The A/Q versus Z plot from LISE3 for a  $^{58}\text{Ni}$  beam on a Be target at 600 MeV/nucleon. The settings have been chosen for the case of  $^{46}\text{Cr}$ , which is seen to be clearly separated from  $^{46}\text{V}$ .**

Figure 5 shows the calculated  $\Delta E$ -A/Q spectrum for the case of  $^{46}\text{Cr}$ . It is clear that it is expected to be very clean. In practice, reactions during implantation will alter this picture but not significantly. Fig.6 shows an example of an on-line spectrum from a recent FRS experiment showing that  $^{55}\text{Ni}$  ions can be readily separated at the focal plane.

The experimental arrangement at the focal plane will be the standard RISING setup with the ions implanted into a double-sided strip detector system (DSSDs) of area  $5 \times 5\text{ cm}^2$  with  $16 \times 16$  strips. The active stopper, the DSSD, will be surrounded by Euroball cluster detectors in close geometry to detect the gamma rays. Fig. 7 shows a schematic view of the overall setup. The overall efficiency of gamma detection will be 11% at 1332 KeV and 20 % at 662 keV.

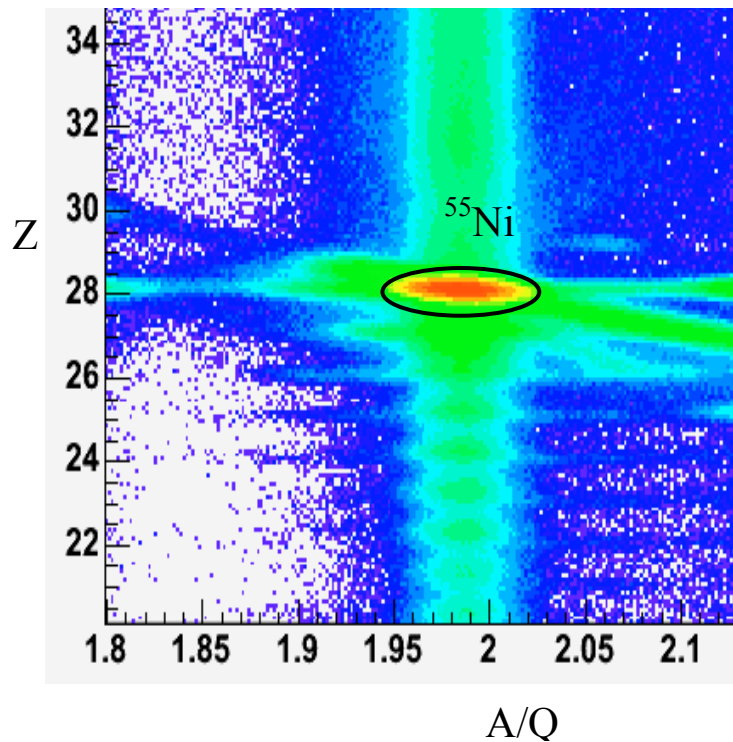


**Figure 6:-The spectrum of ions at the focal plane of the FRS produced in the fragmentation of a  $^{58}\text{Ni}$  beam on a Be target at 600MeV per nucleon. This spectrum was taken on-line.[G.Hammond,M.A.Bentley et al.,private communication]**

Figure 5 shows the calculated  $\Delta E$ -A/Q spectrum for the case of  $^{46}\text{Cr}$ . It is clear that it is expected to be very clean. In practice, reactions during implantation will alter this picture but not significantly. Fig.6 shows an example of an on-line spectrum from a recent FRS experiment showing that  $^{55}\text{Ni}$  ions can be readily separated at the focal plane.

The experimental arrangement at the focal plane will be the standard RISING setup with the ions implanted into a double-sided strip detector system (DSSDs) of area  $5 \times 5 \text{ cm}^2$  with  $16 \times 16$  strips. The active stopper, the DSSD, will be surrounded by Euroball cluster detectors in close geometry to detect the gamma rays. Fig. 7 shows a schematic view of the overall setup. The overall efficiency of gamma detection will be 11% at 1332 KeV and 20 % at 662 keV.

The ions arriving at the detector will be tagged by A and Z in the normal way. Their time of arrival will be correlated with the subsequent detection of the beta particle emitted in the radioactive decay in the same pixel of the DSSD and the beta-delayed gammas which follow. The DSSD will be operated with two sets of electronics in parallel, set on high and low gain in order to be able to detect both the heavy ion and the beta particle. Each event will be time-stamped in order to allow us to determine the correlation in time of the ions, betas and gammas.

If we assume conservatively that the overall efficiency for gamma ray detection is 10% at 1.0 MeV and 5% at 2.0 MeV and that there is a gamma-ray multiplicity of less than two then we can estimate the beta-gamma coincidence rate as  $10^6$  beta-gamma coincidences for the 937 keV level and 1500 counts in the 2010 keV level decay in two days of running. The former was the only gamma ray seen in the study of  $^{54}\text{Ni}$  with a feeding of 22.4(4.4)%. The latter is only seen very weakly in the charge exchange reaction and hence gives us a good measure of how long we need to run if we are to see feeding to the levels of interest.

From the preliminary values of the measured cross-sections in the ( ${}^3\text{He},t$ ) reaction and the feeding of the 937 keV level in the beta decay as measured at Louvain-la-Neuve[6] we can determine the intensities of the decay gamma rays from the 937 and 2010 keV levels as given above. In total we will need 2 days for each isotope. Thus we request 7 days of beamtime for the experiment allowing for the initial setting up and changes of setting for the FRS.

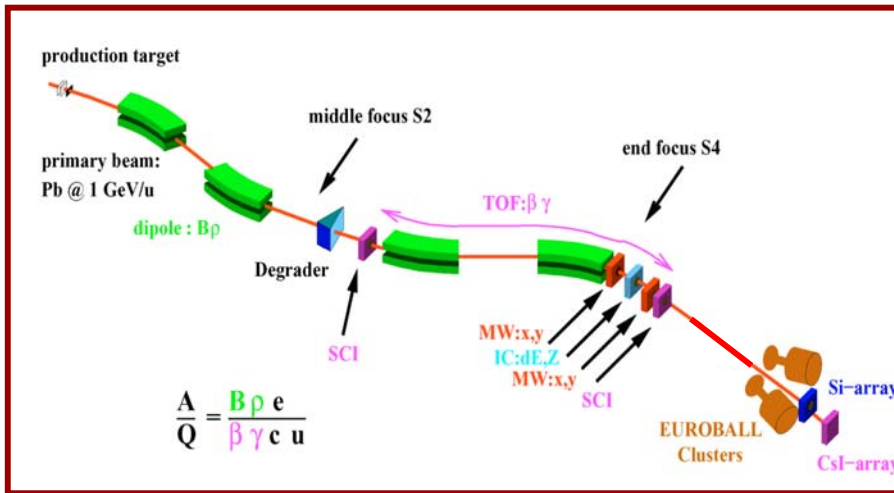


**Figure 7:- Schematic diagram showing the RISING active detector setup at the end of the FRS.**

**References:**

- [1] T.N.Taddeucci et al.,Nucl. Phys. A469 (1987) 125.
- [2] Y.Fujita et al. Phys. Rev. C67 (2003) 064312.
- [3] Y.Fujita et al., Nucl. Instrum. Meth. Phys. Res. B126 (1997) 274, and refs. therein.
- [4] Y.Fujita et al., Nucl. Phys.A687, 311c (2001).
- [5] Y.Fujita et al.,Phys.Rev.C59(1999)90
- [6] I. Reusen et al., Phys. Rev. C 59 (1999) 2416

# Along the N=126 closed shell: nuclei ‘below’ $^{208}\text{Pb}$

Zs. Podolyák<sup>1</sup>, R. Page<sup>2</sup>, J. Jolie<sup>3</sup>, R. Krücken<sup>4</sup>, J. Benlliure<sup>5</sup>, P.M. Walker<sup>1</sup>, P.H. Regan<sup>1</sup>, R. Clark<sup>6</sup>, J. Gerl<sup>7</sup>, H.-J. Wollersheim<sup>7</sup> and the RISING collaboration

<sup>1</sup>University of Surrey, UK; <sup>2</sup>University of Liverpool, UK; <sup>3</sup>University of Köln, Germany; <sup>4</sup>Technical University of München, Germany; <sup>5</sup>University of Santiago de Compostella, Spain; <sup>6</sup>LBL, Berkeley, California, USA; <sup>7</sup>GSI, Darmstadt, Germany

**Abstract:** Excited states have been identified only in two N=126 closed shell nuclei ‘below’  $^{208}\text{Pb}$ :  $^{207}\text{Tl}$  and  $^{206}\text{Hg}$ . We aim to extend our knowledge of the neutron-rich N=126 nuclei by observing isomeric decays in  $^{205}\text{Au}$ ,  $^{204}\text{Pt}$ ,  $^{203}\text{Ir}$  and  $^{202}\text{Os}$  using the RISING setup. It is expected that the following yrast isomeric states are populated in the fragmentation of  $^{208}\text{Pb}$  with sufficient cross section to be observed:  $I^\pi=11/2^-$  (with configuration  $\pi h_{11/2}^{-1}$ ) in the odd-Z  $^{205}\text{Au}$  and  $^{203}\text{Ir}$ ;  $5^-$  ( $\pi s_{1/2}^{-1} h_{11/2}^{-1}$ ) and/or  $7^-$  ( $\pi d_{3/2}^{-1} h_{11/2}^{-1}$ ), and  $10^+$  ( $\pi h_{11/2}^{-2}$ ) in the even-Z  $^{204}\text{Pt}$  and  $^{202}\text{Os}$  nuclei. Proton single-particle energies and polarisation charges will be extracted and the robustness of the N=126 shell-closure will be tested.

## 1. Introduction and motivation

The understanding of how shell structure arises and develops is a major goal in nuclear physics. Nuclei close to the stability line exhibit magic numbers at proton and neutron numbers of 2, 8, 20, 28, 50, 82, 126 etc. By exploring the properties of neutron-rich nuclei it is known that the well established shell structure changes. Evidence for such effects has been observed for N=8,20,28,50 and even 82 [1]. These changes (shell quenching) are generally understood to come from a reduction of the spin-orbit splitting, in other words the Woods-Saxon potential changes towards a harmonic-oscillator type. No such effects have been observed or predicted so far for the N=126 nuclei.

$^{208}\text{Pb}$  with 82 protons and 126 neutrons is a classic shell model core. The present proposal aims to investigate the robustness of the N=126 closed shell, studying E2 polarisability and the shape response of the magic core.

Information on the neutron-rich N=126 nuclei is very scarce. Below the doubly magic  $^{208}\text{Pb}$  nucleus there is experimental information on only three isotones:  $^{207}\text{Tl}$ ,  $^{206}\text{Hg}$  and  $^{205}\text{Au}$ . While in both  $^{207}\text{Tl}$  [3] and  $^{206}\text{Hg}$  [4] excited states have been observed (including isomeric states, see fig. 1), in  $^{205}\text{Au}$  only the ground state is known ( $I^\pi=(3/2^+)$  [2]).

The lack of information on nuclei ‘below’  $^{208}\text{Pb}$  is due to the difficulties in populating these neutron-rich nuclei. However, fragmentation has proved to be an efficient tool to produce exotic nuclear species. When projectile fragmentation is combined with high sensitivity gamma detection arrays, structure information can be gained for otherwise inaccessible nuclei. The highest sensitivity is achieved with the so-called isomer decay

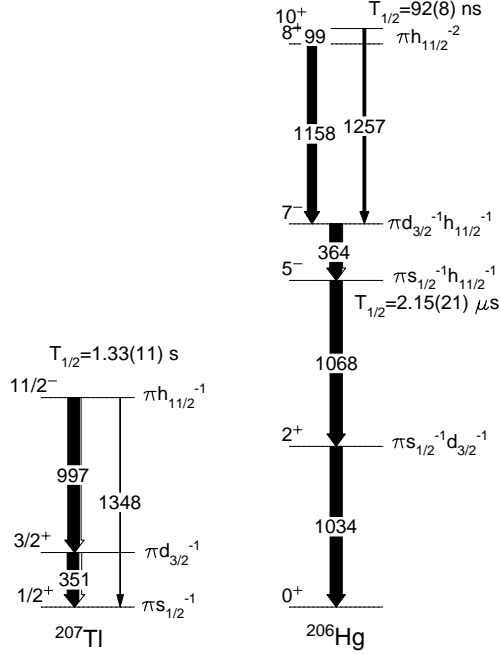


Figure 1: Partial level schemes of the neutron-rich  $N=126$  nuclei (‘below’  $^{208}\text{Pb}$ ) showing the isomers and the states populated by their decay [3, 4]. The configuration of the levels are given. Isomers with similar configurations are expected to be identified as the result of the present proposal in  $^{205}\text{Au}$ ,  $^{204}\text{Po}$ ,  $^{203}\text{Ir}$  and  $^{202}\text{Os}$  nuclei.

spectroscopy. In this technique the delayed gamma rays are correlated with the individually identified ion, therefore there is a minimum of background radiation. Information on the excited states populated in this way can be obtained with only 1000 nuclei produced. In its simple form the technique is sensitive to isomeric decays with lifetimes between 100 ns and 1 ms. The lower limit comes from the flighttime through the fragment separator ( $\approx 300$  ns), the upper limit is from the necessity to correlate the delayed gamma rays with the implanted ion (longer correlation times can be obtained by using active stoppers).

The present proposal seeks to obtain nuclear structure information on four  $N=126$  closed shell nuclei:  $^{205}\text{Au}$ ,  $^{204}\text{Pt}$ ,  $^{203}\text{Ir}$  and  $^{202}\text{Os}$ .

In the yrast structure of the nuclei of interest the following proton single-particle orbitals play a role:  $s_{1/2}$ ,  $d_{3/2}$  and  $h_{11/2}$ . In the even-mass  $^{204}\text{Pt}$  and  $^{202}\text{Os}$  the level schemes should be similar to that of  $^{206}\text{Hg}$  (shown in fig. 1). The  $5^-$  and/or  $7^-$  states with  $\pi s_{1/2}^{-1} h_{11/2}^{-1}$  and  $\pi d_{3/2}^{-1} h_{11/2}^{-1}$  configurations, respectively, could be isomeric. (The  $6^-$  state with  $\pi s_{1/2}^{-1} h_{11/2}^{-1}$  configuration is expected to be non yrast due to the residual interaction.) The existence of isomeric states can be deduced from the systematics of the even- $Z$  platinum isotopes (see fig. 2). In addition we expect a  $10^+$  isomer with the  $\pi h_{11/2}^{-2}$  configuration. This state will decay by a low energy E2 transition to the  $8^+$  state with

the same two proton structure. Since both the  $8^+$  and  $10^+$  states are necessarily pure  $\pi h_{11/2}^{-2}$ , the effective charge of the  $\pi h_{11/2}$  orbital and thus the polarisation charge can be deduced.

The odd- $Z$   $^{205}\text{Au}$  has a ground state with spin-parity  $(3/2^+)$  [2].  $^{203}\text{Ir}$  should have the same  $3/2^+$  or  $1/2^+$  ground state. Both nuclei are expected to have an  $I^\pi=11/2^-$  excited level with  $\pi h_{11/2}^{-1}$  configuration. Since it can decay only via M4 and E5 transitions, with transition strengths close to one Weisskopf unit, this state is isomeric.

In addition, in the same FRS settings, we expect to identify isomeric states in nuclei with  $N=124$  and  $N=125$  (these isomers have similar proton configurations as in the  $N=126$  nuclei).

Figure 3 shows the identification plot and delayed gamma-ray spectrum for  $^{200,201,202}\text{Pt}$  ( $N=122-124$ ) from an experiment performed earlier [5, 6]. (We note that the FRS products were not centred on this region, consequently these nuclei were transmitted with much lower efficiency than normal.)

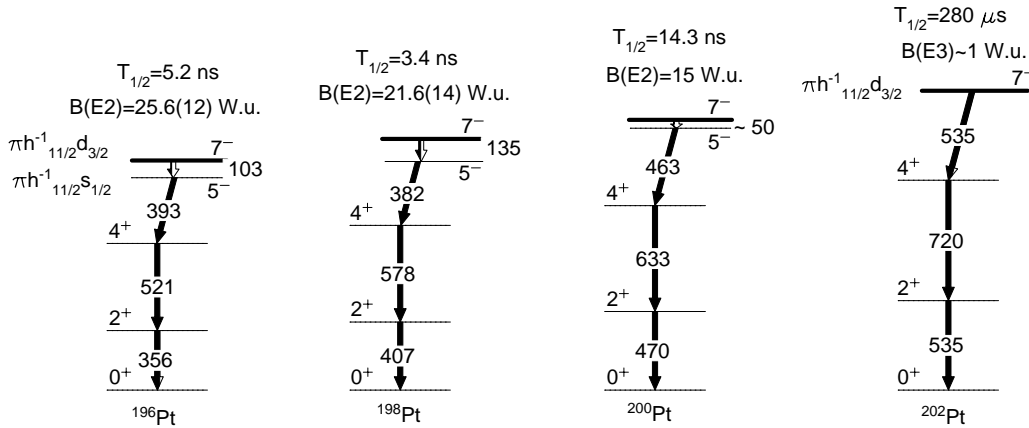
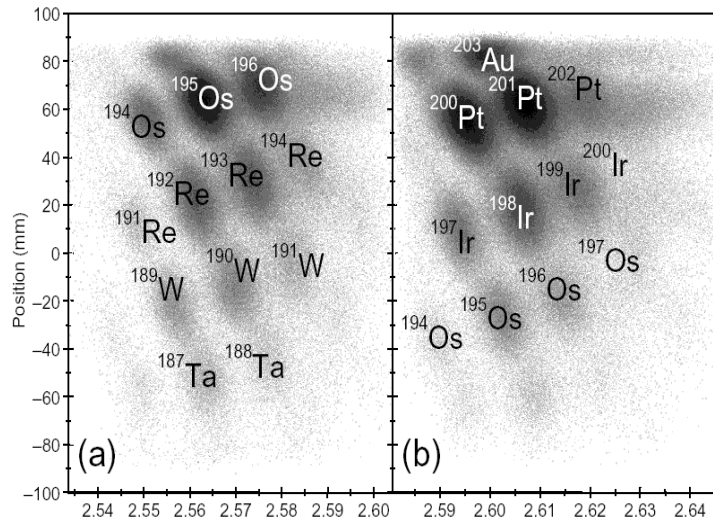


Figure 2: Systematics of isomeric states in even mass Pt isotopes ( $Z=78$ ,  $N=118-124$ ).

## 2. Experiment

The  $N=126$   $^{205}\text{Au}$ ,  $^{204}\text{Pt}$ ,  $^{203}\text{Ir}$ ,  $^{202}\text{Os}$  nuclei will be produced in the fragmentation of a  $^{208}\text{Pb}$  beam. These ions could be produced following the fragmentation of  $^{238}\text{U}$  with comparable production cross sections, but the use of uranium has the disadvantage that the H-like  $^{238}\text{U}$  has exactly the same  $A/q$  ratio as fully stripped  $^{204}\text{Pt}$  ( $238/91=204/78$ ), causing rate problems at the intermediate focal plane of the FRS. The 1 GeV/nucleon  $^{208}\text{Pb}$  beam will be incident on a  $1.6 \text{ g/cm}^2$  Be target ( $1.07 \times 10^{27} \text{ atom/m}^2$ ). The fragment separator will be used in standard achromatic mode with a wedge shape degrader in the intermediate focal plane (S2). The production cross sections can be estimated using both the EPAX (version 2.1) [7] and the COFRA [8] codes. It is believed that in the case of extremely neutron-rich nuclei the COFRA code predicts more reliable cross sections. The rate calculations have been performed using both cross section estimates, with the COFRA predictions given in brackets.  $\sigma(^{205}\text{Au})=7.5$  (13)  $\mu\text{b}$ ,  $\sigma(^{204}\text{Pt})=0.23$  (0.26)  $\mu\text{b}$ ,  $\sigma(^{203}\text{Ir})=7.4 \times 10^{-3}$  ( $3.3 \times 10^{-3}$ )  $\mu\text{b}$ ,  $\sigma(^{202}\text{Os})=2.7 \times 10^{-4}$  ( $0.5 \times 10^{-4}$ )  $\mu\text{b}$ . Considering a primary beam intensity of  $10^8$  ion/s and a typical transmission rate of 50% we obtain the

following yields at the final focal point of the FRS ( $N = \sigma \times I_{beam} \times N_{target}$ ):  $N(^{205}\text{Au}) = 40$  (70) ion/s,  $N(^{204}\text{Pt}) = 1.2$  (1.4) ion/s,  $N(^{203}\text{Ir}) = 2.4$  (1.0) ion/min,  $N(^{202}\text{Os}) = 5$  (1) ion/hour.



# Shape co-existence and the possibility of X(5) behaviour in neutron-rich $A \sim 110$ nuclei.

A.M.Bruce, D.Judson, M.J.Taylor.  
School of Engineering, University of Brighton.  
R.M.Clark.

Nuclear Science Division, Lawrence Berkeley National Laboratory.  
Zs. Podolyak, P.H.Regan, P.M.Walker.  
Centre for Nuclear and Radiation Physics, University of Surrey.

## 1. Introduction.

We propose to study neutron-rich isotopes in the  $A \sim 110$  region using projectile-fission fragmentation at GSI. There are 2 clear aims: a) to look for shape co-existence between prolate and oblate configurations, which are predicted [1,2] to exist in this region; b) to look for X(5) critical point nuclei [3] which are also predicted [4] to exist in this region.

## 2. Motivation.

### 2.1 Shape coexistence in neutron-rich $A \sim 110$ nuclei.

A recent paper, analysing the properties of the Nilsson potential [5], concludes that the relative occurrence of oblate and prolate ground-states is sensitive to the detailed form of the potential and provides a crucial test of the strength of the spin-orbit force. Global shape calculations predict [2] that the region of neutron-rich  $A \sim 110$  nuclei is one where nuclei with both oblate and prolate ground-states are expected to exist. Further calculations by Xu et. al., [1] predict that the oblate shape is stabilised (i.e the oblate potential well becomes deeper) by the addition of angular momentum due to the rotational alignment of pairs of  $g_{9/2}$  protons and  $h_{11/2}$  neutrons.

Of particular interest for this proposal are the predictions for the existence of multi-quasiparticle states in this same mass region. The calculations indicate prolate two-quasineutron states in the heavy zirconium nuclei  $^{112,114}\text{Zr}$ , both of which are predicted to have oblate ground states, and oblate two-quasiproton states in the  $N=66$  nuclei  $^{100}\text{Se}$ ,  $^{102}\text{Kr}$ ,  $^{104}\text{Sr}$  and  $^{106}\text{Zr}$ , all of which are predicted by Xu [1] to have prolate ground states. Skalski [2] predicts that the first two will have oblate ground states and the latter two prolate ground states. Figure 1 shows the location of these states. The grey shaded boxes indicate stable nuclei while the red line marks the limit of nuclei in which excited states have been observed. The purple boxes indicate nuclei where oblate  $\nu 9/2^- [514] \otimes \nu 5/2^+ [420]$ ,  $K^\pi = 5^-$  states have been predicted to exist with excitation energies ranging from 1.4 MeV ( $^{112}\text{Pd}$ ) to 3.0 MeV ( $^{104}\text{Sr}$ ). The light green boxes indicate nuclei where prolate  $\nu 7/2^- [523] \otimes \nu 5/2^+ [402]$   $K^\pi = 6^-$  and  $\nu 9/2^- [514] \otimes \nu 5/2^+ [420]$   $K^\pi = 7^-$  states have been predicted to exist with excitation energies around 2.0 MeV.

Although  $^{114}_{40}\text{Zr}_{74}$  is predicted to have an oblate ground state, the removal of only 8 neutrons leads to the nucleus  $^{106}_{40}\text{Zr}_{66}$  which is one of a range of  $N=66$  nuclei calculated to have a prolate ground state [1]. Thus the removal of only 4 pairs of particles can have a marked change on the predicted shape. The observation of the details of such shape changes would give much quantitative information about the details of the relative energies of the Nilsson orbits and the Fermi surface. It would also have implications for the mean-field potentials used to calculate the nuclear shape and the configuration-constrained calculations used to calculate the multi-quasiparticle states.

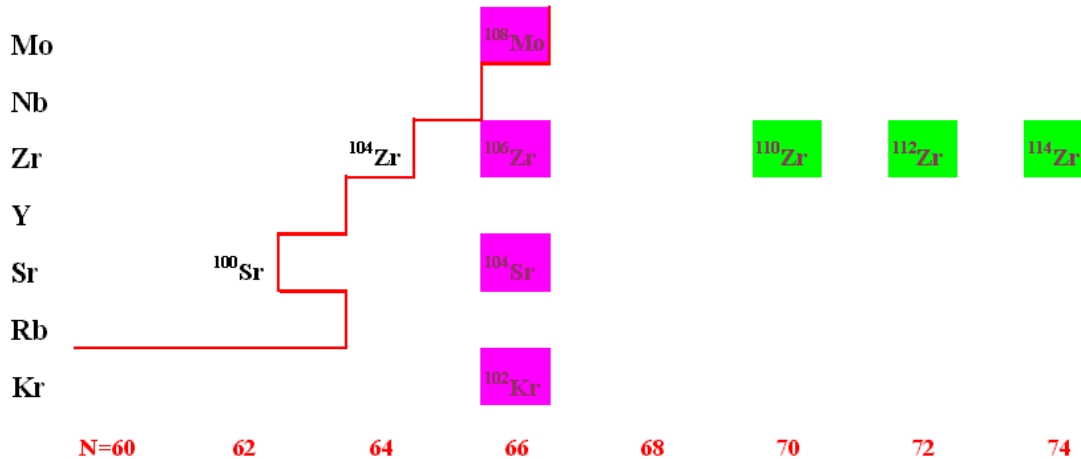


Figure 1: The location of predicted multi-quasiparticle states in this region [1]. Prolate multi-quasiparticle states are predicted in  $^{110,112,114}\text{Zr}$  and oblate multi-quasiparticle states in even-even  $N=66$  nuclei from  $^{100}\text{Se}$  to  $^{112}\text{Pd}$ . The red line marks the limit of nuclei in which excited states have been observed (see text for details).

## 2.2 X(5) Critical point nuclei.

Benchmarks of collective nuclear behaviour are the harmonic vibrator [6], axially deformed rotor [7], and triaxially soft rotor [8]. They correspond to limits of the interacting boson model (IBM) and an algebraic description of the nature of the transition between these limits has been developed in direct analogy with classical phase transitions [9]. Recently, it has been suggested that a useful approach is to find an analytic approximation of the critical point of the shape change as a new benchmark against which nuclear properties can be compared [3].

The critical-point of the transition from a symmetrically deformed rotor to a spherically harmonic vibrator, denoted as X(5), involves the solution of the Bohr collective Hamiltonian with a potential that is decoupled into two components - an infinite square well potential in the quadrupole deformation parameter,  $\beta$ , and a harmonic potential well for the triaxiality deformation parameter,  $\gamma$ . This is an approximation of the true potential found at the critical point of the shape change from IBM calculations [3]. Several examples of nuclei close to the X(5) critical point have been suggested including some of the  $N=90$  isotones, and  $^{126}\text{Ba}$  and  $^{130}\text{Ce}$  [10–12]. However not all the predicted characteristics of X(5) are reproduced and the applicability of the description is still a topic of considerable debate [13].

A recent paper [4] pointed out that a necessary condition for X(5) behaviour is that the number of interactions between valence protons and neutrons is sufficient to induce collective characteristics but not so large as to push the nucleus to full rotational behaviour. This is reflected in the P-factor [14]  $P = N_p N_n / (N_p + N_n)$  where  $N_p$  and  $N_n$  are the numbers of valence protons and neutrons, respectively. Substantial collectivity occurs when the total strength of the p-n valence interactions becomes comparable to the pairing strength, which occurs when  $P > 5$ . Therefore, the loci of nuclei with  $P \sim 5$

are likely to be shape transitional, and may be candidates for X(5) behaviour. This was found to be true for the heavier X(5) candidate nuclei.

The neutron-rich Mo-Zr region also encompasses a locus of nuclei with  $P \sim 5$ . The 2nd column of tables 1 and 2 indicates the value of  $N_p N_n / (N_p + N_n)$  for a selection of nuclei in this region. The decay of high-spin isomeric states, populated in the proposed experiment, will feed the yrast (and possibly non-yrast) sequences of several nuclei of interest. This enables the measurement of quantities, such as energy ratios in the yrast sequence, which should be characteristic of critical-point behaviour. By definition, critical-point behaviour occurs rarely and it is very important to find examples. However, it should be noted that the study of shape transitional nuclei is of considerable interest regardless of the applicability of the critical-point descriptions.

### 3. Experimental details.

The neutron-rich nuclei of interest are difficult to study experimentally but a possible handle is via decay of isomeric states. The existence of the multi-quasiparticle states mentioned earlier provide the possibility of isomerism in these nuclei. In particular, in  $^{106}\text{Zr}_{66}$ , the calculations [1] predict an prolate  $0^+$  ground state and an oblate 2-quasineutron configuration ( $\nu 9/2^- [514] \otimes \nu 1/2^+ [420]$ ) of spin  $5^-$  at an excitation energy of 2.7 MeV. The configuration-constrained potential energy surface calculated for the oblate configuration in  $^{106}\text{Zr}$  is shown in figure 2. The ground state of  $^{106}\text{Zr}$  is predicted to have a  $\beta_2$  deformation of 0.34 [1] or 0.37 [2] which would correspond to an excitation energy of 1400 keV for the  $J^\pi = 6^+$  state of the ground state band. If the  $K^\pi = 5^-$  state decays to this  $J^\pi = 6^+$  state by an E1 transition, a transition rate of 1 W.u. would correspond to a half-life for the state of  $\sim 1.5 \times 10^{-16}$  seconds. The combination of the typical retardation of an E1 transition (by a factor of  $10^4$ ) and the retardation due to the K hindrance of the transition, lead to the expectation of a lifetime for the state in the microsecond region. It is this isomerism which gives the chance of studying these very neutron rich nuclei.  $^{106}\text{Zr}$  has an  $N_p N_n / (N_p + N_n)$  ratio of 6.15 so is a prime candidate for X(5) behaviour. The decay of the isomer would feed exactly the states which are of interest for the X(5) work.

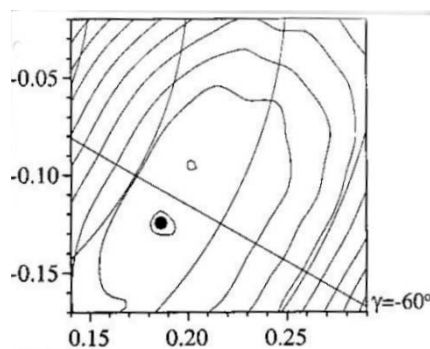


Figure 2: Configuration-constrained potential energy surface [1] for the  $\nu 9/2^- [514] \otimes \nu 5/2^+ [420]$ ,  $K^\pi = 5^-$  state in  $^{106}\text{Zr}$ .

Production rates for the zirconium nuclei in the projectile-fission of  $^{238}\text{U}$  indicate [15] that it will be possible to make spectroscopic measurements for Zr nuclei up to and including  $A=108$ . Bernas et al., [15] indicate a cross-section 100 nb for  $^{108}\text{Zr}$  produced in the projectile fission of 750.A MeV  $^{238}\text{U}$  on  $^9\text{Be}$ . Using a beam current of  $10^8$   $^{238}\text{U}$  particles

Table 1: First attempt at estimating production rates for Zr nuclei using a beam current of  $10^8$   $^{238}\text{U}$  particles per second, a  $2\text{ g/cm}^2$   $^9\text{Be}$  target and an FRS efficiency of 2%.

Nuclide	$N_p N_n$ $N_p+N_n$	cross-section (nb)	fragment rate per second at the focal point	number of gammas [a] per shift
$^{104}\text{Zr}$	5.83	1000000 [b]	267	57600
$^{106}\text{Zr}$	6.15	10000 [b]	2.67	576
$^{108}\text{Zr}$	5.83	100	0.027	5.76
$^{110}\text{Zr}$	5.45	0.4	0.0001	0.023
$^{112}\text{Zr}$	5.00	0.004 [c]	$1 \times 10^{-6}$	0.00023

[a] Calculated assuming a 10% isomeric ratio and an efficiency [18] of 7.5% for RISING.

[b] Calculated assuming a factor of 10 increase in the cross-section for every fewer nucleon from the measured cross-section (100 nb) for  $^{108}\text{Zr}$  [15].

[c] Calculated assuming a factor of 10 reduction in the cross-section for every additional nucleon from the measured cross-section (0.4 nb) for  $^{110}\text{Zr}$  [15].

Table 2: First attempt at estimating production rates for N=66 isotones using a beam current of  $10^8$   $^{238}\text{U}$  particles per second, a  $2\text{ g/cm}^2$   $^9\text{Be}$  target and an FRS efficiency of 2%.

Nuclide	$N_p N_n$ $N_p+N_n$	cross-section (nb)	fragment rate per second at the focal point	number of gammas [a] per shift
$^{100}\text{Se}$	4.36	$2 \times 10^{-6}$ [b]	$5.33 \times 10^{-10}$	$1.15 \times 10^{-7}$
$^{102}\text{Kr}$	5.33	0.005 [b]	$1.33 \times 10^{-6}$	$2.9 \times 10^{-4}$
$^{104}\text{Sr}$	6.15	6.6 [15]	$1.76 \times 10^{-3}$	0.38
$^{106}\text{Zr}$	6.15	10000 [b]	2.67	576
$^{108}\text{Mo}$	5.33	$2.4 \times 10^7$ [b]	6400	1382400

[a] Calculated assuming a 10% isomeric ratio and an efficiency [18] of 7.5% for RISING.

[b] Calculated assuming a factor of 10 difference in the cross-section for a change of 1 in nucleon number from the measured cross-section [15].

per second, a  $2\text{ g/cm}^2$   $^9\text{Be}$  target and an FRS efficiency of 2%, this gives  $\sim 0.027$   $^{108}\text{Zr}$  particles per second arriving at the focal point of the FRS. If we assume that RISING has an efficiency of 7.5% [18] and that the isomeric ratio is 10% then this will give about 5 gammas per shift. Due to the cleanliness of the spectrum, a peak can be identified with  $\sim 100$  counts so 20, 8 hour shifts (i.e. 1 week of run time) would be sufficient to measure  $^{108}\text{Zr}$ . Table 1 shows the rates expected for even-even zirconium nuclei ranging from  $^{104}\text{Zr}$  to  $^{112}\text{Zr}$ . The cross-sections for  $^{108}\text{Zr}$  and  $^{110}\text{Zr}$  have been measured [15] and those for the other nuclei have been estimated assuming the cross-section changes by a factor of 10 for a change of 1 nucleon.

Although the calculations focus on the zirconium nuclei, it is expected that analogous 2 quasiparticle states will be found in neighbouring nuclei. Each experiment is sensitive to  $\sim 30$  nuclei. Table 2 shows the rates expected for the N=66 isotones mentioned earlier.

Delayed spectroscopy of  $A \sim 180$  nuclei has recently been studied using fragmentation of  $^{208}\text{Pb}$  at 1 GeV/nucleon and the results [16, 17] indicate experimental sensitivity to isomers with half-lives up to  $\sim 1$  ms.

The results will have an impact on astrophysicists since the modeling of astrophysical

processes relies heavily on the detailed knowledge of the level schemes and shapes of r-process nuclides. The existence of isomers can have a major effect on calculations of the r-process path [19]. The structure of nuclei in the r-process plays a significant role in the solar elemental abundances for nuclei with  $A \geq 60$ .

## References

- [1] F.R.Xu et al., Phys. Rev. **C65** (2002) 021303(R).
- [2] J.Skalski et al., Nucl. Phys. **A617** (1997) 282.
- [3] F.Iachello, Phys. Rev. Lett. **87** (2001) 052502.
- [4] E.A.McCutchan et al., Phys. Rev. **C69** (2004) 024308
- [5] N.Tajima and N.Suzuki, Phys. Rev. **C64** (2001) 037301.
- [6] G. Scharff-Goldhaber and J. Weneser, Phys. Rev. **98** (1955) 212.
- [7] A. Bohr, Mat. Fys. Medd. K Dan. Vidensk. Selsk. **26** (1952) 1.
- [8] L. Wilets and M. Jean, Phys. Rev. **102** (1956) 788.
- [9] A.E.L. Dieperink et al., Phys. Rev. Lett. **44** (1980) 1747.
- [10] R. Kruecken et al., Phys. Rev. Lett. **88** (2002) 232501.
- [11] R.F. Casten and N.V. Zamfir, Phys. Rev. Lett. **87** (2001) 052503.
- [12] R.M. Clark et al., Phys. Rev. **C68** (2003) 037301.
- [13] R.M. Clark et al., Phys. Rev. **C67** (2003) 041302(R); **C68** (2003) 059801.
- [14] R.F. Casten et al., Phys. Rev. Lett. **58** (1987) 658.
- [15] M.Bernas et al., Phys. Lett. **B415** (1997) 111.
- [16] Zs.Podolyák, A.M.Bruce et al., Phys. Lett. **B491** (2000) 225.
- [17] M.Pfützner, A.M.Bruce et al., Phys. Rev. **C65** (2002) 064604.
- [18] J.Simpson, private communication.
- [19] G.Martínez-Pinedo et al., Phys. Rev. Lett. **83** (1999) 4502.

# Establishing the deformation of proton drip-line nuclei using projectile fragmentation.

D.M. Cullen, D.T. Scholes, S.V. Rigby, A.M. Kishada, J.F. Smith, K. Shehzad.  
*University of Manchester, Manchester M13 9PL, U.K.*

H.J. Wollershiem, M. Gorska and the FRS Collaboration.  
*Gesellschaft für Schwerionenforschung, Planckstr. 1, D-64291, Darmstadt, Germany.*

C. Scholey.  
*Department of Physics, University of Jyväskylä, Jyväskylä, Finland.*

P.H. Regan, Z. Podolyak, G. Jones, P.M. Walker.  
*Department of Physics, University of Surrey, Guildford, Surrey, GU2 7XH, U.K.*

H. Mach  
*The Studsvik Nuclear Research Lab., Uppsala University, S-61182 Nyköping, Sweden.*

We propose to test whether the predicted  $8^-$  isomeric state in  $^{142}\text{Er}$  can be established using projectile fragmentation with the unique combination of the FRS coupled with the RISING array of Ge detectors. We will first test the accuracy of the EPAX production cross section estimates for  $^{140}\text{Dy}$  at the proton drip line before considering searching for the  $8^-$  isomeric state in  $^{142}\text{Er}$ . The decay of these isomers delineate the yrast bands of drip-line nuclei at the FRS focal plane. Their deformations can then be directly measured using the fast-timing method on the delayed yrast  $\gamma$  rays with a series of  $\text{BaF}_2$  detectors. The deformation of these proton drip-line nuclei have recently been the subject of much theoretical discussion since they have been used to characterise and understand the lifetime tunnelling estimates for proton decays, for example in  $^{141}\text{Ho}$ . Population of these isomers using the fragmentation technique was successfully employed near the proton drip-line to populate the  $8^-$  isomer in  $^{138}\text{Gd}$  using a  $^{208}\text{Pb}$  fragmentation reaction at the FRS with only 1 shift of beam time.

## I. INTRODUCTION

A series of  $8^-$  isomeric states are known in all of the *even-even*  $N=74$  isotones,  $^{128}_{54}\text{Xe}$  [1],  $^{130}_{56}\text{Ba}$  [2],  $^{132}_{58}\text{Ce}$  [3],  $^{134}_{60}\text{Nd}$  [4],  $^{136}_{62}\text{Sm}$  [5] and  $^{138}_{64}\text{Gd}$  [6] with differing half-lives ranging from nanoseconds (Xe) to milliseconds (Ba,Ce). Recently, with an experiment at Argonne National Laboratory we were able to extend this chain of measurements right up to the proton drip line. In that experiment an  $8^-$  isomeric state was established in the  $N = 74$  isotone  $^{140}_{66}\text{Dy}$  [7,8].

The importance of measuring nuclei at the proton drip line is that they can determine information about the structure of these nuclei. For example, measurement of the decay half-lives gives information that the ground states of these nuclei are deformed [9]. In addition, our previous experiment on  $^{140}\text{Dy}$ , the daughter of the deformed proton emitter  $^{141}\text{Ho}$ , defined the role of deformation in the proton emission process. This work also supported the previous assignments of single-particle configurations to the two proton emitting states in  $^{141}\text{Ho}$  [7]. The measurement of the isomeric half-life and excitation energy provides one of the few tests of the applicability of the concept of  $K$ -forbiddenness at the proton drip-line and gives additional information about the shape of  $^{140}\text{Dy}$ .

In order to predict the locations of these  $8^-$  isomeric states a series of Woods-Saxon constrained shape polarisation calculations have been performed [11]. These theoretical predictions have, as far as they go, turned out to be quite accurate. For  $^{140}\text{Dy}$  the isomer was predicted to have an excitation energy of 2.15 MeV [12] which compared well with that of the subsequent experimental measurement of 2.16 MeV [7,8]. More recently, these calculations have predicted the existence of a  $K^\pi = 8^-$  isomeric state in  $^{142}\text{Er}$  at 2.20 MeV excitation energy and deformation  $\beta_2=0.25$  [13]. Figure 1 shows the systematics of the yrast  $0^+$ ,  $2^+$ ,  $4^+$ ,  $6^+$ ,  $8^+$  and the  $K^\pi = 8^-$  states across the N=74 chain of isotones, from  $^{130}\text{Ba}$  to  $^{140}\text{Dy}$ . It can be seen that the excitation energy of these yrast states falls with mass number from A=130 to A=140 as the deformation increases. (Note the fall of the  $2^+$  state excitation energy from  $^{130}\text{Ba}$  to  $^{140}\text{Dy}$ .) The prediction for the  $K^\pi = 8^-$  isomers in  $^{136}\text{Sm}$ ,  $^{138}\text{Gd}$ ,  $^{140}\text{Dy}$  and  $^{142}\text{Er}$  are also shown. The systematic trend for the excitation energy of these states are in reasonable agreement with these predictions. However, the predictions show an increasing trend for the isomer excitation energy with mass number while the experimental values are decreasing. In some ways, the measurement of  $^{142}\text{Er}$  is the critical nucleus. The intersection of these experiment and theoretical curves occurs at  $^{140}\text{Dy}$  and a measurement of  $^{142}\text{Er}$  will reveal the true trend and can thereby be used to refine the accuracy of the theoretical predictions at the proton drip line.

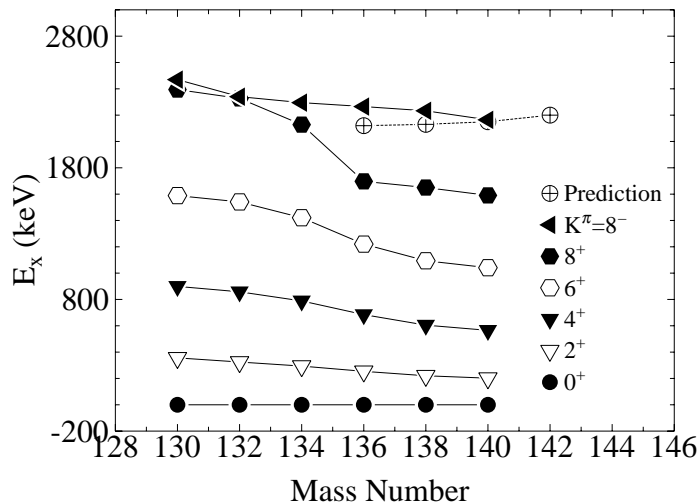


FIG. 1. Excitation-energy systematics of the  $0^+$ ,  $2^+$ ,  $4^+$ ,  $6^+$ ,  $8^+$  and  $K^\pi = 8^-$  states across the N=74 chain of isotones. The predicted values are also shown for  $^{136}\text{Sm}$ ,  $^{138}\text{Gd}$ ,  $^{140}\text{Dy}$  and  $^{142}\text{Er}$ .

The systematic trend of the lifetimes of the  $K^\pi = 8^-$  isomeric states across the N=74 isotone chain show a similarly slow mass dependence [7]. (The half-life of  $^{138}\text{Gd}$  and  $^{140}\text{Dy}$  are  $6\mu\text{s}$  and  $7\mu\text{s}$ , respectively.) Based on these half-lives, the expected lifetime for the  $K^\pi = 8^-$  isomeric state in  $^{142}\text{Er}$  is about  $3\text{--}6\mu\text{s}$ . This lifetime range is well suited for the flight time through the FRS. The predicted excitation energy of the isomer is also well suited for these measurements since it is also similar to that of the  $K^\pi = 8^-$  isomer in  $^{140}\text{Dy}$  and its decay is expected to yield 5  $\gamma$  rays with a similar energy range (200-800 keV) to those involved in the decay of  $^{140}\text{Dy}$ .

With this new proposal, we will use a fragmentation reaction at GSI to establish the  $8^-$  isomeric state in the most proton rich N=74 nucleus  $^{142}_{88}\text{Er}$ . This experiment cannot be done with a fusion-evaporation reaction. However, from previous experience we know that the  $8^-$  isomer in  $^{138}\text{Gd}$  was populated with a  $^{208}\text{Pb}$  fragmentation reaction with one-shift of beam time at the FRS, see Fig. 2.

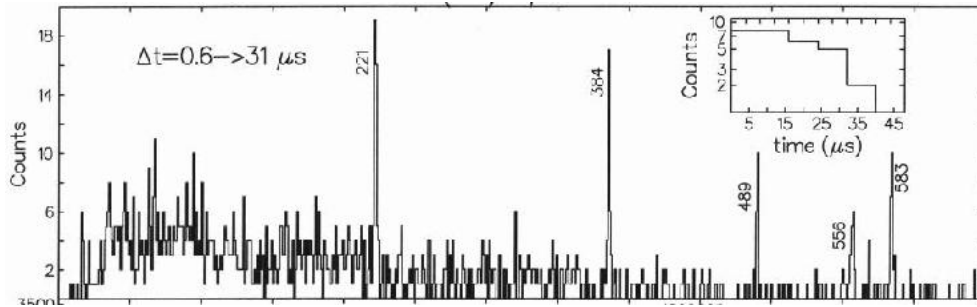


FIG. 2. The decay of the  $6\mu\text{s } 8^-$  isomeric state through the delayed yrast band in  $^{138}\text{Gd}$  produced from 1 shift of  $^{208}\text{Pb}$  fragmentation data.

The predicted cross section from EPAX [10] is  $3\times 10^{-6}$  barns for  $^{138}\text{Gd}$ . In comparison, the experimental cross section estimated from the spectrum shown in Fig. 2 is  $2\times 10^{-7}$  barns with a fairly large uncertainty. (This assumes there were 55 counts in a peak in 1 shift, a  $1.6\text{g}/\text{cm}^2$  target, a beam current of  $10^9$  particles/spill with 3 spills per minute, a  $\gamma$ -ray efficiency of 5%, an isomeric ratio of 5% and an FRS transmission of 70%.) This suggests that the experimental cross section for  $^{138}\text{Gd}$  is reasonably well predicted by the EPAX code. How this translates to the next  $N=74$  isotones  $2n$  ( $^{140}\text{Dy}$ ) and  $4n$  ( $^{142}\text{Er}$ ) nearer the proton dripline will be tested with this proposed experiment.

## II. PHYSICS GOALS OF THIS PROPOSAL

We plan to calibrate and setup on the known isomer in  $^{138}\text{Gd}$ , see Fig. 2 and then try to establish the known isomer in  $^{140}\text{Dy}$  before we consider changing the settings to  $^{142}\text{Er}$ . In this way we will testing the predictive power of Woods-Saxon configuration-constrained shape polarisation calculations [11] at the proton drip-line, and also several other physics issues will be addressed with this proposal:

### (i) Testing EPAX cross sections at the proton drip line.

One of the points of this experiment is to test the EPAX cross sections in this region of nuclei far from stability. There have been no cross section measurements for beams between Xe and Pb for these proton-rich nuclei. The lightest Gd isotope measured, prior to the previous test experiment on  $^{138}\text{Gd}$ , was  $^{145}\text{Gd}$  whose cross section was of the same order as that predicted from EPAX. The lightest Dy isotope measured is  $^{148}\text{Dy}$  with a cross section of 1.6mb. With this experiment we will, at the very least, obtain measurement points to compare with the EPAX cross sections and gain a feeling for what can be done with in this region. In particular, it would be very useful to obtain a cross section for  $^{142}\text{Er}$  which could even be obtained from a few counts in the particle-id spectrum alone.

### (ii) Map out the Proton drip-line in this region.

Since each setting of the FRS produces many nuclei then by searching for the new isomeric states in  $^{142}\text{Er}$  we will also obtain information about the neighbouring nuclei and in so doing be able to map out the proton dripline in this region. As well as  $K$ -isomers, many spin or shell-model isomers are known in this region. This information will be significant because no information is known about these exotic nuclei at the proton drip-line and they cannot be made in other types of reactions.

### (iii) Improved half-life measurement for $^{140}\text{Dy}$ .

The half-life measured for  $^{140}\text{Dy}$  was  $7(1)\mu\text{s}$ . The large error associated with this measurement

was a result of the limited statistics obtained in Ref. [7,8]. The peak height in the previous spectra only contained approximately 50 counts. We expect, dependant on the real production cross section to improve on this with the RISING setup at GSI.

**(iv) Four quasi-particle states in  $^{140}\text{Dy}$  and  $^{142}\text{Er}$ .**

In this mass 130–140 region of the nuclear chart, higher-lying intrinsic states have been observed in the lighter-mass  $N=74$  nuclei, such as  $^{136}\text{Sm}$  [16]. As the deformation of these  $N=74$  nuclei increase toward the proton drip-line, it might be expected that the stability and lifetime of these higher-lying four-quasiparticle states also increases. Hints of these states were observed in  $^{138}\text{Gd}$  [17]. With this measurement of  $^{140}\text{Dy}$  and  $^{142}\text{Er}$  at GSI we will be sensitive to the delayed decay of these higher-lying intrinsic states in a mass-selected low-background environment. In addition, the use of the  $\text{BaF}_2$  detectors and the fast-timing centroid-shift method will allow the lifetimes of these states to be determined with ps resolution. This additional ability to determine lifetimes at the focal plane with RISING has never been attempted before in this region.

**(v) Measuring the deformation of  $^{142}\text{Er}$  at the proton drip-line**

With this experiment, we plan to establish the deformation of the most proton-rich isotope beyond the drip line in the  $N=74$  chain through the observation of the delayed yrast band from the isomer decay. The deformation can be inferred from the ratio of excitation energies of the lowest states but will also be directly measured with the  $\text{BaF}_2$  fast timing method. (The expected lifetime of the collective  $2^+$  state in  $^{140}\text{Dy}$  is expected to be a few ns.) The lightest known Er isotope is  $^{144}\text{Er}$  which was experimentally observed in the proton decay of  $^{145}\text{Tm}$  [14]. In this case, proton decays were established to the first and second excited states in  $^{144}\text{Er}$  [14]. However, the accurate of measuring the excitation energy of states in  $^{144}\text{Er}$  using protons is much less than that which can be achieved with  $\gamma$ -ray measurements. In fact, the lightest known Er nucleus where excited states have been established with  $\gamma$ -ray transitions is  $^{148}\text{Er}$  [15] where evidence was presented for the ( $2^+$ ), ( $4^+$ ) and ( $6^+$ ) states. This new proposed experiment offers an unprecedented method to extend these measurements where gamma rays can be measured, and deformations extracted, by 6 neutrons, right up to the proton drip-line. At the moment, no experimental information about  $^{142}\text{Er}$  is currently known.

This proposed experiment will identify  $\gamma$ -ray transitions in the  $^{142}\text{Er}$  ground-state band from the delayed decay of the  $8^-$  isomeric state. Establishing the yrast ground-state band in  $^{142}\text{Er}$  will reveal its deformation which in turn provides valuable information on calculations and predictions for the existence of deformed proton emitters in this region. In particular, knowledge of the deformation of  $^{142}\text{Er}$  will help with understanding the proton decay tunnelling rates in  $^{143}\text{Tm}$  at the proton drip-line providing refinements to these theoretical nuclear codes. ( $^{142}\text{Er}$  is predicted to be well deformed ( $\beta_2 = 0.25$ ) [13].) Isomer decays, like proton decays, have become a potent spectroscopic tool to characterise states located near the Fermi Surface in nuclei at and beyond the very limits of stability.

**(vi)  $K$ -isomer stability;  $B(E1)$  strength and hindrance factors for the isomer decays.**

Once the  $8^-$  isomer has been identified, at the FRS focal plane, the physics of its  $E1$   $\gamma$ -ray decay strength [ $B(E1)$ ] and hindrance factor, for decay back to the ground state band, will be compared with the systematics of other isomer decays. There is current interest in understanding the large variation in  $B(E1)$  strength observed for these decays across the  $N=74$  chain [6]. These half-life variations have been suggested to be either due to a change in the underlying structure of the isomeric state itself or that of the yrast  $8^+$  state to which the isomer decays [6,11]. Despite these possible explanations, the general feature that the  $B(E1)$  values *increase* as the nuclei become more stably deformed is counter intuitive. It might reasonably be expected that  $^{142}\text{Er}$  will reverse

this trend and show greater robustness of the  $K$  quantum number.

Figure 1 shows that the isomer excitation energy appears to stay approximately constant with increasing neutron number, whereas, the excitation energy of the ground-state band  $2^+$ ,  $4^+$ ,  $6^+$  and  $8^+$  states fall. It would be useful to have the corresponding information for  $^{142}\text{Er}$  to ascertain if it continues this trend at the proton drip-line.

**(vii) Proton decay from the isomeric state?**

If the lifetime of the  $K^\pi = 8^-$  isomeric state in  $^{142}\text{Er}$  is sufficiently long, it might also be possible to speculate on the possibility of observing proton decay from the isomer for the basis of a future experiment. The idea of two-proton decay from an isomeric state in a nucleus not lying beyond the proton-drip line should not be dismissed too readily since this was how the first example of one-proton radioactivity was serendipitously discovered [18]. The identification of two-proton decay, from the isomeric state in  $^{142}\text{Er}$ , would be from the observation of  $^{140}\text{Dy}$  transitions in the  $^{142}\text{Er}$  FRS setting.

### III. EXPERIMENTAL SETUP

#### A. Reasons for performing the experiment at GSI

The experimental setup of the FRS at GSI offers an **unique** possibility to study K-isomers in this mass region. The reasons for this are three-fold. Firstly fragmentation provides the only suitable reaction mechanism which can selectively populate and identify these nuclei, see Fig. 2. In contrast the usual heavy-ion fusion-evaporation reactions tend to populate neutron-deficient mass 140 region nuclei and the best reaction for  $^{142}\text{Er}$  relies on a  $4n$  exit channel. The cross sections for a  $4n$  exit channel at the proton drip-line with this fusion mechanism are very small. Secondly, GSI is the only laboratory in the world which has sufficient beam energy and is coupled to an efficient recoil separator and  $\gamma$ -ray spectrometer. In contrast the maximum beam energy at GANIL is too low to allow separation of these mass 140 recoils. Thirdly, many nuclei can be studied with one fragmentation experiment at the FRS because many nuclei are produced in a single reaction. Isomeric states with half lives in the 100 ns to 1 ms range will be studied using a slow coincidence technique between the emitting nucleus, which has been stopped after its in-flight identification in the FRS, and the isomeric  $\gamma$ -rays. This method was first pioneered at GSI with recoil separators back in the 1970s [19] and was subsequently used at GANIL [20–22].

#### B. Experimental Details

We propose to analyse the products of a fragmentation reaction of a 1 GeV/nucleon  $^{197}_{79}\text{Au}$  beam incident on a thick natural  $^9_4\text{Be}$  target of mass  $6.0\text{ g/cm}^2$  at the entrance to the FRS to search for  $8^-$  isomeric states and map out the proton drip-line in the  $N=74$  neutron-rich nuclei. We will calibrate the setup on the known isomer in  $^{138}\text{Gd}$ , see Fig. 2 and then try to establish the known isomer in  $^{140}\text{Dy}$  before we consider it is sensible to change the settings to  $^{142}\text{Er}$ .

The FRS will be used in standard achromatic mode with an aluminium wedge-shape degrader of thickness  $2\text{ g/cm}^2$  at the intermediate focal plane. Reaction products will be identified by combining the measurements of energy loss ( $\Delta E$ ) and time of flight (TOF) with information from position-sensitive multi-wire counters and the magnetic field readings. From these measurements

of the magnetic rigidity together with position and TOF, the atomic number  $Z$ , and the mass-to-charge ratio ( $A/Q$ ) can be determined for the ions reaching the final focal plane. These procedures rely on the fact that the ions will be fully stripped at these energies. The identified ions will be slowed down in a variable-thickness aluminium degrader and after passing through a 3mm thick plastic scintillator will be implanted into a few mm thick aluminium catcher plate. This final aluminium catcher will be set between the RISING germanium detectors which will be used to identify delayed  $\gamma$  rays in the 100 ns - 1 ms time range with respect to an ion passing through the MUSIC chamber, i.e. a clock will be started by a heavy ion which is detected at the focal plane, and subsequently stopped by the arrival of a  $\gamma$ -ray within a few hundred  $\mu$ s window. Such a setup will greatly reduce the background. The half-life of the delayed  $\gamma$ -ray transitions can be measured by time-to-amplitude converters between these signals.

Data will be taken with an identified recoil, a delayed  $\gamma$ -ray transition, and also delayed  $\gamma - \gamma$  coincidences with the RISING and BaF<sub>2</sub> array which will help in unravelling the decay pattern of these isomers. The known isomeric states in the neighbouring nuclei, e.g. <sup>138</sup>Gd and <sup>140</sup>Dy, will be used as an internal calibration in the lifetime procedure.

RISING provides a high photo-peak efficiency, of the order of 10 %, because its detectors are placed close to the aluminium catcher. (These detectors are placed very close to the aluminium catcher plate since the recoiling nuclei are implanted and are, therefore, stopped which avoids any complications of the  $\gamma$  rays being Doppler broadened). The use of segmented detectors will avoid the problem of  $\gamma$ -ray summing from delayed isomeric cascades below isomeric states. In addition we will use a UK LEPs detector will allow low-energy  $\gamma$ -ray transitions to be identified which are characteristically observed in isomer decays. The BaF<sub>2</sub> detectors will be inserted into the gaps between the RISING germanium detectors and will result in a minimum loss of germanium efficiency.

### C. Beam time requests.

The cross sections for the formation of these nuclei have been estimated from EPAX [10]. The EPAX production rates were as follows, <sup>138</sup>Gd;  $5 \times 10^{-6}$  barns, <sup>140</sup>Dy;  $4 \times 10^{-9}$  barns, and <sup>142</sup>Er;  $2 \times 10^{-13}$  barns.

The beam time estimates have been based on these cross sections and assumed that  $\approx 50\%$  of the secondary fragments survive the optical transmission path through the FRS due to reactions which take place in the degrader and that only approximately 70-80% of the recoils will remain fully stripped. Isomeric ratios are known to be up to 50% [20–22] and a value of  $\approx 10\%$  has been used, see Fig. 2.

With a <sup>197</sup>Au primary beam current of  $10^8$  particles per second and one spill every 8 seconds, then the number of nuclei produced at the focal plane are; <sup>138</sup>Gd; 0.125 per second (10800/day), <sup>140</sup>Dy;  $1 \times 10^{-4}$  per second (9/day), and <sup>142</sup>Er;  $5.3 \times 10^{-9}$  per second (0.0005/day). We note that Pfützner *et al.* [23] with <sup>238</sup>U fragmentation at GSI were able to clearly identify isomers in <sup>212</sup>Pb and determine half-lives for isomeric transitions with as little as 370 implanted ions. [One of the points of this experiment is to test the EPAX cross sections this far from stability. (There have been no cross section measurements for beams between Xe and Pb for these proton-rich nuclei. The lightest Gd isotope measured was <sup>138</sup>Gd which was of the same order as that predicted from EPAX. The lightest Dy isotope measured was <sup>148</sup>Dy with a cross section of 1.6mb).]

We plan to spend 1 day setting up the FRS, 2 shifts to optimise the FRS settings and then to

measure  $^{138}\text{Gd}$  for 1 shift with the  $^{197}\text{Au}$  beam to compare with the previous results with the  $^{208}\text{Pb}$  beam, see Fig. 2. We then plan to run for 7 days at the  $^{140}\text{Dy}$  setting and in this time expect to get about 63 counts based entirely on the EPAX cross sections. If it turns out that we can produce  $^{140}\text{Dy}$  with a higher cross section than EPAX predicts then we will switch to running  $^{142}\text{Er}$  as soon as we have sufficient counts to obtain a good half-life measurement. If not then we will at least have a measurement point to compare with the EPAX cross sections and gain a feeling for what can be done with in this region.

In total we request 9 days of beam time.

- 
- [1] L. Goettig, Nucl. Phys. **A357**, 109 (1981).
  - [2] H.F. Brinkman, Nucl. Phys. **81**, 233 (1966).
  - [3] D. Ward, Nucl. Phys. **A117**, 309 (1968);  
Yu. V. Sergeenkov, Nuclear Data Sheets **65**, 277 (1992).
  - [4] D.G. Parkinson, Nucl. Phys. **A194**, 443 (1972).
  - [5] A.M. Bruce, Phys. Rev. **C50**, 480 (1994).
  - [6] A.M. Bruce, Phys. Rev. **C55**, 620 (1997).
  - [7] D.M. Cullen *et al.* Phys. Lett. **B 529**, 42 (2002).
  - [8] W. Krolas *et al.* Phys. Rev. **C65**, 031303(R) (2002).
  - [9] C. Davids *et al.* Phys. Rev. Lett. **80**, 1849 (1998).
  - [10] K. Sümmerer *et al.* Phys. Rev. C **35**, 1687 (1987) and Phys. Rev. C **42**, 2546 (1990).
  - [11] F.R. Xu *et al.*, Phys. Rev. **C59**, 731 (1999).
  - [12] F.R. Xu *et al.*, Private communication (2002).
  - [13] F.R. Xu *et al.*, Private communication (2004).
  - [14] J.C. Batchelder *et al.* Phys. Rev. **C57**, R1042 (1998),  
M. Karny *et al.* Phys. Lett. **C90**, 012502 (2003).
  - [15] Z. Phys. **A306**, 211 (1982) and Z. Phys. **A306**, 223 (1982).
  - [16] P.H. Regan *et al.*, Phys. Rev. **C51**, 1745 (1995).
  - [17] D.M. Cullen *et al.* Phys. Rev. **C 58**, 846 (1998).
  - [18] K.P. Jackson *et al.* Phys. Lett. **B 33**, 281 (1970).
  - [19] J.W. Grüter, *et al.* Phys. Lett. **B 33**, 474 (1970).
  - [20] R. Grzywacz *et al.* Phys. Lett. **B 355**, 439 (1995).
  - [21] R. Grzywacz *et al.* Phys. Rev. C **55**, 1126 (1997).
  - [22] C. Chandler *et al.* Phys. Rev. C **56**, R2924 (1997).
  - [23] M. Pfützner *et al.* Phys. Lett. **B 444**, 32 (1998).